Doctoral Dissertation

Metabolomics Approach for Characterization of Kopyor (*Cocos nucifera* L. var Kopyor), Indonesian Unique Coconut

Mercy Bientri Yunindanova

January 2025

Division of Biotechnology

Graduate School of Engineering,

Osaka University

List of Abbreviations

(*in alphabetical order*)

GC	Gas chromatography
MS	Mass Spectrometry
MSTFA	N-Trimethylsilyl-N-methyl trifluoroacetamide
PCA	Principal Component Analysis
OPLS-R	Orthogonal Projections to Latent Structures Regression
FCP	Free Choice Profiling
GPA	Generalized Procrustes Analysis
ANOVA	Analysis of variance

Table of Contents

Chapter 1

General Introduction

1.1 Coconut (*Cocos nucifera* L.)

Coconut is a vital tropical palm fruit with considerable economic significance. The coconut palm (*Cocos nucifera* L.), part of the Arecaceae family, is predominantly cultivated in tropical regions, with Asia being the leading producer. Major coconut-growing countries include Indonesia, the Philippines, India, Myanmar, Thailand, and several other tropical nations. These five countries including Indonesia, the Philippines, India, Sri Lanka, and Thailand account for approximately 90% of global coconut production, yielding around 61.5 million tons annually (Patil & Benjakul, 2018).

Coconuts possess 32 chromosomes, organized into 16 pairs of homologous chromosomes, and are classified as monocotyledonous plants (Abraham & Mathew, 1963; Pereira et al., 2017). This classification is characterized by features such as parallel leaf venation, a single cotyledon in the embryo, and a fibrous root system. The edible part of the coconut is the endosperm, which consists of both coconut water and flesh. This coconut flesh, also known as coconut meat, is not only structurally complete but also recognized for its high nutritional value (Azra et al., 2021).

The development of the coconut endosperm begins with the formation of coconut water during the early stages of growth. Throughout the first six months, the endosperm remains in a liquid state, and after this period, the liquid endosperm begins to deposit and transition into a solid form. By approximately 12 months of maturity, the endosperm fully solidifies, forming the firm, whitish mass known as coconut flesh (Ohler, 1999). The liquid endosperm is characterized as a syncytial structure, consisting of cytoplasm with free nuclei. In contrast, the solid endosperm comprises cells with varying chromosomal ploidy levels, including 3n, 6n, and 12n, whereas the diploid (wild-type) condition is $2n = 32$ (Abraham & Mathew, 1963).

This transformation from liquid to solid endosperm is marked by significant shifts in the metabolite profile, with primary metabolites playing a key role in these developmental processes (Kumar et al., 2021).

Coconut varieties, or cultivated varieties (cultivars), are classified based on several factors, including plant height (tall or dwarf), fruit characteristics (size, shape, color), and maturity period (early vs. late maturing) (Nayar, 2017; Rahayu et al., 2021; Samarajeewa, 2024; Wicaksono et al., 2021). Hybrid varieties, which combine traits from tall and dwarf coconuts, are also developed to enhance yield, early maturity, and disease resistance. Other unique types of coconuts exist, distinguished by specific properties or uses. Varieties differ in resistance to pests and diseases, as well as environmental adaptability (climate and salt tolerance). Some varieties are cultivated primarily for oil production, others for coconut water, and some for ornamental purposes.

Additionally, coconuts exhibit variations based on their endosperm, including normal coconuts and unique varieties with irregular endosperm structures. Among these distinctive varieties, several stand out for their remarkable characteristics, such as Kopyor from Indonesia, Curd Coconut or Macapuno from the Philippines/ Dikiri Pol from Sri Lanka/ Wax Coconut (Kelapa Lilin) from Indonesia/ Dong Kathi from Cambodia/ Thairu Tengai from India/ Niu Garuk from Papua New Guinea/ Pia from Polynesia/ Maphrao Kathi from Thailand/ Dua Sap from Vietnam (Chomchalow, 2013; Wicaksono et al., 2021). The uniqueness of these coconuts is evident not only in their external appearance but also in the distinctive properties and composition of their endosperm.

Kopyor coconut is characterized by a modified solid endosperm that is less firm and partially detached from the endocarp, while its liquid endosperm is cloudy but not viscous. On the other hand, Curd Coconut is an uncommon abnormality in coconut flesh, identified by its thicker consistency compared to regular coconuts, with a light, fluffy, and soft texture similar

to curd, along with viscous water. The occurrence of Curd Coconut is extremely rare, with a frequency of about 0.15% (**Figure 1.1**) (Chomchalow, 2013).

A. B. C.

Figure 1.1. Solid endosperm of A. Curd coconut (Chomchalow, 2013), B. Kopyor coconut, C. Normal coconut

Variations in coconut species across the world, though not yet fully explored in detail, including differences in plant height, endosperm type, and hybridization potential, play a critical role in determining the suitability of each variety for specific agricultural and commercial purposes. Understanding these variations is essential for optimizing coconut breeding programs and improving the economic value of coconut crops.

1.2 Kopyor (*Cocos nucifera* L. var Kopyor)

Among the various types of coconut, the Kopyor variety (*Cocos nucifera* L. var. Kopyor) is particularly notable for its unique characteristics and is indigenous to Indonesia (Maskromo et al., 2016; Maskromo & Sudarsono, 2013; Maskromo et al., 2014). Kopyor is a naturally occurring mutant, distinguished by its distinct endosperm properties. Unlike normal coconuts, the solid endosperm of Kopyor coconuts is partially or fully detached from the endocarp (shell), leading to the mixing of solid and liquid endosperm. This phenomenon is attributed to the weak integration of the cell walls in the solid endosperm of Kopyor coconuts.

The phenomenon of changes in the endosperm of Kopyor coconuts has been frequently attributed to natural genetic modifications. The first viewpoint, as stated by (Pesik et al., 2017), suggests that the formation of Kopyor endosperm in coconuts is potentially due to a mutation in a single regulatory gene, which leads to pleiotropic effects that influence multiple developmental processes in the coconut plant. Further support for this idea comes from (Setiawan et al., 2020), who proposes that the unique characteristics of Kopyor coconuts are linked to genetic modification governed by duplicate dominant epistasis. In this form of epistasis, two different genes can each independently produce the same phenotype when a dominant allele is present at either gene locus. This means that as long as at least one dominant allele is present in either of the two gene pairs, the phenotype will be expressed, making it a highly resilient genetic trait.

In addition, several studies have noted that Kopyor coconuts, characterized by a reduction in the enzyme α-D-galactosidase, exhibit altered endosperm development (Maskromo & Sudarsono, 2013; Novarianto et al., 2014; Sudarsono et al., 2019). These changes are attributed to mutations in the α-Gal gene, which, when derived from coconut, is referred to as the CnAGal gene. This gene encodes the enzyme α-D-galactosidase. The full-length cDNA sequence of CnAGal in normal coconuts (KJ957156) comprises 1,194 nucleotides, encoding a protein of 398 amino acids with a molecular weight of 43.575 kD. The amino acid sequence was analyzed using the SignalP 3.0 program (Bendtsen et al., 2004).

The formation of Kopyor coconut involves distinct physiological and biochemical processes that set it apart from the development of normal coconuts. In both normal and Kopyor coconuts, the early development of the endosperm progresses similarly through the syncytial phase. However, during the cellular phase, Kopyor coconuts experience a disruption in cell wall formation, as highlighted by (Wicaksono et al., 2021) (**Figure 1.2**). This disruption is attributed to a deficiency in the enzyme α-galactosidase, which is crucial for the hydrolysis of

galactomannans into their component sugars, galactose and mannose. The α-galactosidase deficiency leads to an imbalance in the galactomannan composition, characterized by an elevated galactomannan content and reduced mannan levels. As a result, the cell walls in the Kopyor endosperm exhibit reduced structural integrity. Mannans play a vital role in maintaining the hardness and mechanical resistance of the endosperm, as noted by (Petkowicz et al., 2001) (**Figure 1.3**).

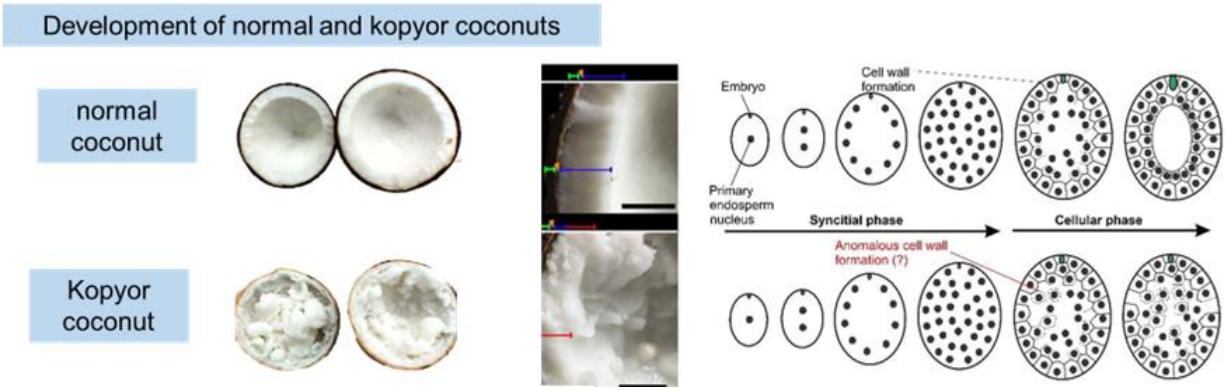

Figure 1.2. Developmental comparison between normal and Kopyor coconuts: morphological and cellular phases (Wicaksono et al., 2021)

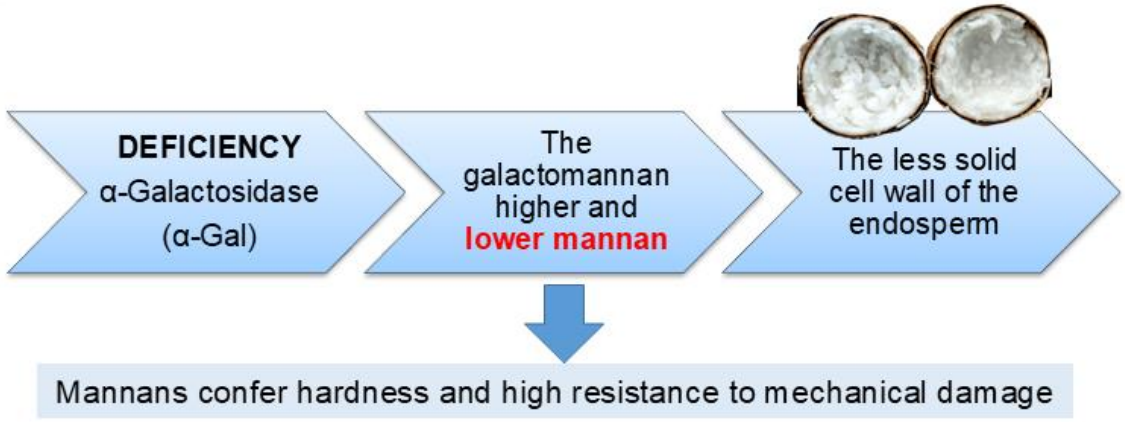

Figure 1.3. Impact of α-galactosidase deficiency on endosperm structure via altered galactomannan composition (Petkowicz et al., 2001)

Kopyor coconuts are naturally generated through the crossbreeding of heterozygous coconut plants that carry the Kopyor trait; however, this method typically results in less than

25% of the offspring exhibiting the Kopyor phenotype. Traditionally, Kopyor seedlings cannot be propagated directly from Kopyor embryos due to the detachment of the endosperm from the shell, which prevents the embryo from sustaining normal seedling development (Novarianto et al., 2014). An alternative approach to overcome this limitation is the use of embryo rescue via in vitro culture, which has been shown to produce seedlings with up to 99% kopyor fruit production (Sisunandar et al., 2018).

The unique characteristics of mutant coconuts have driven high market demand. Kopyor coconuts, known for their fragile solid endosperm, offer a distinctive texture and superior taste, making them highly valued in traditional Indonesian desserts. Due to their rarity, Kopyor coconuts command a premium price, and demand continues to grow (Faramitha et al., 2024; Rozaki et al., 2021; Santoso et al., 1996a; Wicaksono et al., 2021). Similarly, Macapuno coconuts from the Philippines are prized for their jelly-like endosperm, which sets them apart from regular coconuts. Their unique texture is highly sought after in Filipino desserts, with increasing demand in the Philippines and Vietnam (Bao Toan & Cong Thanh, n.d.; Nguyen et al., 2016).

Previous research on Kopyor coconut has primarily focused on its genomic aspects (Maskromo et al., 2016; Maskromo et al., 2014; Rahayu et al., 2021; Rahmawati et al., 2021; Setiawan et al., 2020; Sudarsono et al., 2019), highlighting genetic differences and the mutations responsible for its irregular endosperm. While studies have examined Kopyor's proximate composition, including macronutrient content, there remains a gap in metabolomic and sensory analyses. Despite its reputation for being highly desirable, with strong consumer demand and premium pricing, formal sensory evaluations that elucidate the sensory attributes contributing to Kopyor's appeal remain insufficient. To date, no comprehensive study has systematically analyzed the sensory components that distinguish Kopyor from other coconut varieties. Moreover, the correlation between these sensory

characteristics and the underlying metabolic profiles has not yet been investigated. Conducting such research is crucial to scientifically validate the sensory attributes that drive consumer preference and provide a substantiated explanation for Kopyor's elevated market value.

1.3 Metabolomic approach

Metabolomics is an omics discipline focused on the comprehensive analysis of metabolites; the small molecules produced by living organisms. It enables detailed differentiation of biological systems and provides insights into metabolic profile changes in response to environmental or biological processes (Hanifah et al., 2022; Ikram et al., 2021; Putri & Fukusaki, 2016). The broad scope of metabolomics, allowing simultaneous analysis of multiple metabolites, has proven valuable in fields such as medical research, food science, agriculture, and environmental studies. Metabolomics employs chromatography to separate metabolites based on parameters like molecular weight and retention time, with library-based identification of individual compounds. The approach is divided into targeted metabolomics, which focuses on specific metabolites, and non-targeted metabolomics, which analyzes all detectable metabolites.

Several analytical instruments are commonly used in metabolomics, including nuclear magnetic resonance (NMR), gas chromatography-mass spectrometry (GC-MS), and liquid chromatography-mass spectrometry (LC-MS) (Putri & Fukusaki, 2016). GC-MS is widely utilized for its robustness, stability, affordability, and ease of use, making it particularly suitable for profiling small hydrophilic molecules. It has been applied to various types of food, such as soy sauce, cheese, and coffee (Dixon et al., 2006; Pavagadhi & Swarup, 2020; Rocchetti & O'Callaghan, 2021; Xiao et al., 2019). LC-MS is also a key technique in metabolomics, used for profiling targeted metabolites, like amino acids, as well as unknown metabolites. Unlike

GC-MS, LC-MS does not require derivatization, allowing for broader metabolite detection and a more comprehensive analysis.

Due to the large amount of data generated in metabolomics studies which often range from tens to thousands of metabolites, multivariate analysis techniques are employed to interpret the data effectively. Commonly used methods include Principal Component Analysis (PCA), which helps reduce data dimensionality and identify patterns or trends, and Orthogonal Partial Least Squares Discriminant Analysis (OPLS-DA), which is used for classification and identifying differences between sample groups. Additionally, Orthogonal Partial Least Squares Regression (OPLS-R) can be applied when correlating metabolite data with specific variables of interest. The choice of multivariate technique depends on the goals of the analysis and the ease of interpreting the resulting information. These tools are crucial for extracting meaningful insights from complex metabolomic datasets (Ikram et al., 2020).

In the fields of food science and agriculture, metabolomics plays a crucial role in determining the origin and authenticity of food products, assessing the impact of cultivation methods, and optimizing processing techniques to improve both quality and safety. In agriculture, metabolomics helps to understand how factors such as cultivated variety, post-harvest handling, farming practices, soil conditions, and environmental influences affect crop quality and nutritional value. By analyzing metabolic profiles, metabolomics helps to identify unique biomarkers in both food and agricultural products that contribute to their nutritional, sensory, and safety attributes. This enhances product traceability, quality, and overall sustainability in food production systems.

1.4 Metabolomics of coconut

Metabolomics studies on coconuts have primarily focused on examining metabolic profiles based on maturity stages and varietal differences. Additionally, the impact of post-harvest handling, particularly in coconut water, a widely traded product, has been extensively investigated (Kumar et al., 2021; Prades et al., 2012). In recent years, there has been an increase in metabolomics studies on coconuts, driven by the recognition of the importance of a more comprehensive analysis of coconut metabolites, given that coconuts are a globally traded commodity. A better understanding of the complex metabolic composition of coconuts can enhance product quality, traceability, and commercial value.

However, there remains a significant gap in the metabolomics study of unique coconut types, such as kopyor and macapuno (Wicaksono et al., 2021), which have distinct characteristics compared to regular coconuts. These unique varieties have not been extensively studied, primarily due to challenges related to the availability of specific samples, as their cultivation is often limited to specific geographic regions. The scarcity of samples and the localized nature of their production have made it difficult to perform comprehensive metabolomics analyses on these coconuts.

Expanding research into these unique varieties could provide valuable insights into their metabolic profiles and offer opportunities to better understand their nutritional and commercial potential, as well as their distinct sensory attributes. Comprehensive metabolomics studies on these coconuts would significantly contribute to broadening our understanding of coconut biodiversity and enhancing its applications in food science, agriculture, and global commerce.

1.5 Objective and strategy

This research aims to characterize the unique Indonesian Kopyor coconut (*Cocos nucifera* L. var. Kopyor) using a metabolomics-based approach. The strategy consists of three

main steps: first, comparing Kopyor with normal coconuts through metabolomics and sensory evaluation; second, analyzing Kopyor's phenotypic diversity using metabolomics alongside proximate and physicochemical analyses; and third, characterizing various Kopyor varieties based on their metabolomic profiles and sensory attributes. These steps work together to provide a comprehensive understanding of Kopyor's distinctive properties and unlock its potential in niche markets.

1.6 Thesis outline

This thesis consists of five chapters. Chapter 1 serves as an introduction, providing a general overview of coconuts, including the unique Kopyor coconut (*Cocos nucifera* L. var. Kopyor), and recent research surrounding Kopyor. It also discusses how metabolomics can support the future development and commercialization of Kopyor.

Chapter 2 presents the characterization process of the unique Indonesian Kopyor coconut (*Cocos nucifera* L. var. Kopyor), highlighting its differences from regular coconuts. The strategy involves comparative metabolomics using data profiling and discrimination approaches, alongside sensory evaluation. Notably, the sensory attributes were developed for the first time in this research to strengthen the unique characteristics of Kopyor as a food product. This stage aims to identify the metabolite characteristics and sensory attributes of Kopyor, serving as a foundation for further analysis.

Chapter 3 explores the metabolomics-based approach and proximate, as well as physicochemical analysis of various Kopyor phenotypes. Since Kopyor exhibits different levels of endosperm quantity, a metabolomic approach utilizing regression analysis is employed. This allows for the examination of how endosperm levels influence compound concentrations and aids in identifying potential biomarkers.

Chapter 4 delves deeper into the relationship between plant variety and Kopyor's sensory and metabolic profiles, demonstrating how different varieties influence consumer preferences. Sensory evaluations, grounded in the research presented in Chapter 2, serve as the foundation for identifying the most favored varieties. This analysis provides critical insights for selecting the optimal varieties for both cultivation practices and consumer markets.

Chapter 5 concludes the thesis by summarizing the key findings and offering recommendations for future research and commercial opportunities.

Chapter 2

Characteristics of kopyor coconut (*Cocos nucifera* L. var Kopyor) using sensory analysis and metabolomics-based approach

2.1 Introduction

Kopyor (*Cocos nucifera* L. var. Kopyor) is a unique coconut variety indigenous to Indonesia, renowned for its distinct endosperm modification. Despite sharing an identical external appearance with regular coconuts, Kopyor coconuts can be distinguished at the mature stage by their significantly altered internal endosperm structure. Among the numerous coconut varieties worldwide and within Indonesia, Kopyor coconuts have attracted considerable attention due to their unique characteristics and limited availability, both of which contribute to their high demand in niche markets (Rozaki et al., 2021; Santoso et al., 1996). Kopyor coconuts stand out for their substantial economic value, making them a distinct asset in the diverse coconut farming industry (Antu et al., 2021; Novarianto et al., 2014; Sisunandar et al., 2018).

Despite their growing popularity, the utilization of Kopyor coconuts is still relatively limited, primarily centered around the food and beverage sector, where they are used in the production of desserts and specialty drinks. Additionally, there is untapped potential for Kopyor in the pharmaceutical and cosmetic industries, as its natural components, such as virgin coconut oil, offer promising applications (Mahbub et al., 2022). Moreover, Kopyor coconuts hold significant promise as an ingredient for healthy food products due to their unique nutritional profile, and they have the potential to be developed into functional products, expanding into broader markets beyond traditional uses (Antu et al., 2021). On the other hand, there is a lack of comprehensive studies that focus on its chemical composition and sensory attributes, particularly those that influence consumer acceptance. To fully unlock the potential

of Kopyor as a valuable food commodity, detailed investigations encompassing chemical profiling and sensory evaluation are essential.

Metabolomics is an advanced approach in food science, providing detailed analysis of the chemical composition within food products (Rocchetti & O'Callaghan, 2021). Additionally, this approach facilitates the identification of biomarkers, enabling the differentiation of the samples. Consequently, metabolomic analysis is highly suitable for characterizing Kopyor coconuts in comparison to normal coconuts, encompassing both immature and mature stages.

Sensory evaluation plays a vital role in food products, as it is directly linked to the assessment of sensory attributes, which are crucial for defining the overall quality and characteristics of a product (Lawless & Heymann, 2010; Stone & Sidel, 1993). Sensory analysis offers valuable insights into how consumers perceive key attributes such as taste, texture, aroma, and appearance. These attributes not only shape the product's identity but also have a significant impact on consumer acceptance and preference. However, in the case of Kopyor coconuts, there has been no established sensory profile, and the compounds associated with these sensory attributes remain unidentified. Therefore, identifying the sensory attributes of Kopyor is critical as an initial step and will serve as a reference for future research in this area.

The aim of this research is to combine sensory analysis with metabolomic approaches, using gas chromatography mass spectrometry (GC-MS), to comprehensively characterize the unique attributes of Kopyor coconuts.

2.2 Materials and methods

2.2.1 Samples of Kopyor coconut, immature (young) normal coconut, and mature normal coconut

This experiment used Kopyor, normal mature (11 months old), and normal young coconuts (6-7 months old). Kopyor is only distinguishable at maturity, while young Kopyor resembles normal young coconuts (**Figure. 2.1.A**). The endosperm of the three coconut types is shown in Fig. 2.1.B, and the liquid and flesh are illustrated in **Figure. 2.1.C.** Coconuts were collected from Central Java, including Kopyor Brown Dwarf (KBD) and Pati Dwarf Brown varieties (normal coconut) from Pati Regency, Indonesia and Kebumen Tall from Kebumen Regency, Indonesia for young coconuts. Five coconuts of each type were harvested, with average weights of 1324 ± 241 g for Kopyor, 1590 ± 365 g for normal mature, and 2075 ± 122 g for normal young. After collection, water and flesh were immediately extracted, stored at -30°C, and prepared for sensory and metabolomic analysis.

2.2.2 Reagents

In this analysis, several reagents were employed for the extraction and preparation of coconut water and flesh samples. A solvent mixture of methanol, water, and chloroform in a 5:2:2 ratio (v/v/v) was used to extract the necessary compounds from both sample types. Methanol for GC-MS analysis was obtained from Kanto Chemical Co., Inc. (Tokyo, Japan), and chloroform for GC-MS was sourced from Kishida Chemical Co., Ltd. Ribitol, at a concentration of 100 µg/mL, was used as an internal standard to ensure accurate quantification, following previous studies. Ribitol and pure pyridine were supplied by Fujifilm Wako Pure Chemical Industries, Ltd. (Osaka, Japan). Ultrapure water, required for the extraction solvent and sample preparation steps such as diluting supernatant fractions and preparing aqueous layers, was obtained from Genpure (Thermo Scientific, Osaka, Japan). Additional reagents included methoxyamine hydrochloride, purchased from Sigma-Aldrich Japan (Tokyo, Japan),

and N-methyl-N-(trimethylsilyl) trifluoroacetamide (MSTFA), along with an alkene mix (C9-C40), sourced from GL Sciences (Tokyo, Japan). These reagents played a crucial role in the effective extraction, separation, and preparation of the coconut samples for GC-MS analysis.

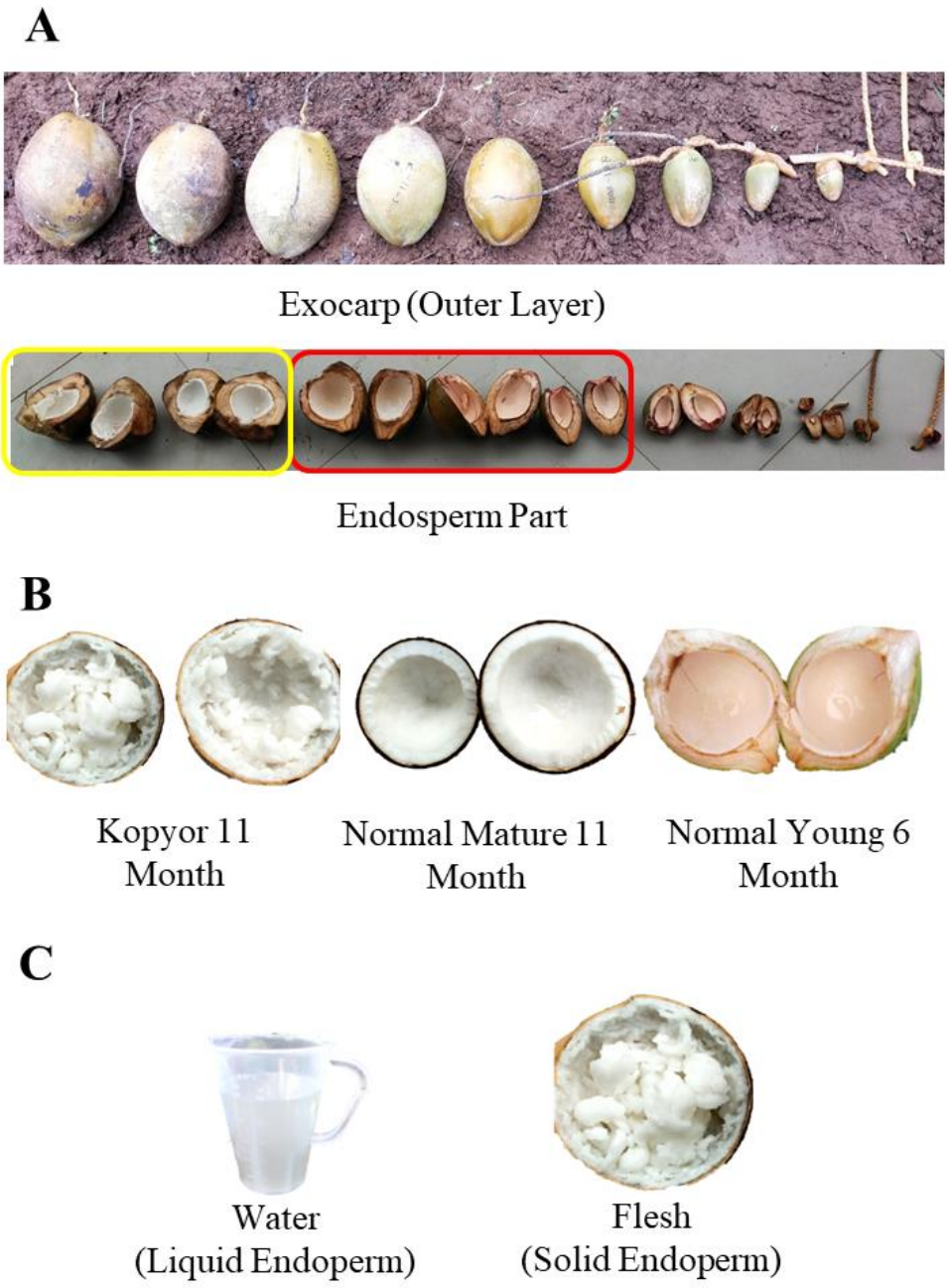

Figure 2.1. A. Developmental stages of coconuts, highlighting exocarp and endosperm structures. B. Endosperm morphology comparison between Kopyor (11 months), normal mature (11 months), and young coconuts (6 months). C. Kopyor's liquid (water) and solid (flesh) endosperm.

2.2.3 Extraction process for hydrophilic low-molecular-weight compounds in GC-MS analysis

The analysis involved separating coconut water and flesh samples. For each sample, 1 mL of coconut water was collected. The coconut flesh was freeze-dried for 48 hours, followed by lyophilization in liquid nitrogen and grinding into a homogeneous powder using a multi-bead shocker (Yasui Kikai, Osaka, Japan) at 2000 rpm for 20 seconds. A 5 mg portion of the resulting powder was used for further analysis. Both water and flesh samples were extracted using a solvent mixture of methanol, water, and chloroform in a 5:2:2 ratio (v/v/v). Ribitol (100 μg/mL) was added as an internal standard based on prior studies. To each sample, 1 mL of the extraction solvent was added, followed by vortex mixing and incubation at 37°C and 1200 rpm for 30 minutes. The mixture was then centrifuged at 4°C and 10,000 rpm for 3 minutes to separate the solids from the liquid. Subsequently, 300 μL of ultrapure water was added to a 1.5 mL tube, along with 600 μL of the supernatant from the previous step. This mixture was centrifuged again at 4°C and 10,000 rpm for 3 minutes. From the resulting solution, 50 μL of the aqueous phase was transferred into new 1.5 mL microtubes, with an additional 50 μL from each sample pooled into a 2 mL tube for quality control (QC). The blank, sample, and QC tubes were sealed with perforated caps and centrifuged under vacuum at 25°C and 1500 rpm for 60 minutes using a centrifugal concentrator (TAITEC, Saitama, Japan) to obtain the extracts.

2.2.4 Derivatization process for hydrophilic low-molecular-weight compounds in GC-MS analysis

The derivatization process was conducted using both oximation and silylation procedures. To initiate the analysis, 100 μL of methoxyamine hydrochloride was added to the samples, followed by incubation in a shaker at 30°C for 90 minutes at 1200 rpm.

Methoxyamine hydrochloride facilitates the oximation process, which stabilizes carbonyl compounds during derivatization. After incubation, 50 µL of N-Methyl-N-trimethylsilyl-trifluoroacetamide (MSTFA) (GL Sciences) was added to the samples. MSTFA is commonly used for silylation, a procedure that enhances the volatility and thermal stability of analytes for GC-MS analysis. The samples were then incubated at 37°C for 30 minutes at 1200 rpm. Following this, the samples were centrifuged at 10,000 rpm for 3 minutes at 25°C. Finally, 100 µL of the supernatant was transferred into GC/MS vials for injection into the GC-MS system.

2.2.5 GC-MS conditions

For GC-MS analysis, each flesh sample was analyzed once, while water samples underwent two analyses, one with the filament on and the other with it off. During the filament-off analysis, the filament was deactivated at the sucrose retention time (19.1–19.4 min) to exclude the sucrose peak. The GC-MS analysis was conducted using a GC-MS-QP2010 Ultra (Shimadzu, Kyoto, Japan), equipped with an AOC-20i/s autoinjector and an InertCap 5MS/NP column (35 m length, 0.18 mm I.D., 0.18 µm film thickness). Before analysis, the inner seal connector and inert silica capillary tube (GL Sciences, Tokyo, Japan) were preconditioned at 250 °C for one hour and assembled with the column. A 1 µL sample was injected at 230 °C with a split ratio of 25:1, using hydrogen as the carrier gas at a linear velocity of 39.0 cm/s. The column temperature was initially held at 80 °C for 4 minutes, then increased to 330 °C at a rate of 15 °C/min, and maintained at 330 °C for 8 minutes. The interface and ion source temperatures were set at 310 °C and 280 °C, respectively. Electron ionization (EI) at 70.0 V was applied, and spectra were recorded over a mass range of m/z 85–500 with a scan time of 0.15 seconds. A standard alkane mixture (C10–C40) was injected at the start of each analysis to calculate retention indices (RI) for peak identification.

2.2.6 GC-MS data analysis

The GC-MS data were converted to AIA format using the GC-MS solution software (Shimadzu, Kyoto, Japan) and processed with MS-DIAL ver. 4.00, utilizing the GC-MS-5MP Library (Riken, Kanagawa, Japan) for peak alignment, filtering, and annotation. Peak intensities of annotated metabolites were normalized to the ribitol internal standard. Metabolites were further validated through an in-house library via MS-DIAL (GL-Sciences DB). Only metabolites with a relative standard deviation (RSD) below 30% in the quality control (QC) samples were retained. Principal component analysis (PCA) was then conducted using SIMCA P+ ver. 13.0 (Umetrics, Umea, Sweden) for data visualization.

2.2.7 Free Choice Profiling (FCP) test for sensory evaluation and sample preparation

Sensory evaluation was conducted using Free Choice Profiling (FCP) following the procedures outlined in previous studies (Deliza et al., 2005; Heo et al., 2023). FCP involves two main phases: an attribute-generation session and a rating session. The evaluation was repeated three times, with a panel of 21 participants who provided informed consent prior to the sessions. During the first phase, panelists underwent training and participated in focus group discussions to generate sensory attributes. These attributes, identified by the panelists themselves, were subsequently used in the rating phase.

Before tasting each sample, panelists were instructed to rinse their mouths with mineral water to minimize carryover effects. In the rating session, panelists evaluated the intensity of sensory attributes such as color, aroma, taste, flavor, mouthfeel, and aftertaste. The samples were presented in a randomized order to reduce bias. Each panelist rated the intensity of the attributes using a line scale, which is commonly recommended for FCP to quantify sensory descriptors (Gomide et al., 2021). Between samples, panelists cleansed their palates by consuming crackers and water, and were asked to wait for 20–30 seconds after rinsing to ensure

their palate was neutral before proceeding with the next sample. This process ensured consistent and reliable sensory data across the panelists and sessions.

2.2.8 Statistical analysis

The internal standard was utilized to normalize peak height data, ensuring accurate quantification across samples. Metabolites with a relative standard deviation (RSD) below 30% were selected for further analysis to ensure data reliability. These selected metabolites were subjected to multivariate analysis, starting with principal component analysis (PCA) using SIMCA-P version 13 (Umetrics, Umea, Sweden). PCA, a widely used multivariate technique, enables the extraction of meaningful patterns from complex datasets and aids in identifying clusters and outliers. Autoscaling was applied as the scaling method without data transformation to maintain uniformity across variables.

In addition to PCA, orthogonal projections to latent structures regression (OPLS-R) were also performed using SIMCA-P version 13, allowing for further discrimination between variables. The variable importance in projection (VIP) scores and regression coefficients were derived from the OPLS-R analysis, offering insights into the significance of each metabolite's contribution to the model.

Statistical significance between groups was assessed through one-way analysis of variance (ANOVA), followed by Tukey’s post-hoc test, using MetaboAnalyst 5.0, with a significance threshold of $p < 0.05$. To further explore metabolite differences, a volcano plot was constructed, combining p-value from a t-test ($p < 0.05$) with fold change (FC) values, highlighting significant metabolites that show both statistical relevance and biologically meaningful fold changes.

2.3 Result and discussion

2.3.1 Comparative metabolite assessment of normal and Kopyor coconuts

GC-MS analysis of coconut water revealed distinct differences between Kopyor, normal mature, and young coconuts. In the score plot, Kopyor water was separated from both mature and young coconut water along Principal Component (PC)1, which accounted for 64.1% of the variation. This separation was driven by endosperm type, with Kopyor water clustering on the positive side of PC1, while normal mature and young coconut water grouped on the negative side. PC2, explaining 21.3% of the variance, distinguished between mature and young coconut water based on maturity. The loading plot for PC1, containing 79 metabolites, indicated Kopyor water had higher metabolite accumulation than normal coconut water, including elevated levels of amino acids, organic acids, sugars, and sugar alcohols, as detailed in the supplementary table.

The coconut flesh showed clear clustering. PC1, accounting for 77.6% of the variance, distinguished the flesh based on maturity, with young normal coconut flesh on the positive side and Kopyor and mature coconut flesh on the negative side. PC2, explaining 12.5% of the variance, separated the flesh by endosperm type, with Kopyor on the positive side and normal mature and young coconuts on the negative side. A supplementary table lists 52 hydrophilic metabolites, with young normal coconuts having more metabolites than Kopyor and mature coconuts. The loading plot highlights the variables driving this separation.

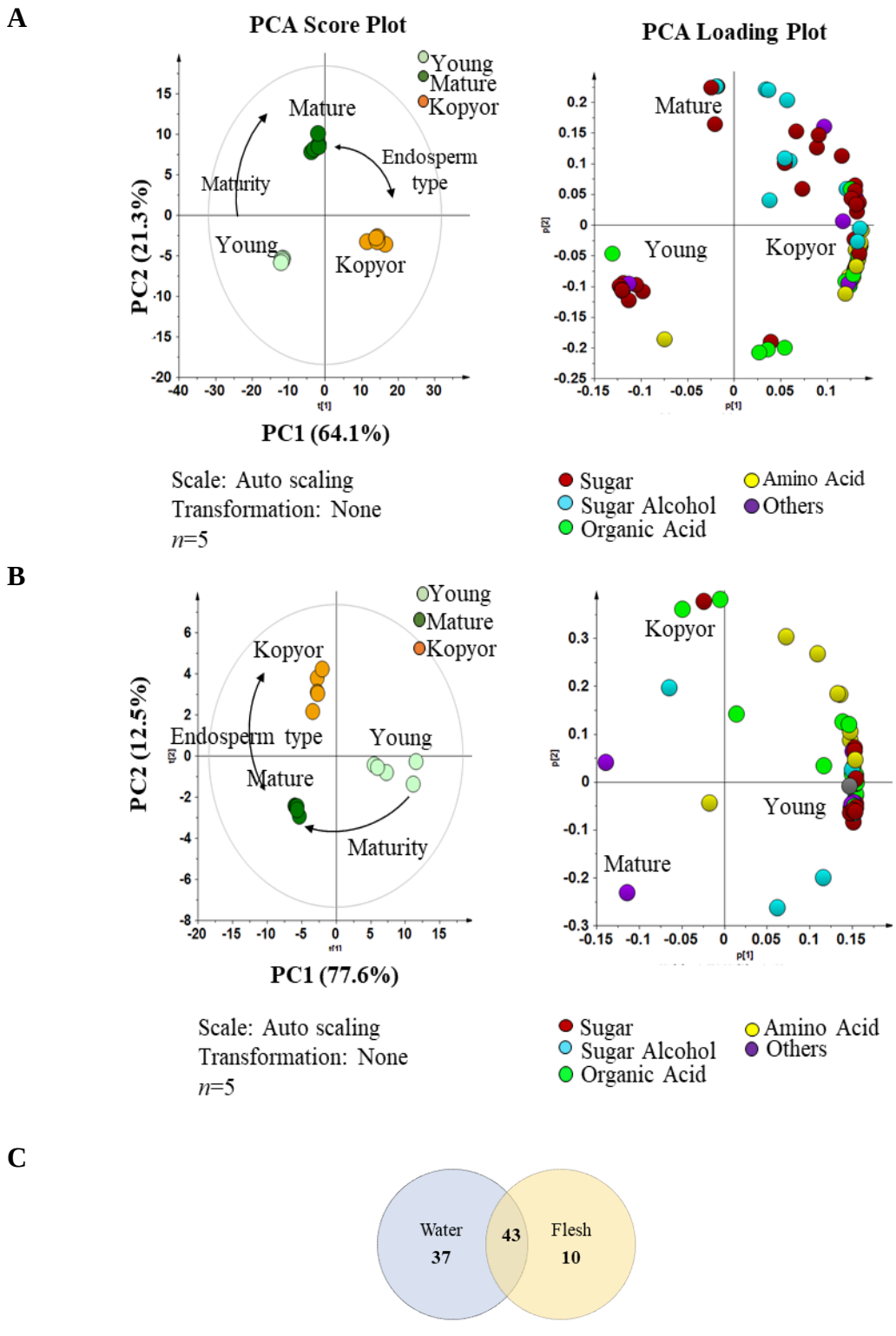

Figure 2.2. Metabolomic analysis of Kopyor, normal mature, and young coconuts using GC-MS. (A) Water analysis: PCA score and loading plots based on 79 metabolites. (B) Flesh analysis: PCA score and loading plots based on 52 metabolites. (C) Venn diagram showing metabolite composition in water and flesh.

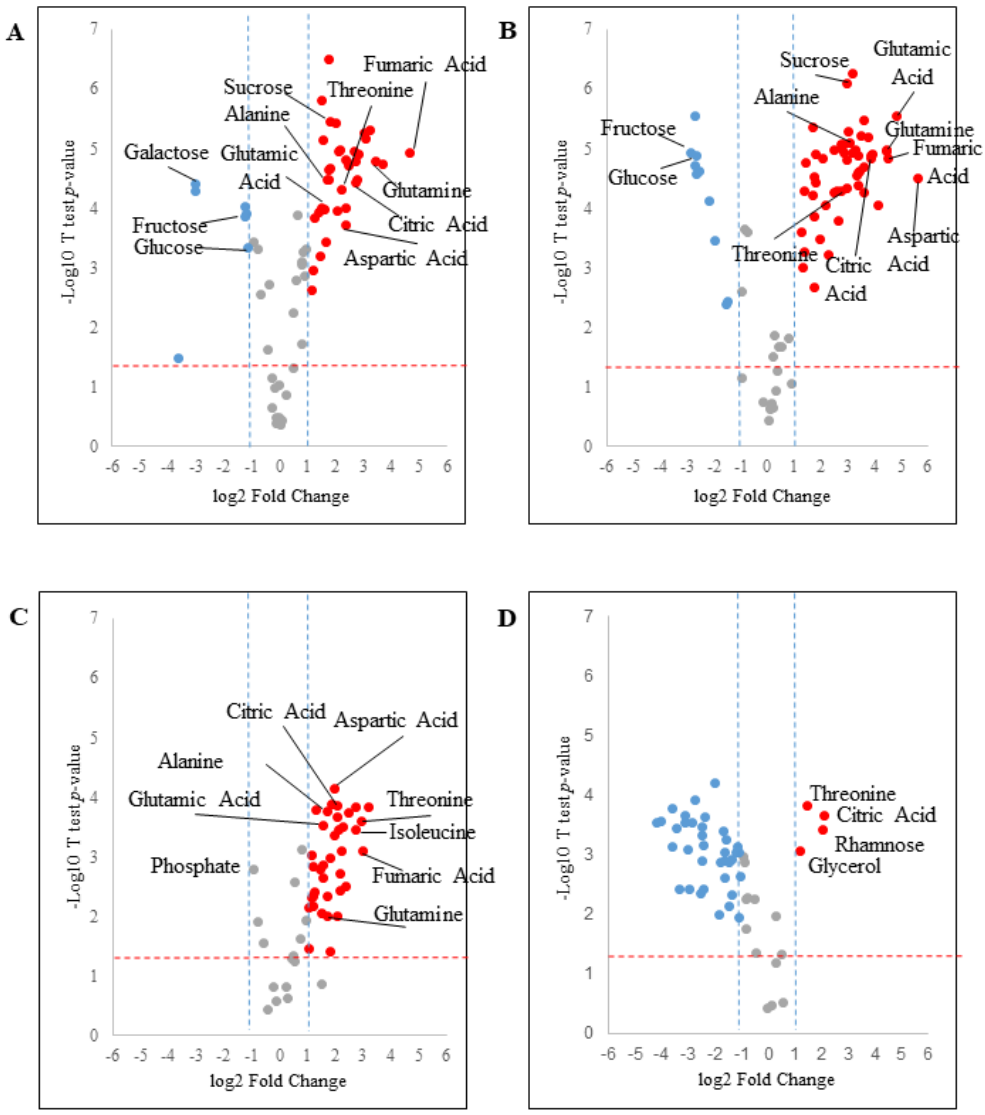

Figure 2.3. Differential analysis of metabolites in Kopyor water and flesh compared to mature and young coconuts. Volcano plots display fold changes (x-axis) and *p*-values (y-axis) from pairwise Student's t-tests. (A) Kopyor vs. mature coconut water, 67 metabolites had *p*-values < 0.05. (B) Kopyor vs. young coconut water, 62 metabolites showed *p*-values < 0.05. (C) Kopyor vs. mature coconut flesh, 37 metabolites had *p*-values < 0.05. (D) Kopyor vs. young coconut flesh, 40 metabolites had *p*-values < 0.05. The differential analysis of mature and young normal coconuts is presented in **Figure S1**.

Differential analysis identified significant metabolite differences, as shown in a volcano plot. Comparing Kopyor water to mature coconut water, 69 metabolites differed significantly

(*p*-value < 0.05), with 36 upregulated (log2 Fold Change > 1), 21 moderately changed, and 12 downregulated (log2 Fold Change < -1) (Figure 4A, Table S3). Similarly, 69 metabolites differed between Kopyor and young coconut water, with 52 higher in Kopyor (log2 Fold Change > 1) (Figure 4B, Table S4). Fumaric acid was abundant in Kopyor compared to mature coconut water, while aspartic acid was higher in Kopyor than in young coconut water. Kopyor water also had elevated levels of glutamine, citric acid, aspartic acid, threonine, alanine, and glutamic acid, contributing to flavor, but lower amounts of reducing sugars like fructose and glucose, with sucrose as the main sugar.

Significant differences were observed in the coconut flesh. Comparing Kopyor flesh to mature coconut flesh, 44 metabolites differed significantly (*p*-value < 0.05), with 36 metabolites higher in Kopyor (log2 Fold Change > 1), including amino acids like aspartic acid, fumaric acid, and glutamic acid. Kopyor flesh had higher sucrose content than mature coconuts but fewer metabolites than young coconut flesh. Of 48 significant metabolites, only glycerol, threonine, rhamnose, and citric acid were higher in Kopyor. These findings suggest more pronounced metabolic changes in Kopyor water compared to its flesh.

The differences in metabolite accumulation between Kopyor and normal coconut flesh and water were influenced endosperm type. Kopyor's unique endosperm with the breakdown of solid endosperm allowing more metabolites to diffuse into the water, enriching Kopyor water. Additionally, Kopyor's mutation, causing soft flesh due to galactomannan buildup, was indicated by lower galactose levels in Kopyor water compared to normal coconut water. Sucrose accumulation in Kopyor water was higher than in both young and mature normal coconut water, consistent with previous findings (Santoso et al., 1996). This results from disrupted endosperm metabolism in Kopyor coconuts, leading to reduced sucrose absorption by the embryo and greater sucrose accumulation compared to normal mature coconut water.

The influence of the maturation process may occur because Kopyor is a type of coconut that reaches a mature stage. As the liquid endosperm matures, it becomes richer in metabolites, leading to higher levels in Kopyor compared to young coconuts (Abraham & Mathew, 1963; Balasubramaniam, 1976; Sudha et al., 2019). Amino acid accumulation supports fruit growth and embryo development. However, this requires further investigation by comparing young coconuts with the potential to develop into Kopyor at maturity, such as young coconuts derived from Kopyor embryo culture with recessive genes, resulting in 100% kopyor from the outset.

2.3.2 Sensory evaluation of Kopyor and normal coconuts

Sensory analysis compared Kopyor coconuts with normal mature and young coconuts to objectively describe their characteristics. Young coconuts (6-7 months old) were included due to their popularity for fresh coconut water, while normal mature coconuts were used to compare endosperm types. Although the sensory attributes of young coconuts have been extensively studied, Kopyor's attributes had not been previously explored.

This study identified 32 sensory attributes for Kopyor water, covering taste, flavor, aroma, aftertaste, mouthfeel, and color, and 34 sensory attributes for Kopyor flesh, encompassing taste, flavor, aroma, aftertaste, mouthfeel, and appearance. The sensory wheel, illustrating these attributes, is shown in **Figure 2.4.**

The sensory profile of Kopyor water revealed a milky, nutty, creamy, and bitter taste, with oily, astringent, and salty aftertastes. Kopyor flesh was characterized by a nutty, creamy bitter, astringent taste, aroma of nutty, creamy, and coconut, with a white appearance, a soft, moist, and sandy texture. This characteristic is more comprehensive compared to the sensory attributes described by (Faramitha et al., 2024), which stated that Kopyor flesh possesses a white appearance, coconut aroma, and soft texture. These findings distinguish Kopyor from other elite coconuts, such as Macapuno and wax coconut from Indonesia. The FCP analysis, presented as a biplot in **Figure 2.5**, shows the sensory distinctions between Kopyor, normal

young, and mature coconuts. The sensory attributes provided in this study serve as a crucial reference for future research on elite coconuts.

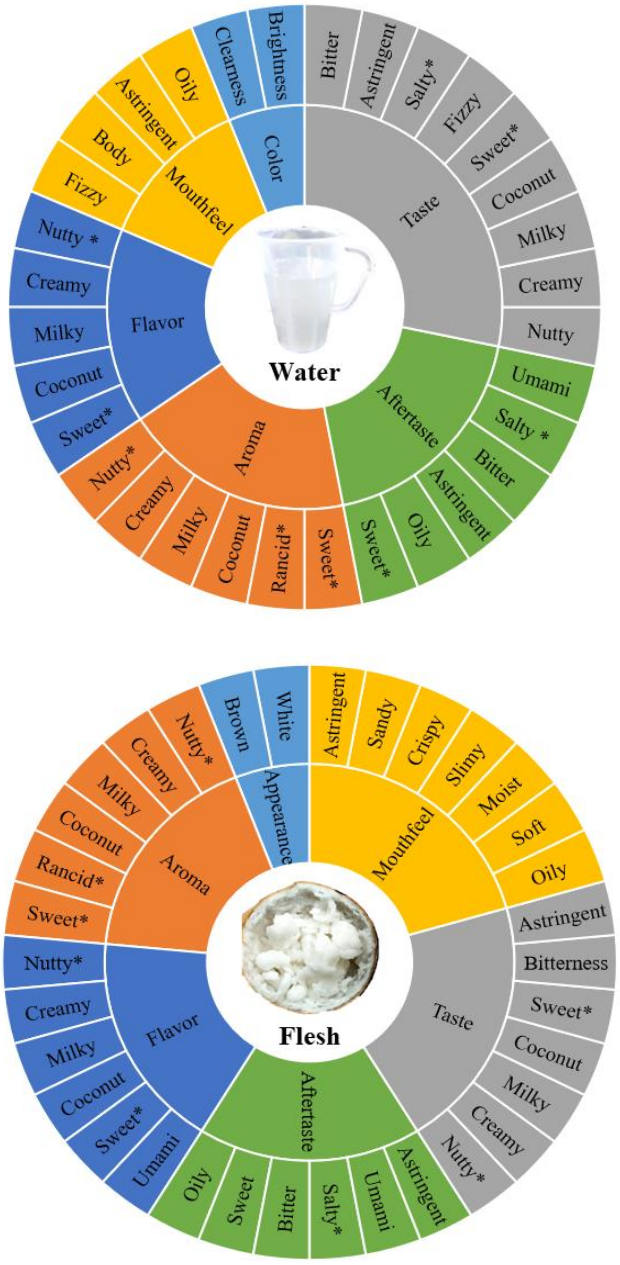

Figure 2.4. Sensory wheel of Kopyor illustrating 32 attributes for water (Upper part) and 34 for flesh (Below part). These attributes were developed through panel consensus based on a coconut lexicon, with additional input from normal coconut, virgin coconut oil, and coconut milk lexicons. Previously reported attributes are marked with asterisks (Adubofuor et al. (2016); Rachel (2013); Chowdhury et al. (2005); Villarino et al. (2007); Wattanapahu et al. (2012)).

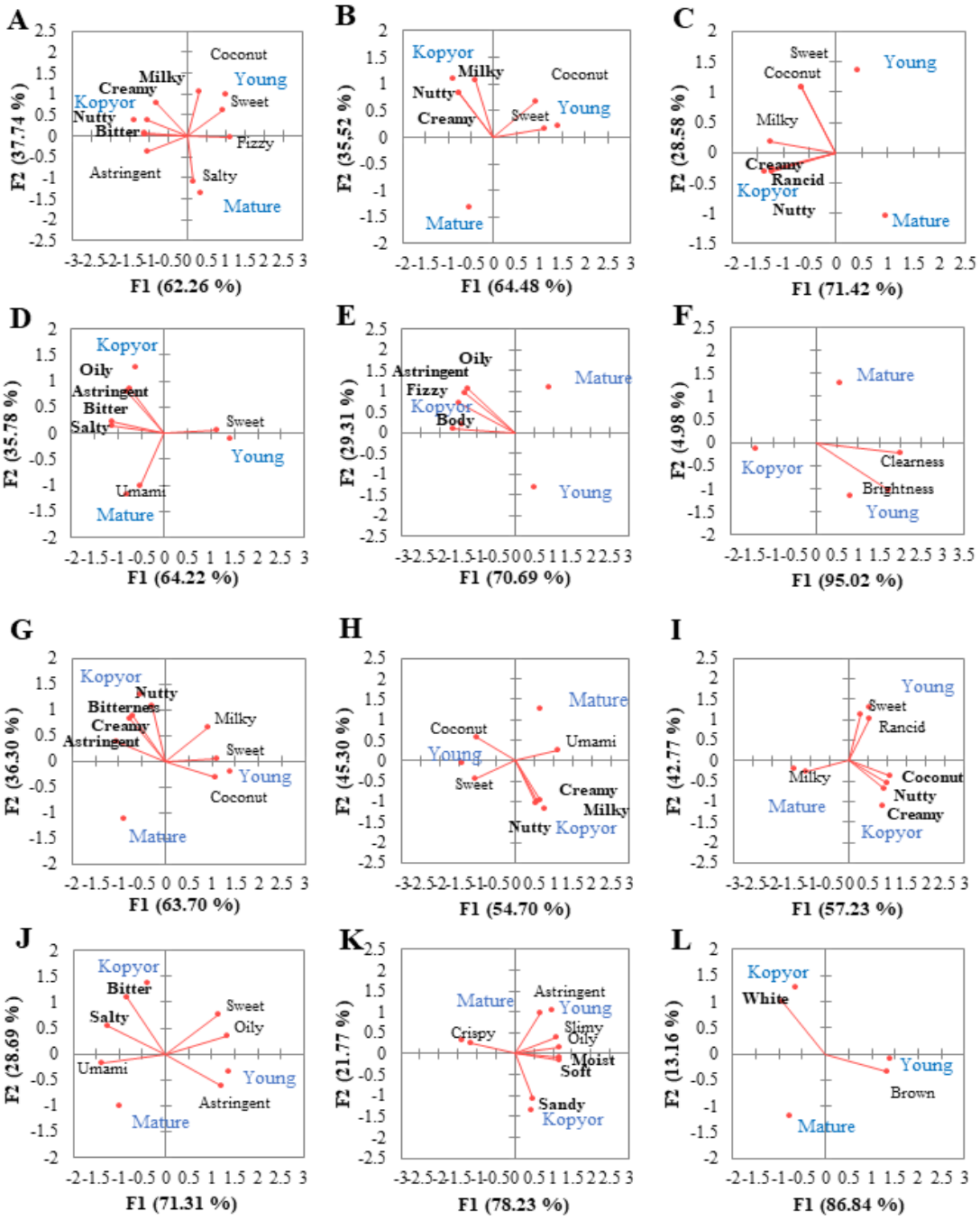

Figure 2.5. Biplot (F1 and F2 axes: 100%) of sensory data analysis for water and flesh from *Kopyor*, mature, and young coconuts. (1) Water, (2) Flesh, displaying attributes: (A) Taste of water, (B) flavor of water, (C) aroma of water, (D) aftertaste of water, (E) mouthfeel of water, (F) color of water, (G) taste of flesh, (H) flavor of flesh, (I) aroma of flesh, (J) aftertaste of flesh, (K) mouthfeel of flesh, (L) appearance of flesh. The biplot shows the separation of sensory attributes across different coconut types. Data was analyzed using Generalized Procrustean Analysis (GPA) via XLSTAT software.

2.3.3 OPLSR-based correlation between sensory evaluation and metabolite analysis

The correlation between sensory attributes and metabolite profiles was examined using OPLS-R to identify the metabolites responsible for specific sensory characteristics. It identified key metabolites responsible for the distinct sensory characteristics of Kopyor water, which has a unique milky, creamy, nutty, and bitter taste, linked to metabolites such as valine, 4-aminobutyric acid, and butanoic acid. The nutty taste is further driven by alanine, sucrose, and proline, while the rancid aroma is associated with fatty acids like butanoic acid. The oily, astringent, and fizzy mouthfeel of Kopyor water is influenced by glutamic acid and glycerol. Tables 2.1 presents the OPLSR results, highlighting the metabolites contributing to Kopyor water.

Table 2.1. Sensory attributes of Kopyor water and metabolites in Kopyor water (R^2-value (linearity), Q^2-value(robustness), RMSEE (prediction residual)

Number	Attributes	Latent Variable	R^2	Q^2	RMSEE	Metabolites
1	Taste Milky	1+1+0	0.991	0.984	0.04398	Valine, 4-Aminobutyric acid, Butanoic acid, Isoleucine, Leucine, Fumaric acid, 2-Aminoethanol, Allothreonine, Succinic acid, Phosphoric acid
2	Taste Creamy	1+1+0	0.994	0.99	0.04642	4-Aminobutyric acid, Isoleucine, Butanoic acid, Leucine, Allothreonine, 2-Aminoethanol, Fumaric acid, Valine, Glutamine, Succinic acid
3	Taste Nutty	1+1+0	0.995	0.992	0.05075	β-Alanine, Sucrose, Alanine, Palatinose, Serine, Inositol, Butane, Proline, Glutamic acid, Glycine
4	Taste Bitter	1+1+0	0.995	0.992	0.01525	β-alanine, Sucrose, Alanine, Palatinose, Butane, Inositol, Proline, Serine, Glycine, Aspartic acid
5	Flavor Nutty	1+1+0	0.994	0.991	0.04769	Glutamine, Isoleucine, Leucine, Butane, Glycine, Sucrose, Citric acid, Allothreonine, Inositol, Proline

Number	Attributes	Latent Variable	R^2	Q^2	RMSEE	Metabolites
6	Flavor Creamy	1+1+0	0.994	0.991	0.03975	Glutamine, Isoleucine, Leucine, Butane, Glycine, Sucrose, Citric acid, Allothreonine, Inositol, Proline
7	Aroma Creamy	1+1+0	0.994	0.990	0.04762	Isoleucine, Leucine, 4-Aminobutyric acid, Butanoic acid, Allothreonine, 2-Aminoethanol, Fumaric acid, Glutamine, Succinic acid, Citric acid
8	Aroma Rancid	1+1+0	0.993	0.989	0.02141	Valine, 4-Aminobutyric acid, Butanoic acid, Isoleucine, Leucine, Fumaric acid, 2-aminoethanol, Allothreonine, Succinic acid, Glutamine
9	Aroma Nutty	1+1+0	0.994	0.991	0.04823	Isoleucine, Leucine, Glutamine, Allothreonine, 2-Aminoethanol, Fumaric Acid, Butanoic Acid, Citric Acid, Glycine, 4-Aminobutyric Acid
10	Aftertaste Oily	1+1+0	0.995	0.989	0.03269	β-alanine, Alanine, Sucrose, Serine, Glutamic acid, Palatinose, Inositol, Butane, Proline, Aspartic acid
11	Aftertaste Astringent	1+1+0	0.995	0.993	0.03631	Glutamic acid, β-Alanine, Alanine, Serine, Sucrose, Palatinose, Inositol, Aspartic acid, Butane, Proline
12	Aftertaste Bitter	1+1+0	0.994	0.99	0.00902	Tetradecylglycerol, Lyxose, Ribose, Glycerol, Quinic acid, Lactulose, Trehalose, Meso erythritol, Sugar compound1, α-D-Xylopyranose
13	Aftertaste Salty	1+1+0	0.993	0.989	0.01488	Tetradecylglycerol, Lyxose, Trehalose, Ribose, Quinic acid, Glycerol, Unknown3, Lactulose, Meso erythritol, Gentiobiose
14	Mouthfeel Oily	1+1+0	0.995	0.989	0.037515	Lyxose, Lactulose, Glutamic acid, Glycerol, Ribose, α-D-Xylopyranose, Serine, Alanine, β-Alanine, Quinic acid

Number	Attributes	Latent Variable	R^2	Q^2	RMSEE	Metabolites
15	Mouthfeel Astringent	1+1+0	0.995	0.992	0.03381	Glutamic acid, Lactulose, Lyxose, Serine, Alanine, β-Alanine, Glycerol, α-D-Xylopyranose, Ribose, Sucrose
16	Mouthfeel Fizzy	1+1+0	0.995	0.993	0.00296	Glutamic acid, β-Alanine, Alanine, Serine, Sucrose, Palatinose, Inositol, Aspartic acid, Butane, Proline
17	Mouthfeel Body	1+1+0	0.993	0.99	0.05607	4-Aminobutyric acid, Butanoic acid, Isoleucine, Leucine, Valine, 2-Aminoethanol, Fumaric acid, Allothreonine, Glutamine

*Sensory attributes were selected based on the R^2 -values and Q^2 -values of the model. The model was developed using OPLSR. These metabolites were the ten highest VIP metabolites and those with scores over 1.0. These metabolites have positive coefficients for the attributes, indicating that they enhance these attributes.

For Kopyor flesh, the astringent taste is correlated with raffinose and glycerol, while its coconut aroma is linked to threonine and fumaric acid. The soft, moist, and sandy mouthfeel is associated with glycine, sucrose, and leucine, while citric acid contributes to the flesh's white color. This study provides the first scientific foundation for characterizing Kopyor coconuts by correlating their sensory attributes with metabolite profiles using OPLS-R analysis. Tables 2.2 detail the OPLS-R results, highlighting the metabolites contributing to Kopyor flesh characteristics.

Table 2.2. Sensory attributes of Kopyor flesh and metabolites in Kopyor flesh (R^2 -value(linearity), Q^2 -value(robustness), RMSEE (prediction residual)

No	Attributes	Latent Variable	R^2	Q^2	RMSEE	Metabolites
1	Taste Nutty	1+1+0	0.968	0.949	0.03820	Rhamnose, Citric acid, Threonine, Phenylalanine, Leucine, Sorbitol
2	Taste Bitter	1+1+0	0.965	0.944	0.03421	Citric acid, Rhamnose, Threonine, Sorbitol, Glycerol

No	Attributes	Latent Variable	R^2	Q^2	RMSEE	Metabolites
3	Taste Creamy	1+2+0	0.993	0.969	0.02383	Citric acid, Rhamnose, Threonine, Glutamine, Putrescine, Glycerol
4	Taste Astringent	1+2+0	0.996	0.977	0.01623	Raffinose, Maltose, Glycerol, Glutamine, Putrescine, Glutamic acid, Unknown1, Valine, Methionine
5	Flavor Creamy	1+1+0	0.967	0.948	0.10107	Citric acid, Rhamnose, Threonine, Phenylalanine, Sorbitol
6	Flavor Milky	1+1+0	0.968	0.949	0.09054	Rhamnose, Citric acid, Threonine, Phenylalanine, Leucine, Sorbitol
7	Flavor Nutty	1+1+0	0.968	0.949	0.05004	Rhamnose, Citric acid, Threonine, Phenylalanine, Leucine, Sorbitol
8	Aroma Coconut	1+1+0	0.968	0.95	0.05277	Threonine, Rhamnose, Phenylalanine, Leucine, Citric acid, Isoleucine, Glycine, Fumaric acid, Succinic acid, Proline
9	Aroma Nutty	1+1+0	0.968	0.95	0.02566	Threonine, Rhamnose, Citric acid, Phenylalanine, Leucine, Isoleucine, Glycine, Sorbitol, Succinic acid, Fumaric acid
10	Aroma Creamy	1+1+0	0.968	0.95	0.10532	Rhamnose, Threonine, Citric acid, Phenylalanine, Leucine, Isoleucine, Sorbitol, Glycine
11	Aftertaste Bitter	1+1+0	0.963	0.942	0.01227	Citric acid, Rhamnose, Threonine, Glycerol
12	Aftertaste Salty	1+2+0	0.996	0.977	0.00791	Glycerol
13	Mouthfeel Moist	1+2+0	0.984	0.953	0.179539	Glycine, Leucine, Isoleucine, Fumaric acid, Proline, Succinic acid, Phenylalanine. α-D-Glucopyranoside, Sucrose, Allothreonine
14	Mouthfeel Soft	1+1+0	0.962	0.942	0.19972	Leucine, Glycine, Isoleucine, Phenylalanine, Fumaric acid, Proline, Succinic acid, α-D-Glucopyranoside, Sucrose, Allothreonine
15	Mouthfeel Sandy	1+1+0	0.968	0.949	0.07194	Rhamnose, Citric acid, Threonine, Phenylalanine, Leucine, Sorbitol
16	Color White	1+1+0	0.965	0.944	0.03998	Citric acid, Rhamnose, Threonine, Sorbitol, Glycerol

*Sensory attributes were selected based on the R^2 -values and Q^2 -values of the models. The model was developed using OPLS-R. These metabolites were the ten highest VIP metabolites

and those with scores over 1.0. These metabolites have positive coefficients for the attributes, indicating that they enhance these attributes.

This analysis not only offers insights into the unique soft texture and mouthfeel traditionally associated with Kopyor coconuts but also serves as a scientific reference for other unique coconut varieties worldwide.

2.4 Conclusion

The findings revealed that Kopyor coconuts possess distinctive characteristics, both in terms of metabolomic analysis and sensory attributes, that differentiate them from normal mature and young coconuts. Metabolomic analysis showed that Kopyor contains a wider variety of metabolites, contributing to its sensory complexity. This study also marks the first sensory analysis of Kopyor endosperm. Additionally, the research confirmed that endosperm type significantly influences metabolite accumulation in Kopyor.

Chapter 3

Phenotypic Diversity of Kopyor (*Cocos nucifera* L. var. Kopyor): Insights from Metabolomics, Physicochemical, and Proximate Analyses

3.1 Introduction

Kopyor coconuts (*Cocos nucifera* L. var. Kopyor) exhibit phenotypic diversity, including variations in endosperm quantity (EQ) and variety (Rahayu et al., 2021; Setiawan et al., 2020). EQ refers to the amount of flesh separated from the endosperm, and studies have shown it can be used to classify kopyor coconuts. The EQ is controlled by a genetic mechanism known as duplicate dominant epistasis. It is measured on a scale from 1 to 9, with 1 indicating minimal kopyor content and 9 indicating a completely filled cavity (Maskromo et al., 2014). More research is needed to further explore EQ characteristics in Kopyor coconuts.

Kopyor coconuts come in several varieties, including Kopyor Green Dwarf (KGD), Kopyor Yellow Dwarf (KYD), and Kopyor Brown Dwarf (KBD) (Novarianto et al., 2014), which are distinguishable by the color of their exocarp. This makes it easier to identify Kopyor coconuts for trade based on their variety. These three varieties show high morphological diversity, with differences between them reaching 95% (Sudarsono et al., 2019).

The use of Kopyor remains limited due to insufficient research on its diverse phenotypic traits. With increasing consumer demand for health-conscious and functional foods driven by the rise in chronic diseases, researchers are beginning to explore the potential of underutilized foods like Kopyor (Baker et al., 2022; Liñán et al., 2019). Although coconut's benefits as a functional food are well-documented, the unique characteristics of Kopyor coconuts still need further investigation. Understanding its metabolite composition and phenotypic diversity is essential to fully realize Kopyor’s potential.

Metabolomics, a high-throughput technology, is used to study metabolite profiles across different phenotypes. In food and agriculture, it helps evaluate the effects of plant variety, nutrition, and environmental factors on metabolites, providing complex data to better understand food composition (Billet et al., 2018; Guo et al., 2008; Ikram et al., 2021). This information can improve crop traits, benefiting diet and health.

To explore the phenotypic diversity of Kopyor, metabolomics, along with proximate and physicochemical analyses, was utilized to address challenges in developing functional and sensory-rich food products. A key focus of this research is determining whether variety or endosperm quantity plays a more significant role in shaping Kopyor's unique characteristics, as well as identifying biomarkers that can provide insights into these traits.

3.2 Material and methods

4.3.1 Kopyor with phenotypic diversity samples

This study analyzed both liquid and solid endosperm from three Indonesian kopyor varieties: Kopyor Green Dwarf (KGD), Kopyor Yellow Dwarf (KYD), and Kopyor Brown Dwarf (KBD). The endosperm quantities (EQ) assessed were normal (0 kopyor) and at 10%, 20%, 30%, 40%, and 50%. EQ measures the amount of flesh detached from the coconut's endosperm or shell. The EQ classification follows a scale from 1 to 9, with 10% corresponding to a score of 2, 20% to 3, and so on. All samples, aged 11 months, were collected from Pati, Central Java, Indonesia, and stored at -30°C after harvest to preserve their quality.

Table 3.1. Sample information for Kopyor and normal coconut flesh and water analysis

Type of Coconut	Sample	Number of fruits
Normal	Normal Brown, Normal Green, Normal Yellow	7
Kopyor 10%	Kopyor Brown Dwarf, Kopyor Yellow Dwarf	3
Kopyor 20%	Kopyor Brown Dwarf, Kopyor Green Dwarf, Kopyor Yellow Dwarf	4
Kopyor 30%	Kopyor Green Dwarf, Kopyor Yellow Dwarf	3
Kopyor 40%	Kopyor Brown Dwarf, Kopyor Yellow Dwarf	4

Type of Coconut	Sample	Number of fruits
Kopyor 50%	Kopyor Brown Dwarf, Kopyor Green Dwarf, Kopyor Yellow Dwarf	3

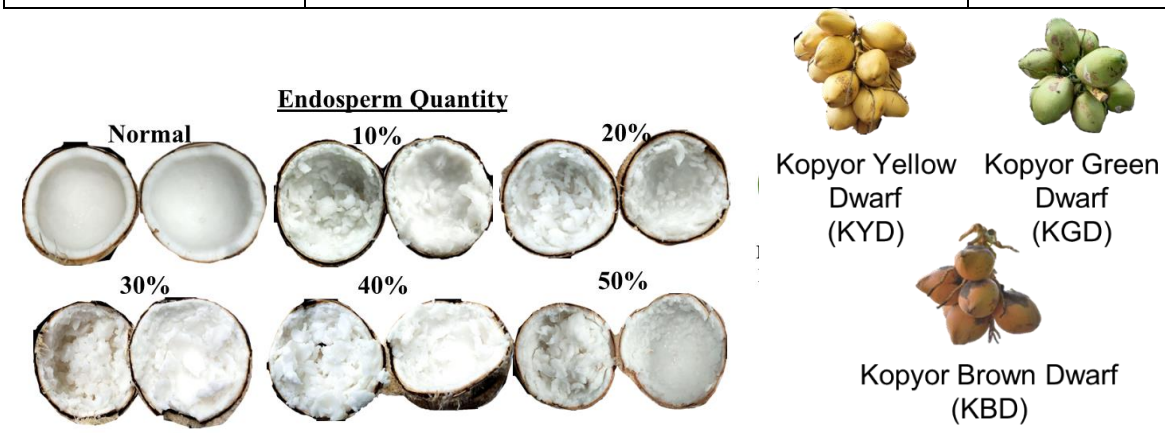

Figure. 3.1: Endosperm quantity (EQ) of normal coconut (0%) and Kopyor coconut with EQ levels of 10%, 20%, 30%, 40%, and 50% (left) and different Kopyor varieties: Kopyor Green Dwarf (KGD), Kopyor Yellow Dwarf (KYD), and Kopyor Brown Dwarf (KBD) (Right).

4.3.2 Metabolite analysis using Gas Chromatography-Mass Spectrometry (GC-MS)

For GC-MS analysis of Kopyor water and flesh, samples underwent extraction and derivatization. Lyophilized water (1 mL) and flesh (5 mg) were extracted using a solvent mixture (methanol, chloroform, water) in a 5:2:2 ratio, with ribitol as the internal standard. After vortex mixing and incubation at 37°C for 30 minutes, the samples were centrifuged at 10,000 rpm and 4°C. The supernatant was collected, mixed with ultrapure water, and centrifuged again. The final extract was concentrated before derivatization using MSTFA.

GC-MS analysis utilized a Shimadzu GCMS-QP2010 Ultra with an InertCap 5MS/NP column. The temperature program ranged from 80°C to 330°C, with samples injected at a split ratio of 25:1 and ionized at 70 eV. The spectra were recorded over m/z 85–500, with retention indices calculated using a standard alkane mixture for peak identification.

4.3.3 Physicochemical characterization of water and proximate analysis of flesh

In this study, the physicochemical properties of coconut water and proximate analysis of the flesh were compared between Kopyor and normal coconuts. Water properties were measured as follows: absorbance at 370 nm with a spectrophotometer, pH with a pH meter, electrical conductivity (EC) with an EC meter, and sweetness (Brix value) with a hand refractometer. Turbidity, indicating cloudiness from suspended particles, was assessed via absorbance. For the flesh, fat content was measured using Soxhlet extraction, crude fiber through acid-base hydrolysis, carbohydrates with specific methods, protein via the Kjeldahl method, ash content by dry ashing at 550°C, and moisture content through gravimetric drying at 105°C.

4.3.4 GC-MS analysis and data analysis

The raw data from the GC-MS analysis was first converted to .cdf format using GC-MS solution software (Shimadzu). These files were then transformed into .abf format with an Abf converter (Reifycs). MS-DIAL (version 4.00) was used for baseline correction, peak detection, denoising, alignment, and automatic compound annotation, utilizing RI and mass spectral data from GL-Science and NIST-11 libraries. Both automatic and manual annotations had a similarity threshold of 70%.

Before conducting multivariate analysis, metabolite data were normalized using an internal standard to adjust peak heights. Principal Component Analysis (PCA) with autoscaling and Orthogonal Projections to Latent Structures Regression (OPLSR) were performed using SIMCA-P version 13. One-way ANOVA and Tukey’s post hoc test were conducted using MetaboAnalyst 6.0 to compare group means with a significance threshold of $p < 0.05$. Pearson correlation analysis was also performed in GraphPad Prism 10. Additionally, physicochemical data were analyzed using one-way ANOVA and Tukey's post hoc test with MetaboAnalyst 6.0,

followed by Pearson correlation tests in GraphPad Prism 10, applying the same significance level of $p < 0.05$.

4.4 Results and discussion

4.3.1 Metabolite results from water and flesh based on GC-MS analysis

The PCA plot illustrates the distribution of Kopyor water samples based on principal component scores, with PC1 accounting for 43.9% of the variance and PC2 for 15.7% (**Figure 3.2.A.**). Using a GC-MS metabolomic approach, 41 annotated hydrophilic compounds were identified (see Table S1 for details). The plot reveals three distinct clusters: normal samples, a group of 10%, 20%, 30%, and a separate cluster for 40% and 50% EQ. This suggests that EQ levels, rather than cultivated variety, are key in differentiating samples. Higher EQ levels are linked to increased metabolites such as amino acids, organic acids, and sugars, causing distinct clustering.

A similar clustering pattern is observed in Kopyor flesh. The PCA analysis (**Figure 3.3.B.**) based on GC-MS identified 39 annotated metabolites, with details in Table S2. The PCA plot shows distinct clusters: normal samples, 10%, 20%, 30% clustering around negative PC1 and PC2, and 40%, 50% grouping on the positive side of PC1. Normal coconuts have a consistent metabolite profile, while Kopyor coconuts separate into clusters based on increasing EQ. As EQ rises, Kopyor flesh accumulates more amino acids, sugars, and organic acids compared to normal coconuts.

The three varieties in this study (KGD, KYD, and KBD) appear across all clusters in both water and flesh analysis, suggesting that varietal differences have minimal impact on the metabolite profile. Despite this, variations in EQ within each variety led to significant differences in metabolites, confirming that EQ plays a more crucial role in shaping the metabolomic profile of Kopyor coconuts than the specific variety. This study highlights EQ as a key factor influencing the unique metabolic composition of Kopyor coconuts, offering new

insights into their biochemical characteristics. To the best of our knowledge, this is the first study to establish a direct correlation between EQ and metabolite diversity in Kopyor coconuts.

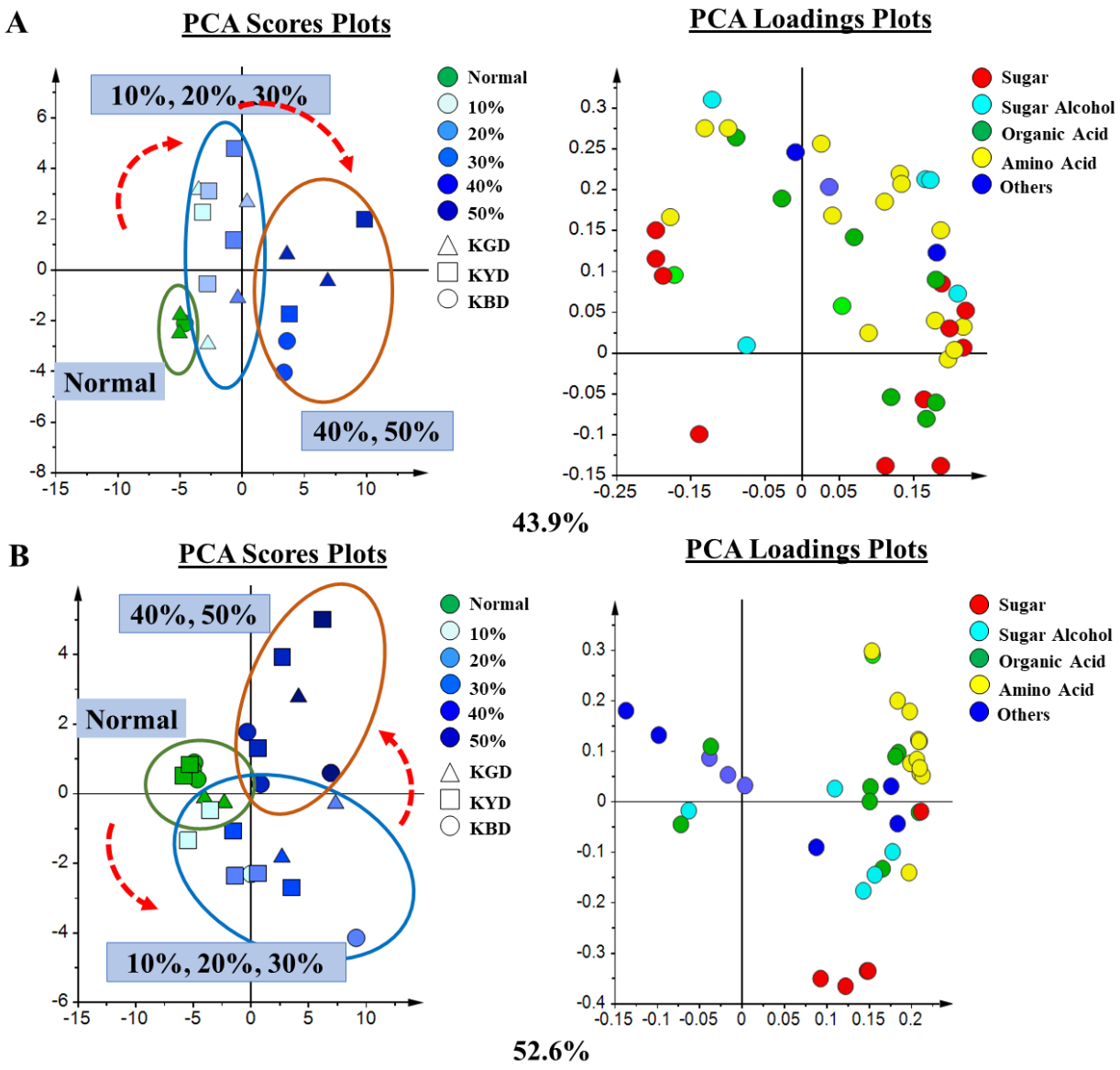

Figure. 3.2 (A) Water Analysis: A PCA based on 41 auto-scaled annotated metabolites from GC-MS analysis was used as explanatory variables. The score plot (Left) shows clear separation based on endosperm quantity in Kopyor. The loading plot (Right) illustrates the metabolites that contribute to this separation. (B) Flesh Analysis: The PCA was conducted using 39 auto-scaled annotated metabolites from GC-MS as explanatory variables. The score plot (Left) distinguishes Kopyor types by endosperm quantity, while the loading plot (Right) highlights the metabolites responsible for this differentiation.

4.3.2 Identification of important compounds in Kopyor water and flesh

Based on the PCA clustering patterns, further analysis was conducted to identify metabolites significantly affected by EQ in Kopyor. One-way ANOVA was performed to compare metabolite levels across different EQ groups. Significant differences ($p < 0.05$) were followed by Tukey's post-hoc test to pinpoint specific group differences. In the water samples, 21 out of 41 metabolites were significantly influenced by EQ, as detailed in Table S3. Pearson correlation analysis revealed that 16 metabolites had a significant correlation with EQ ($p < 0.05$), shown in Table S4. Five metabolites (citric acid, fructose, glucose, tagatose, and tyrosine) showed negative correlations, meaning their levels decreased as EQ increased, while 11 metabolites (including alanine, glutamic acid, sucrose, and valine) had positive correlations, indicating higher levels with increased EQ.

Galactose, glutamine, maltitol, pyroglutamic acid, and threonine were significantly impacted by EQ ($p < 0.05$) but did not show a clear correlation with increasing EQ ($p > 0.05$). Galactose remained low across all samples, while threonine levels increased, both independent of EQ. Among the metabolites that increased with higher EQ, valine stands out as an essential amino acid important for human health (Che et al., 2019; Kim et al., 2020; Reeds & Garlick, 2003). Glutamic acid, glycine, sucrose, and xylitol also followed this trend, known for enhancing food sensory properties (Bachmanov et al., 2016; Tanase et al., 2022). Additionally, gluconic acid, important for food preservation, and inositol, vital for cellular health (Ma et al., 2022), showed significant increases with EQ. These results emphasize the role of EQ in shaping Kopyor water's metabolomic profile. **Figure 3.3**. illustrates how valine, glutamic acid, glycine, sucrose, xylitol, gluconic acid, and inositol increase with higher EQ levels.

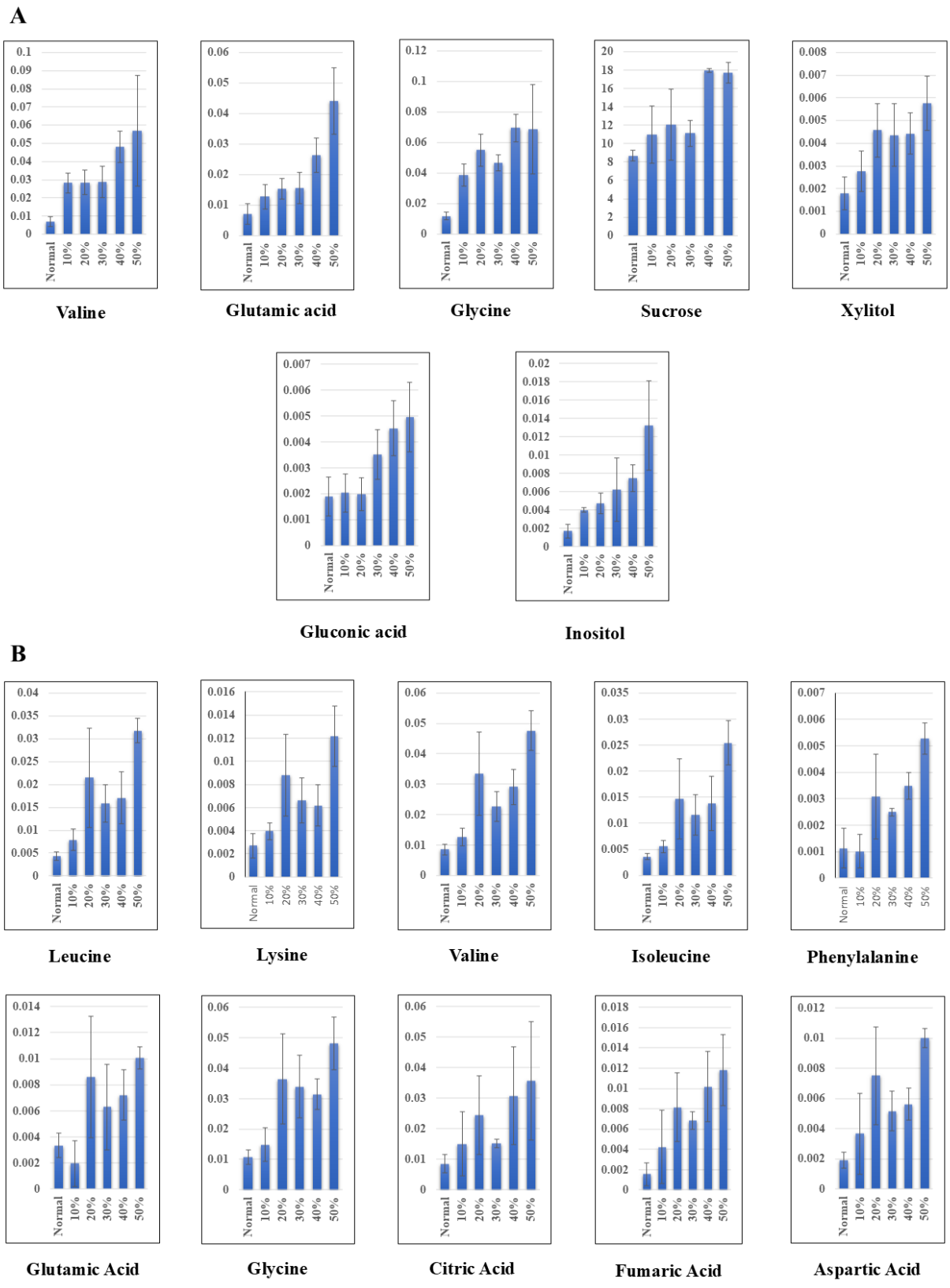

Figure. 3.3. Overview of key metabolite trends in water and flesh: (A) Metabolites in water and (B) metabolites in flesh were evaluated using One-Way ANOVA and Tukey's HSD test to identify significant differences.

In addition to the water analysis, ANOVA and Tukey's post-hoc test ($p < 0.05$) were applied to 39 annotated metabolites in Kopyor flesh to examine the impact of EQ on metabolite levels. The analysis identified 25 metabolites with significant differences based on EQ, as detailed in Table S5. Pearson correlation analysis ($p < 0.05$) further revealed that 17 metabolites were significantly correlated with increasing EQ, with details including *p*-values and correlation coefficients provided in Table S6.

Among the 17 identified metabolites, five metabolites namely isoleucine, leucine, lysine, phenylalanine, and valine are essential amino acids. Additionally, aspartic acid, glutamic acid, fumaric acid, glycine, and citric acid, known for enhancing sensory properties (Bachmanov et al., 2016; Tanase et al., 2022), were also detected. As shown in **Figure 3.3.**, the concentrations of these metabolites increase with rising EQ in the flesh. This indicates that Kopyor flesh with higher EQ not only contains more essential amino acids but also higher levels of sensory-related compounds, enhancing taste and flavor. Galactose, glucose, fructose, and phosphate levels were consistently low in kopyor flesh, regardless of EQ, as indicated by Pearson correlation results ($p > 0.05$, Table S7). This aligns with previous findings that Kopyor is low in phosphate (Yunindanova et al., 2024), which is advantageous since it does not promote embryo development, making it a more suitable food source.

OPLS regression analyses were performed on both water and flesh metabolite profiles to examine the relationship with EQ. As shown in **Figure 3.4.,** the regression for Kopyor water metabolites showed a strong model fit with an R^2 -value of 0.905, indicating that 90.5% of the variance in EQ could be explained. The Q^2 -value of 0.803 further demonstrated high predictive accuracy, explaining 80.3% of the variance during cross-validation. The Root Mean Square Error of Estimation (RMSEE) was 0.588, indicating good precision with low error. Similarly, **Figure 3.5.** shows the OPLS regression analysis for Kopyor coconut flesh based on metabolite profiles. The model had a strong fit with an R^2 -value of 0.862, explaining 86.2% of the variance

in EQ. The Q^2 -value of 0.859 demonstrated high predictive accuracy, accounting for 85.9% of the variance in cross-validation. The RMSEE was 7.103, reflecting the prediction error in the model.

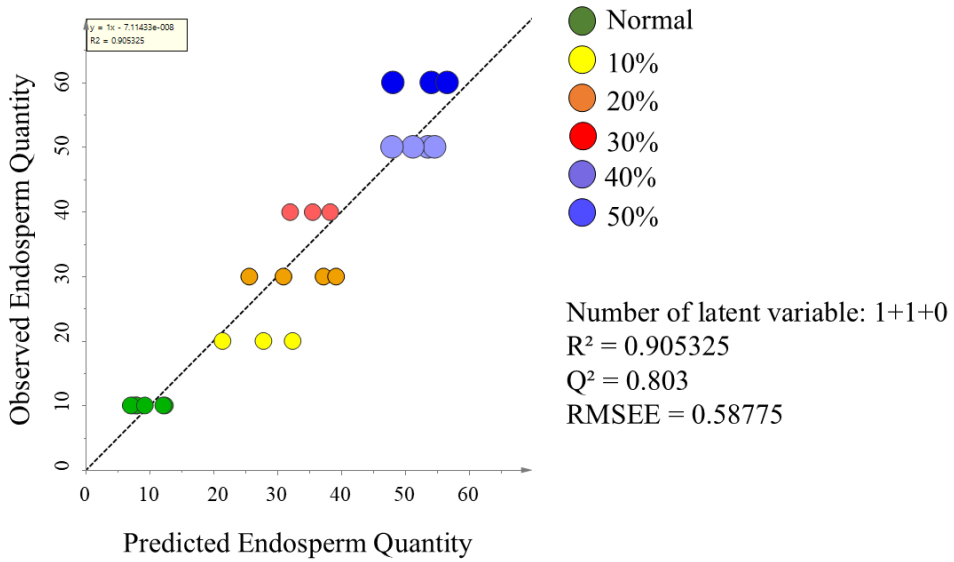

Figure 3.4. OPLS Regression analysis of the relationships between metabolomics profiles in water and endosperm quantity in kopyor

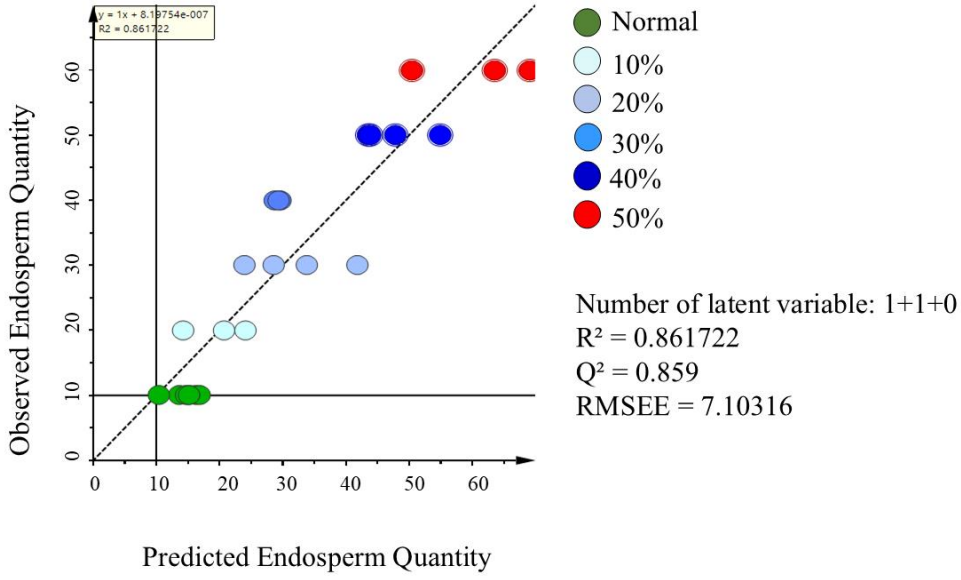

Figure 3.5. OPLS Regression analysis of the relationships between metabolomics profiles in flesh and endosperm quantity in kopyor

Both OPLS regression analyses identified several metabolites in water (**Table S8**) and flesh (**Table S9**) with VIP scores over 1 and positive coefficients. Notably, valine appeared consistently in both water and flesh, with a VIP score above 1 and positive coefficients. These results, supported by ANOVA, Tukey's test, and OPLS, highlight valine's key role in Kopyor coconuts based on EQ. Valine is the only compound consistently detected across all analyses, showing significant and consistent increases in both matrices. Thus, valine is suggested as a potential biomarker for endosperm quantity in Kopyor coconuts.

The hypothesis that valine levels increase with higher EQ stems from the role of coconut flesh (endosperm) as a nutrient reserve, where storage proteins like globulins are abundant, similar to those in other seeds. Globulins, making up to 40% of the protein content in coconut flesh, contain branched-chain amino acids like valine, which are prevalent in oilseed proteins. When these proteins break down, valine is released, raising its levels in the flesh or water (Chen et al., 2024; Kotecka-Majchrzak et al., 2020; Kwon et al., 1996). In Kopyor coconuts, the breakdown of flesh likely accelerates this process, as supported by proximate analysis showing lower total protein content due to increased protein degradation.

4.3.3 Physicochemical characteristics of water and proximate composition of flesh

This part investigates the correlation between metabolomics data, physicochemical properties, and proximate analysis, recognizing the practical importance of physicochemical assessments in the food industry for quality control, safety, nutrition, and product development. In Kopyor water, changes in absorbance, pH, Brix, and EC values correspond with variations in EQ. **Figure 3.6.A.** shows that absorbance increases from 0.59 in normal samples to 2.49 at the highest EQ, indicating a positive trend as endosperm development becomes more Kopyor.

Figure 3.6.B. shows an upward trend in pH values for Kopyor water, increasing from 5.57 in normal samples to between 6.30 and 6.53 for EQ levels 2 to 6, indicating a shift towards a more alkaline environment. This rise in pH aligns with changes in water composition as EQ

increases, potentially affecting taste. The Brix value, which indicates sweetness, shows a slight decline from 5.31 in normal samples to 4.98 at the highest EQ (**Figure 3.6.C.**), suggesting a decrease in sugar content. **Figure 3.6.D**. highlights an increase in electrical conductivity (EC) from 6.26 µS/cm in normal samples to 8.07 µS/cm at higher EQ, indicating a rise in ionic content, which enhances Kopyor water's potential value in the food industry.

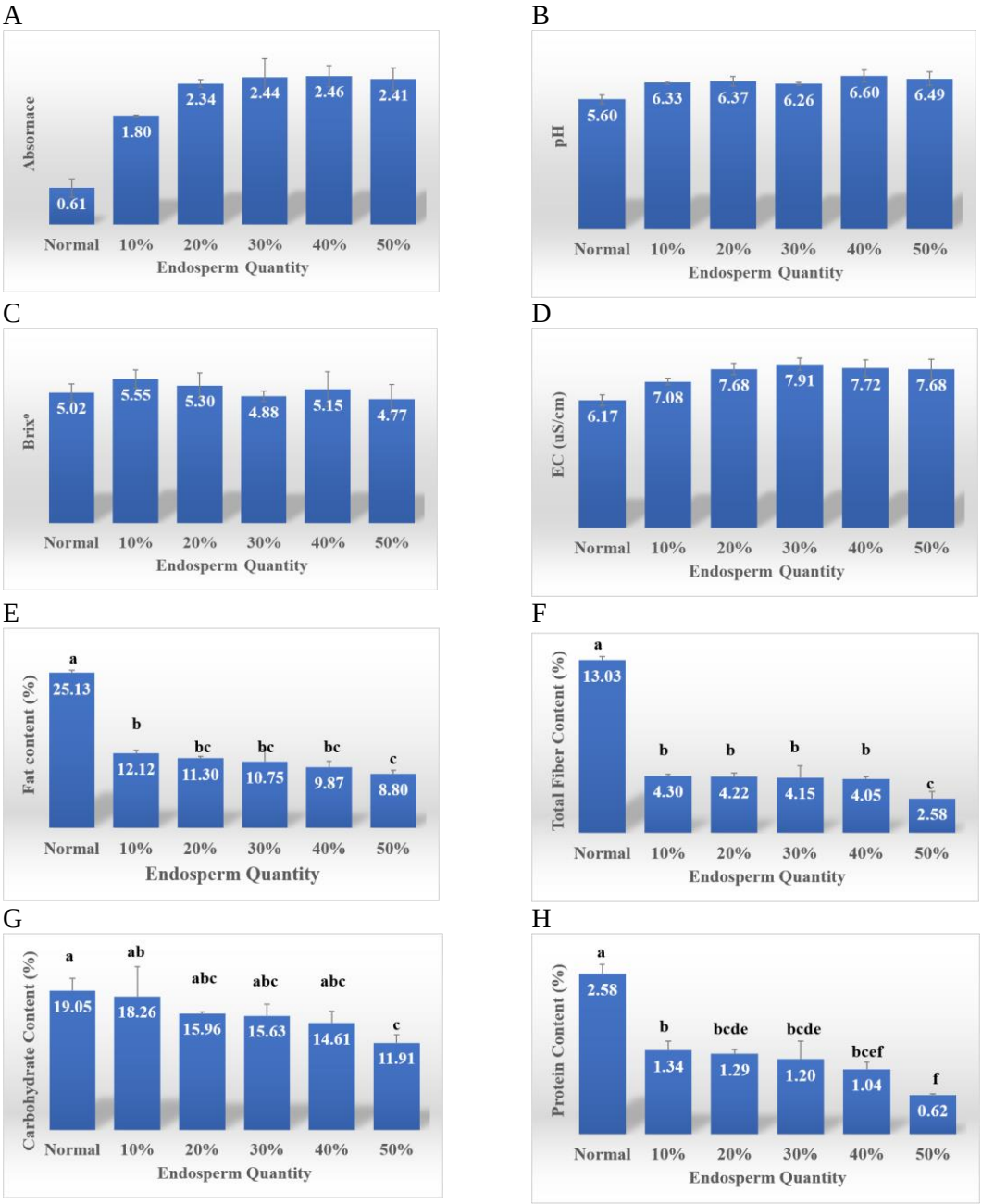

Figure 3.6. Effect of EQ on the physicochemical properties of water (A: absorbance, B: pH, C: Brix, D: electrical conductivity) and the proximate composition of flesh (E: fat content, F: total fiber content, G: carbohydrate content, H: protein content) in Kopyor coconut.

Proximate analysis of Kopyor flesh shows its nutritional composition, including fat, fiber, protein, and carbohydrates. **Figure 3.6.E.** highlights a decrease in fat content as EQ increases. Normal coconuts have the highest fat content at 25.13%, while Kopyor samples see a drop from 12.12% to 8.80% as EQ rises from 10% to 50%. These differences are statistically significant. The decline in fat suggests that endosperm modification affects lipid storage, where the majority of coconut fat is saturated, with 62–70% consisting of medium-chain (Bach & Babayan, 1982).

Figure 3.6.F. shows that total fiber content decreases significantly in Kopyor coconuts compared to normal ones. Normal coconuts have 13.03% fiber, while Kopyor coconuts range from 4.30% at 10% EQ to 2.58% at 50% EQ. This reduction is linked to lower mannan levels in Kopyor, due to decreased α-D-galactosidase enzyme activity. Mannan is a key component of soluble dietary fiber in coconuts (Saittagaroon et al., 1983).

Carbohydrate and protein levels in kopyor follow a similar pattern (**Figures 3.6.G. and 3.6.H.**), with normal coconuts having the highest amounts. There is a significant decline in both as EQ increases, especially at 50% EQ. After coconut milk extraction, the remaining coconut meal is rich in carbohydrates (43-45%), primarily mannose polysaccharides (61%). Other polysaccharides include cellulose and galactomannan (Balasubramaniam, 1976; Saittagaroon et al., 1983). Normal desiccated coconut contains about 5% protein (Kotecka-Majchrzak et al., 2020). In Kopyor, protein breakdown, indicated by rising amino acid levels like valine, reduces total protein content, as globulin proteins disintegrate into more easily absorbed amino acids. The reduction in proximate analysis values indicates the breakdown of large molecules into simpler metabolites, highlighting the potential for improved nutrient bioavailability.

4.3.4 The connection between physicochemical properties and proximate composition in relation to EQ

A Pearson correlation test was performed to analyze the relationship between EQ, water physicochemical properties, and flesh proximate composition. **Table 3.2.** shows significant correlations, including between EQ and flesh carbohydrate (p = 0.008), protein (p = 0.030), and ash content (p = 0.040). Additionally, Kopyor water absorbance is significantly correlated with EQ (p = 0.030). These results indicate that as EQ increases, there are notable changes in flesh composition and water absorbance.

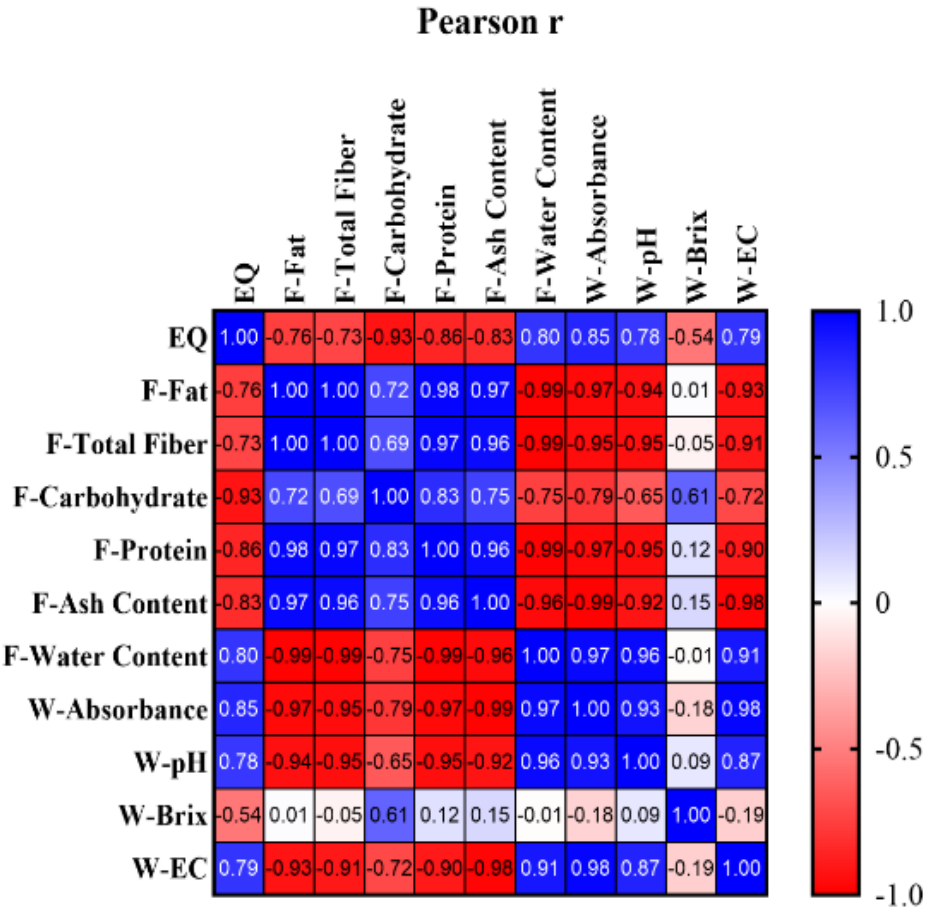

Figure 3.7. Pearson correlation coefficients (r) between endosperm quantity (EQ) and flesh proximate analysis and water physicochemical properties

The correlation coefficients in **Figure 3.7.** reveal a strong negative correlation between EQ and carbohydrate (r = -0.93), protein (r = -0.86), and ash content (r = -0.83) in the flesh, indicating that these components decrease as EQ increases. In contrast, a strong positive correlation exists between EQ and water absorbance (r = 0.85), showing that higher EQ corresponds with increased absorbance. Confidence intervals ($CI(r)$) for these correlations are provided in Table S10. Absorbance is key for maintaining consistency, visual appeal, and quality control in Kopyor coconut products. The study emphasizes the role of absorbance in indicating turbidity, an important quality marker, which complements traditional identification methods like shaking or knocking on the fruit. Although absorbance is measured after opening the coconut, it scientifically supports the effectiveness of local techniques based on turbidity.

Combining metabolomics, proximate, and physicochemical analyses offers valuable insights for Kopyor development in food and health, though further research is needed to assess the health benefits of these compounds.

Table 3.2. *p*-values for the correlation analysis between endosperm quantity (EQ) and flesh proximate analysis and water physicochemical properties

	EQ	F-Fat	F-Total Fiber	F-Carbohydrate	F-Protein	F-Ash Content	F-Water Content	W-Absorbance	W-pH	W-Brix	W-EC
EQ		0.079	0.097	0.008*	0.030*	0.040*	0.058	0.030*	0.066	0.272	0.059
F-Fat	0.079		0.000*	0.108	0.001*	0.001*	0.000*	0.002*	0.006*	0.987	0.008*
F-Total Fiber	0.097	0.000*		0.128	0.001*	0.003*	0.000*	0.003*	0.004*	0.919	0.012*
F-Carbohydrate	0.008*	0.108	0.128		0.043*	0.089	0.086	0.061	0.161	0.198	0.108
F-Protein	0.030*	0.001*	0.001*	0.043*		0.003*	0.000*	0.001*	0.004*	0.820	0.013*
F-Ash Content	0.040*	0.001*	0.003*	0.089	0.003*		0.002*	0.000*	0.009*	0.776	0.000*
F-Water Content	0.058	0.000*	0.000*	0.086	0.000*	0.002*		0.002*	0.002*	0.979	0.012*
W-Absorbance	0.030*	0.002*	0.003*	0.061	0.001*	0.000*	0.002*		0.008*	0.740	0.001*
W-pH	0.066	0.006*	0.004*	0.161	0.004*	0.009*	0.002*	0.008*		0.862	0.025*
W-Brix	0.272	0.987	0.919	0.198	0.820	0.776	0.979	0.740	0.862		0.720
W-EC		0.079	0.097	0.008*	0.030*	0.040*	0.058	0.030*	0.066	0.272	0.059

The asterisk (*) indicates that *p*-values less than 0.05 represent a statistically significant correlation.

4.4 Conclusion

The results demonstrated that endosperm quantity (EQ) had a stronger impact on metabolite accumulation than the variety of Kopyor. Higher EQ levels enhance metabolite accumulation in both the water and flesh. The breakdown of large molecules in Kopyor increases nutrient bioavailability. Valine (Val) is identified as a candidate biomarker for endosperm quantity in Kopyor coconuts.

Chapter 4

Metabolomics-Based Characterization and Sensory Analysis of Kopyor (*Cocos nucifera* L. var. Kopyor) Based on Cultivated Variety

4.4 Introduction

Kopyor coconut (*Cocos nucifera* L. var. Kopyor) is highly valued for its unique endosperm. This characteristic makes Kopyor coconuts particularly popular in the Indonesian market for various food and beverage applications (Rozaki et al., 2021). However, while previous research has highlighted the importance of endosperm quantity (EQ) in determining the quality and marketability of Kopyor coconuts, identifying EQ remains a challenge because it requires destructive testing, opening the fruit to measure it directly.

Given that Kopyor coconuts are typically sold whole for ease of transport and storage, it becomes impractical to rely on destructive methods for EQ determination. To address this, alternative methods for identifying cultivated varieties are crucial as the non-destructive method. Kopyor coconut varieties, such as Kopyor Dwarf Green (KDG), Kopyor Dwarf Yellow (KDY), and Kopyor Dwarf Brown (KDB), are more easily recognized from their external appearance. However, limited information is available about the metabolite profiles that differentiate these varieties, leaving a gap in our understanding of how metabolomics could support the identification of these products.

To better support the trade of Kopyor coconuts, it is essential to characterize these cultivated varieties in terms of their metabolomic and sensory attributes. This study aims to bridge this gap by conducting a comprehensive metabolomics-based characterization and sensory evaluation of Kopyor cultivated varieties. The sensory attributes used in this study are based on previous research by (Yunindanova et al., 2024), providing consistency in evaluating the sensory characteristics of Kopyor.

By combining metabolomics and sensory analysis, this research will offer insights into how plant variety influences both the biochemical composition and sensory appeal of Kopyor coconuts, helping to support the market demand for this unique product. The findings will be valuable for breeders, producers, and the food industry, providing a scientific basis for promoting Kopyor coconuts as a premium agricultural product.

4.4 Material and methods

4.3.1 Sample of Kopyor coconuts of three cultivated varieties

In this study, Kopyor coconuts of three cultivated varieties, Kopyor Green Dwarf (KGD), Kopyor Yellow Dwarf (KYD), and Kopyor Brown Dwarf (KBD) were selected as the plant material. The coconuts used were 11 months old and were sourced from Pati, Central Java, Indonesia. The analysis focused on both the water and flesh components of the endosperm, which are the edible parts of the coconut. After harvesting, the coconuts were opened, and the samples were immediately stored at -30°C to preserve their integrity before being subjected to further analysis.

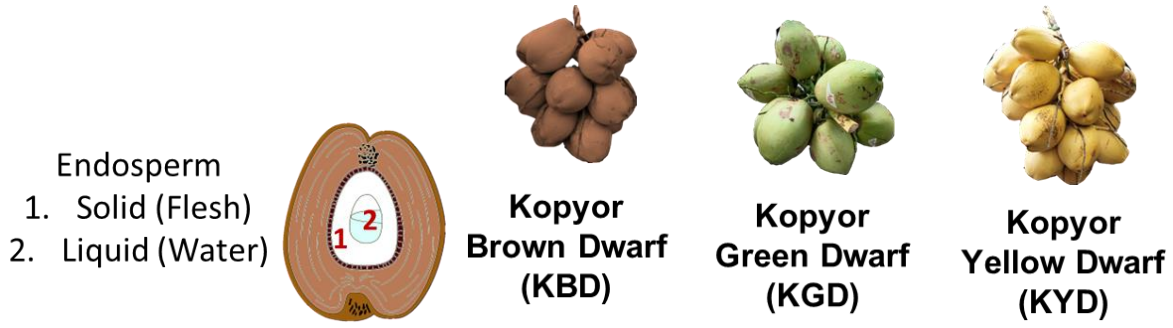

Figure 4.1. Plant varieties and edible endosperm components of Kopyor Coconuts. This figure illustrates three different varieties of kopyor coconuts, Kopyor Green Dwarf (KGD), Kopyor Yellow Dwarf (KYD), and Kopyor Brown Dwarf (KBD) alongside their edible components, including the water and flesh parts of the endosperm.

4.3.2 Sample preparation and GC-MS analysis

Coconut water and flesh were analyzed separately. One milliliter of coconut water was prepared per sample, while the flesh was freeze-dried, lyophilized in liquid nitrogen, and crushed into a homogeneous powder. Five milligrams of flesh powder were used for analysis. Both water and flesh were extracted using a methanol, water, and chloroform mixture (5:2:2 v/v/v), with ribitol as the internal standard. After vortexing and incubating the samples, they were centrifuged to separate solids from the liquid. The extracts were collected and processed further, with derivatization based on a previous study.

GC-MS analysis was performed using a GC-MS-QP2010 Ultra (Shimadzu) with an AOC-20i/s autoinjector. The system was equipped with an InertCap 5MS/NP column (35 m length, 0.18 mm I.D., and 0.18 mm film thickness). For the flesh samples, a single analysis was done, while for water samples, two analyses (with filament on and off) were conducted to exclude the sucrose peak. Samples were injected at 230°C with a 25:1 split ratio. The column temperature was ramped from 80°C to 330°C, with a carrier gas velocity of 39.0 cm/s. Electron ionization at 70 V generated ions, with spectra recorded over m/z 85-500. Retention indices were calculated using a C10-C40 alkane mixture.

4.3.3 Sensory evaluation using Free Choice Profiling (FCP)

The method used in this research is Free Choice Profiling (FCP), a descriptive sensory analysis technique, consistent with the approach in **Chapter 1**. The sensory attributes identified in Chapter 1, which consist of 32 attributes for both Kopyor water and 34 attributes for flesh, were applied in Chapter 4, ensuring a systematic and coherent approach throughout. FCP allows panelists to use their own terms to describe sensory attributes, making it ideal for novel products like Kopyor coconut, where no expert panelists or standards exist. In this study, 21 panelists completed 3 replications for reliable results. The materials used were the same as those analyzed in the metabolomics study, providing a link between sensory attributes and

chemical composition. The evaluation involved three steps: an attribute generation session where panelists described the sensory characteristics of Kopyor flesh and water, followed by a rating session where they scored these attributes, and finally, analysis using statistical tools.

The attributes generation session for Kopyor coconut water identified 32 sensory attributes, categorized into color, aroma, taste, mouthfeel, flavor, and aftertaste. The color of the water is described by attributes like brightness and clearness. Aromatic qualities include descriptors such as nutty, creamy, milky, coconut, rancid, and sweet. The taste is characterized by attributes such as nutty, creamy, milky, coconut, sweet, fizzy, salty, astringent, and bitter. The mouthfeel of the coconut water is described by sensations like oily, astringent, body, and fizzy. The flavor profile includes nutty, creamy, milky, coconut, and sweet notes. The aftertaste is captured by attributes such as sweet, oily, astringent, bitter, salty, and umami.

The attributes generation session for Kopyor coconut flesh identified 34 key sensory attributes. These attributes are divided into several categories: appearance, aroma, taste, mouthfeel, flavor, and aftertaste. The appearance is described by the colors white and chocolate. The aroma includes descriptors such as nutty, creamy, milky, coconut, rancid, and sweet. In terms of taste, the coconut flesh can be characterized by flavors like nutty, creamy, milky, coconut, sweet, bitterness, and astringent. The mouthfeel attributes encompass sensations like oily, soft, moist, slimy, crispy, sandy, and astringent. The flavor profile consists of nutty, creamy, milky, coconut, sweet, and umami notes. Additionally, the aftertaste is described by sensations such as oily, sweet, bitter, salty, umami, and astringent.

4.3.4 Data analysis of sensory evaluation and GC-MS results

Sensory data were analyzed using Generalized Procrustes Analysis (GPA) in XLSTAT to cluster terms and identify shared attributes. For GC-MS data, raw files were converted to CDF and ABF formats, followed by baseline correction, peak detection, and alignment in MS-DIAL (v4.00). Compound annotation was conducted using GL-Science and NIST-11 mass

spectral libraries with a 70% similarity threshold. Metabolites with a relative standard deviation below 30% were selected, and peak heights were normalized using an internal standard.

Principal component analysis (PCA) was used to identify patterns in the metabolomic data, while Orthogonal Projection to Latent Structures Regression (OPLS-R) was employed to correlate sensory and metabolite data. Both PCA and OPLS-R were performed in SIMCA-P (v13). One-way ANOVA with Tukey's post-hoc test ($p < 0.05$) and heat map generation were carried out in MetaboAnalyst 6.0, with metabolites normalized to ribitol. Pearson correlation analysis was performed using GraphPad Prism 10.

4.4 Result and discussion

4.3.1 Metabolite results from water and flesh based on GC-MS analysis by plant cultivated variety

The PCA results for the GC-MS analysis of kopyor water from different cultivated varieties (KBD, KGD, and KYD) reveal distinct clustering patterns (**Figure 4.2.A**). The score plot shows the distribution of samples based on the first two principal components (PC1 and PC2), which explain 56% and 19.6% of the total variance, respectively. These distinct clusters indicate significant differences in the metabolite profiles of each variety. KYD is positioned on the positive side of PC1, while KBD and KGD are on the negative side. KBD and KGD are further separated along PC2, indicating additional variation between these two varieties. The loading plot reveals that KYD has a higher accumulation of metabolites, especially amino acids, in the water. Other metabolites, including organic acids, sugars, and sugar alcohols, also show higher accumulation in KYD, contributing to the observed separation in the PCA score plot.

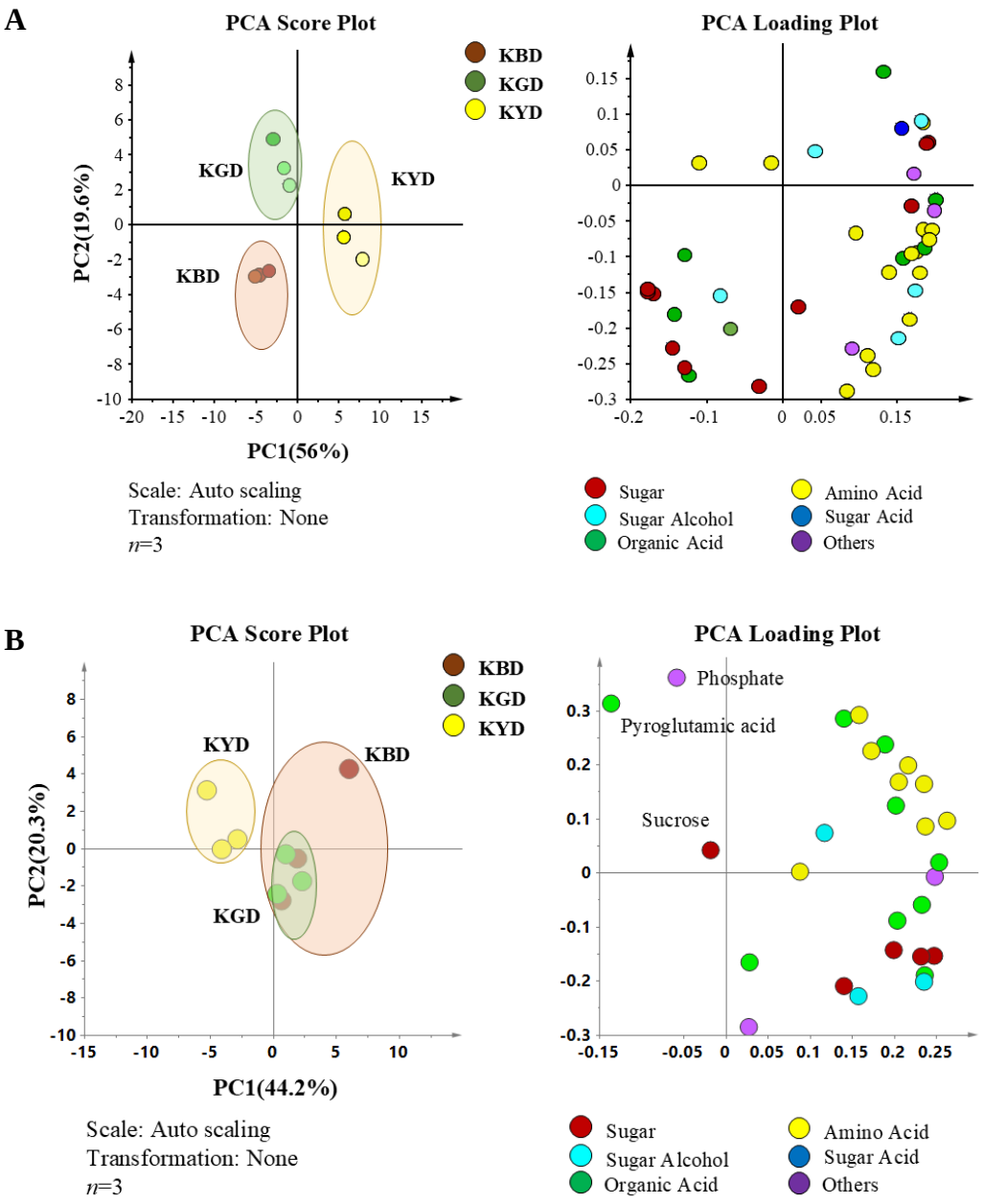

Figure 4.2. Metabolomic analysis of water and flesh from Kopyor coconuts of different cultivated varieties using GC-MS. (A) Water analysis: PCA was performed using 44 auto-scaled annotated metabolites derived from GC-MS analysis. The left panel shows the score plot, while the right panel displays the loading plot, indicating the metabolites contributing to the separation observed in the score plot. (B) Flesh analysis: PCA was conducted using 28 auto-scaled annotated metabolites from GC-MS analysis. The left panel represents the score plot, and the right panel illustrates the loading plot, corresponding to the separation shown in the score plot.

A different pattern is observed between the metabolomic profiles of kopyor coconut flesh and water. Firstly, the PCA results indicate that the metabolomic differences in water are explained to a greater extent compared to the flesh. In the flesh **(Figure 4.2.B)**, PC1 accounts for 44.2% of the variance, while PC2 explains 20.3%. Secondly, in terms of clustering, although KBD and KGD group together, both are located on the positive side of PC1, while KYD is positioned on the negative side of PC1. This pattern contrasts with the PCA clustering observed in the water. Despite this difference, the score plot clearly illustrates a distinct separation between the metabolomic profiles of the different Kopyor varieties. The loading plot, based on 28 auto-scaled annotated metabolites, identifies the metabolites contributing to this variance. KBD shows a higher accumulation of amino acids, sugars, organic acids, and sugar alcohols. Meanwhile, KGD is characterized by a greater accumulation of sucrose, and KYD displays higher levels of phosphate and pyroglutamic acid. This pattern is also reflected in the heatmap. This inverse relationship, where varieties that accumulate more metabolites in the flesh accumulate fewer in the water, and vice versa, highlights the significant metabolic variations between Kopyor varieties.

4.3.2 Identification of key metabolites in the flesh and water of three Kopyor coconut varieties

After conducting a PCA to observe the distribution of compounds across the three Kopyor coconut varieties and to identify key metabolites, a heatmap analysis and ANOVA test were performed. The heatmap, as shown in **Figure 4.3**, provides a detailed visualization of metabolite profiles in Kopyor coconut water (A) and flesh (B) from three different varieties. The clustering of metabolites reveals distinct patterns between the varieties, suggesting that specific metabolites are differentially regulated based on the Kopyor variety. This differential metabolite expression indicates variety-dependent biochemical pathways that may influence the flavor, nutritional content, or other biochemical properties of Kopyor coconut.

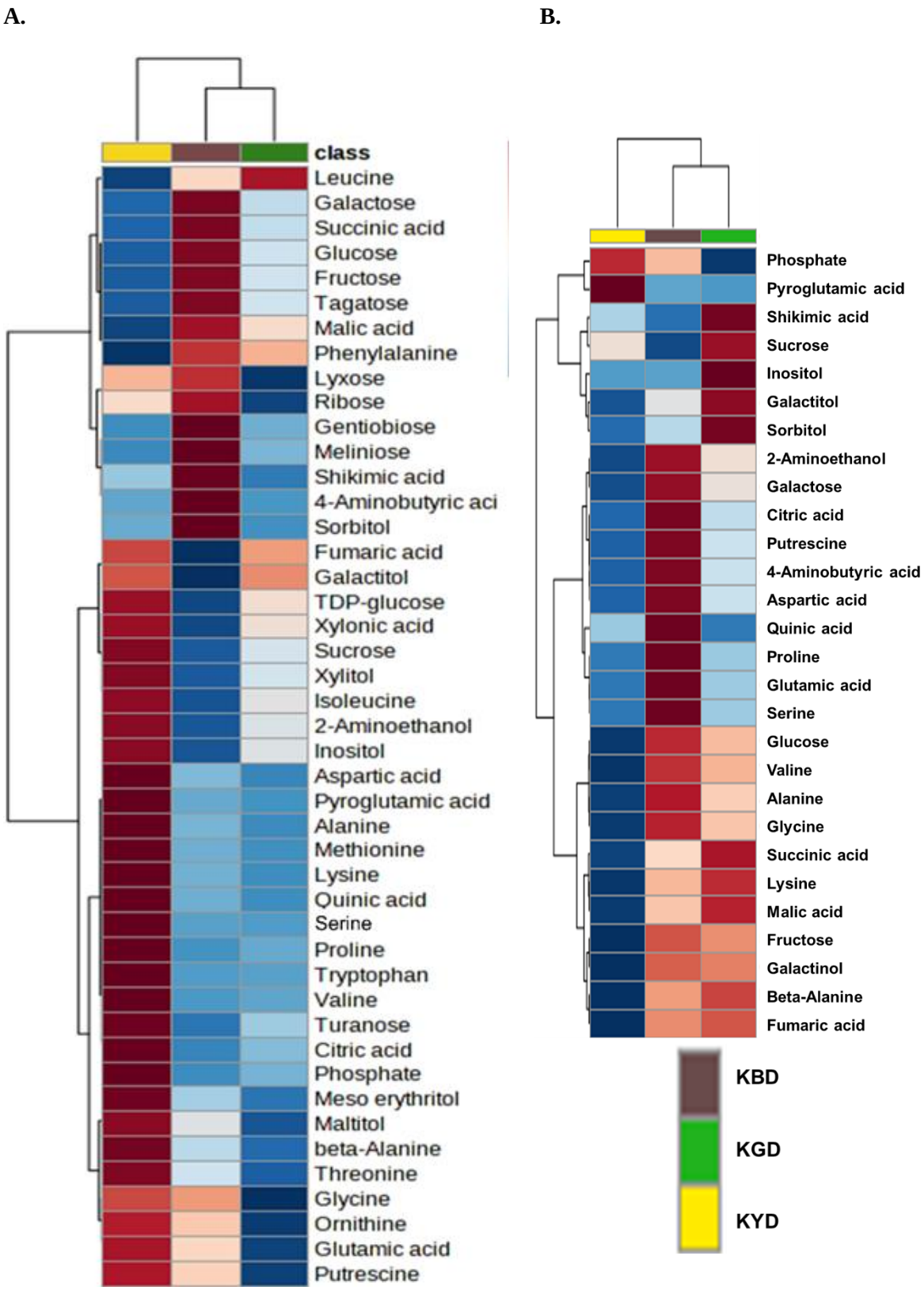

Figure 4.3. Heatmap analysis of metabolite profiles in Kopyor coconut water (A) and flesh (B) from three different varieties. The color classes indicate the varieties. The red to blue color gradient on the heatmap indicates the relative intensity levels.

Table 4.1. Metabolite analysis of water from three Kopyor varieties with significant differences based on ANOVA and Tukey's HSD Test

No	Metabolite	*F*-value	*p*-value	Tukey's HSD
1	Gentiobiose	401.63	0.000	KGD-KBD; KYD-KBD
2	Melibiose	346.32	0.000	KGD-KBD; KYD-KBD
3	Phosphate	312.35	0.000	KYD-KBD; KYD-KGD
4	Glucose	271.26	0.000	KGD-KBD; KYD-KBD; KYD-KGD
5	Citric acid	261.43	0.000	KGD-KBD; KYD-KBD; KYD-KGD
6	Fructose	184.18	0.000	KGD-KBD; KYD-KBD; KYD-KGD
7	Tagatose	159.45	0.000	KGD-KBD; KYD-KBD; KYD-KGD
8	4-Aminobutyric acid	159.12	0.000	KGD-KBD; KYD-KBD
9	Tryptophan	93.309	0.000	KYD-KBD; KYD-KGD
10	Pyroglutamic acid	44.927	0.000	KYD-KBD; KYD-KGD
11	Inositol	29.65	0.001	KGD-KBD; KYD-KBD; KYD-KGD
12	Galactose	29.505	0.001	KGD-KBD; KYD-KBD
13	Valine	25.447	0.001	KYD-KBD; KYD-KGD
14	Glycine	24.116	0.001	KGD-KBD; KYD-KGD
15	Isoleucine	23.888	0.001	KGD-KBD; KYD-KBD; KYD-KGD
16	Sucrose	23.558	0.001	KYD-KBD; KYD-KGD
17	Quinic acid	21.836	0.002	KYD-KBD; KYD-KGD
18	Proline	19.08	0.003	KYD-KBD; KYD-KGD
19	Xylitol	17.631	0.003	KYD-KBD; KYD-KGD
20	Maltitol	17.105	0.003	KYD-KBD; KYD-KGD
21	Serine	17.063	0.003	KYD-KBD; KYD-KGD
22	β-Alanine	16.894	0.003	KYD-KBD; KYD-KGD
23	Meso erythritol	14.533	0.005	KYD-KBD; KYD-KGD
24	Ornithine	12.164	0.008	KGD-KBD; KYD-KGD
25	Lysine	11.105	0.010	KYD-KBD; KYD-KGD
26	Aspartic acid	10.394	0.011	KYD-KBD; KYD-KGD
27	Methionine	10.123	0.012	KYD-KBD; KYD-KGD
28	Ribose	9.0858	0.015	KGD-KBD
29	Succinic acid	8.611	0.017	KYD-KBD

Aside from the heat map analysis, **Table 4.1**. provides a comprehensive overview of the metabolites that significantly differ among the three Kopyor coconut water varieties, as determined by ANOVA and Tukey’s HSD test. This table identifies 29 metabolites with statistically significant differences between the varieties. Each metabolite is accompanied by

its respective *F*-value and *p*-value, quantifying the level of variance and statistical significance. Highly significant compounds such as Gentiobiose, Melibiose, Phosphate, and Glucose demonstrate substantial differences between the varieties, as evidenced by notably low *p*-values. Furthermore, Tukey's HSD test results, detailed in the final column, illustrate the specific pairwise comparisons where these significant differences occur among the three varieties (KGD, KBD, KYD).

Table 4.2. Metabolite analysis of flesh from three Kopyor varieties with significant differences based on ANOVA and Tukey's HSD Test

No	Metabolite	*F*-value	*p*-value	Tukey's HSD
1	Fructose	91.795	0.000	KYD-KBD; KYD-KGD
2	Glucose	50.068	0.000	KYD-KBD; KYD-KGD
3	Fumaric acid	18.046	0.003	KYD-KBD; KYD-KGD
4	Galactitol	11.144	0.010	KYD-KGD
5	4-Aminobutyric acid	10.98	0.010	KYD-KBD
6	2-Aminoethanol	10.503	0.011	KYD-KBD
7	Sorbitol	10.394	0.011	KYD-KGD
8	Galactose	9.1481	0.015	KYD-KBD
9	Galactinol	9.0485	0.015	KYD-KBD; KYD-KGD
10	Glutamic acid	8.293	0.019	KYD-KBD

In contrast to the 29 significantly different metabolites identified in the water of kopyor coconut varieties, only 10 metabolites were found to differ significantly in the flesh, as shown in **Table 4.2.** This observation is consistent with the findings in **Chapter 2**, which noted that the differences in metabolite compounds are more pronounced in Kopyor coconut water than in the flesh. Each metabolite listed in **Table 4.2.** is accompanied by an *F*-value and *p*-value, indicating the degree of variance and the statistical significance of the differences across the varieties. Notably, compounds such as fructose, glucose, and fumaric acid exhibit highly significant differences, as reflected by their low *p*-values. Tukey's HSD test results provide

further insight into specific pairwise comparisons between the three varieties (KGD, KBD, KYD) where significant differences were detected.

4.3.3 Sensory analysis of three Kopyor coconut varieties based on FCP

The sensory evaluation using FCP reveals distinct profiles for the three Kopyor coconut water varieties, as shown in the biplot data from **Figure 4.3. (A, B, C, D, E, F)**. KGD water is characterized by a nutty, milky, and slightly bitter taste, with a sweet, creamy coconut flavor, and a full-bodied mouthfeel, noted for its brightness. KYD water has a more astringent, salty taste with an umami aftertaste and a fizzy mouthfeel. KBD water offers a sweet, coconut, creamy taste but is marked by a rancid aroma and a salty, bitter aftertaste, with a clear appearance.

The sensory evaluation of Kopyor flesh, based on the biplot data in **Figure 4.3 (G, H, I, J, K, L)**, highlights distinct characteristics of flesh among the three varieties. KGD flesh is sweet, with a milky flavor and an oily aftertaste, and has a slimy, moist, soft texture. KYD flesh has a coconut and astringent taste, with umami and coconut flavors, a sweet milky aroma, an oily, astringent mouthfeel, and a white color. KBD flesh presents a milky, bitter, creamy, and nutty taste, with a nutty flavor, a rancid aroma, and an aftertaste that combines salty, bitter, umami, astringent, and sweet notes.

The sensory evaluation of both the flesh and water reveals distinct characteristics unique to each Kopyor variety. These variations suggest that each variety holds potential for targeted applications based on its sensory profile. The key next step is to investigate the underlying factors driving these sensory differences. A correlation analysis will be conducted to identify the metabolites responsible for the sensory attributes.

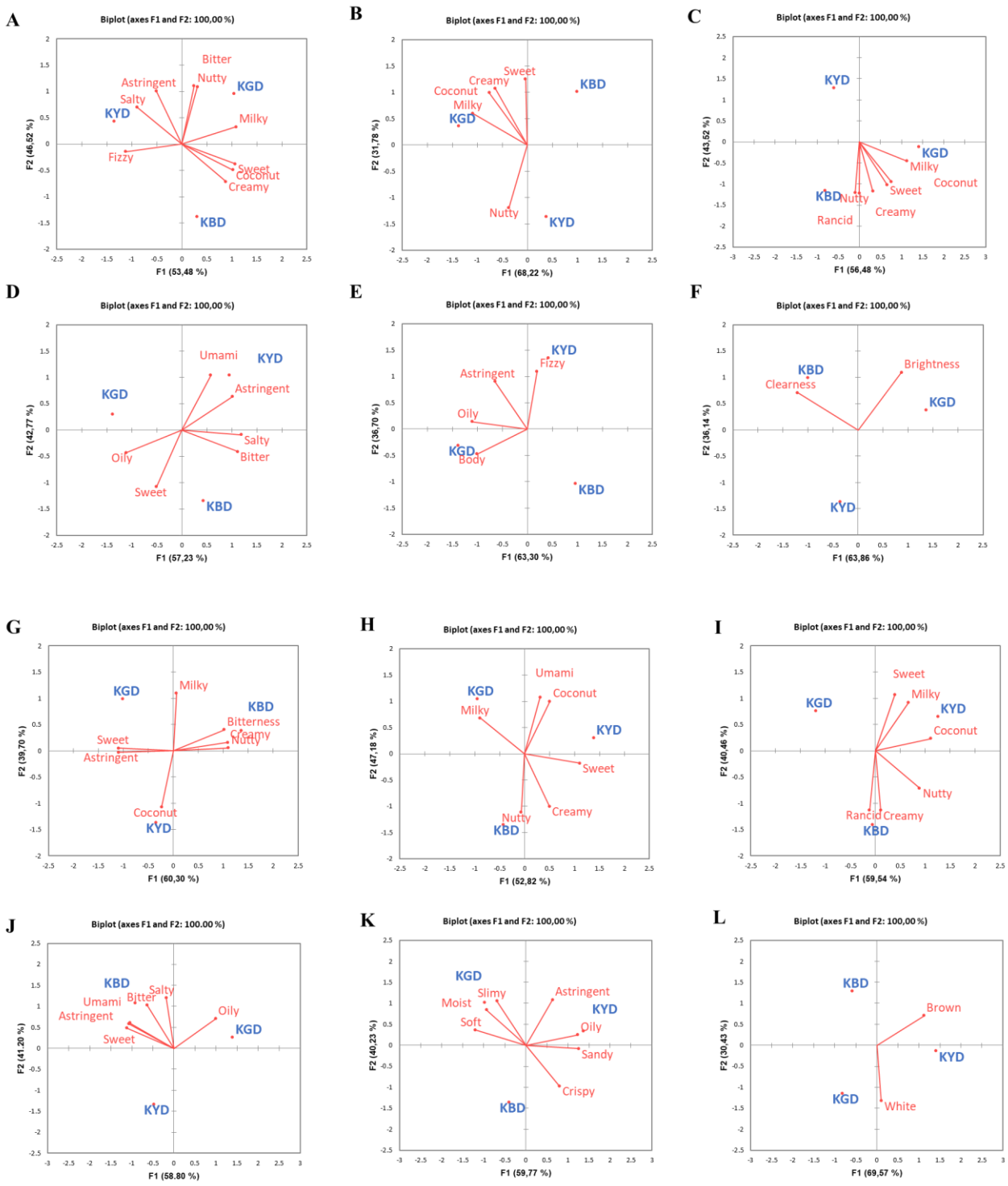

Figure 4.4. Biplot (axes F1 and F2: 100%) illustrating the sensory analysis of Kopyor water and flesh across three varieties. It covers the following aspects: (A) taste of the water, (B) flavor of the water, (C) aroma of the water, (D) aftertaste of the water, (E) mouthfeel of the water, (F) color of the water, (G) taste of the flesh, (H) flavor of the flesh, (I) aroma of the flesh, (J) aftertaste of the flesh, (K) mouthfeel of the flesh, and (L) appearance of the flesh.

The correlation analysis was conducted using Pearson correlation with a 95% confidence level to assess the relationship between each sensory attribute and the metabolites identified in Kopyor variety. For the water, 32 sensory attributes were correlated with 44 annotated metabolites obtained from GC-MS analysis. In the case of the flesh, 34 sensory attributes were correlated with 28 metabolites. The results demonstrate that each attribute is linked to specific compounds, which may act individually or in combination with other compounds to create the sensory impressions perceived by the panelists. The findings are presented in **Table 4.3.** for the water the flesh, focusing on sensory attributes that exhibit statistically significant correlations with specific metabolites at the 95% confidence level. Additionally, the metabolites can exhibit either positive or negative correlations with the sensory attributes. The details of these positive and negative correlations are provided in Supplementary Table 4.7 and Table 4.9, respectively.

Table 4.3. Sensory attributes of water and flesh and the number of metabolites correlated from metabolomic analysis based on Pearson Correlation at the 95% confidence level.

No	Water		Flesh	
	Attribute	Number of correlated metabolites	Attribute	Number of correlated metabolites
1	Color-Brightness	19	Appearance-White	11
2	Color-Clearness	11	Appearance-Chocolate	7
3	Aroma-Nutty	29	Aroma-Nutty	10
4	Aroma-Creamy	28	Aroma-Creamy	11
5	Aroma-Milky	13	Aroma-Milky	2
6	Aroma-Coconut	22	Aroma-Coconut	9
7	Aroma-Rancid	28	Aroma-Rancid	5
8	Aroma-Sweet	24	Taste-Nutty	9
9	Taste-Nutty	7	Taste-Creamy	11
10	Taste-Creamy	29	Taste-Milky	7
11	Taste-Milky	17	Taste-Coconut	6
12	Taste-Coconut	28	Taste-Bitter	6

No	Water		Flesh	
	Attribute	Number of correlated metabolites	Attribute	Number of correlated metabolites
13	Taste-Sweet	25	Taste-Astringent	2
14	Taste-Fizzy	18	Mouthfeel-Oily	9
15	Taste-Salty	29	Mouthfeel-Soft	5
16	Taste-Astringent	22	Mouthfeel-Moist	8
17	Taste-Bitter	6	Mouthfeel-Slimy	11
18	Mouthfeel-Oily	6	Mouthfeel-Crispy	3
19	Mouthfeel-Astringent	19	Mouthfeel-Sandy	10
20	Mouthfeel-Body	6	Mouthfeel-Astringent	6
21	Mouthfeel-Fizzy	28	Flavor-Nutty	3
22	Flavour-Nutty	27	Flavor-Creamy	12
23	Flavour-Creamy	24	Flavor-Milky	1
24	Flavour-Milky	13	Flavor-Coconut	2
25	Flavour-Coconut	19	Flavor-Umami	7
26	Flavour-Sweet	29	After taste-Oily	6
27	After taste-Sweet	29	After taste-Bitter	6
28	After taste-Oily	19	After taste-Salty	10
29	After taste-Astringent	22	After taste-Umami	10
30	After taste-Bitter	4	After taste-Astringent	9
31	After taste-Salty	7		
32	After taste-Umami	28		

4.3.4 Hedonic test of three Kopyor coconut varieties and its relationship with metabolomics

In previous analysis, we conducted a sensory evaluation to assess the specific sensory attributes of Kopyor varieties. However, while the sensory evaluation was crucial in understanding the characteristics of Kopyor, it did not answer the critical question of consumer preference which attributes consumers enjoy or prefer most. To address this gap, we implemented a hedonic test to measure overall consumer liking and preferences (Lim, 2011; Wichchukit & O'Mahony, 2015). Unlike the sensory evaluation, which focuses on the strength and presence of individual attributes, the hedonic test captures how much consumers like or

prefer the product as a whole. Through the combined use of sensory evaluation and hedonic testing**,** we can achieve a comprehensive understanding, linking detailed sensory attributes with overall consumer acceptance.

The hedonic test results presented in **Figure 4.4.**, based on ANOVA and Tukey Post Hoc Test, reveal significant differences in consumer preferences for Kopyor coconut water across the different cultivated varieties. For coconut water, the KBD variety, with a hedonic score of 6.02, is the most preferred by consumers, followed closely by the KGD variety (5.87). In contrast, the KYD variety is the least preferred, with a significantly lower score of 5.03, highlighting distinct consumer preferences for water among the varieties. In terms of coconut flesh, however, there are no significant differences in consumer preference, as all varieties received similar scores, indicating that the flesh is equally well-liked across varieties. These findings suggest that while KBD stand out for their coconut water, consumer preferences for the flesh do not vary significantly between varieties.

This information, provides valuable insights for producers aiming to optimize product development and marketing strategies. The results suggest a focus on the KBD variety for coconut water production, while all varieties can be equally targeted for flesh-based products, as consumer preferences are consistent across the varieties for this component.

A. B.

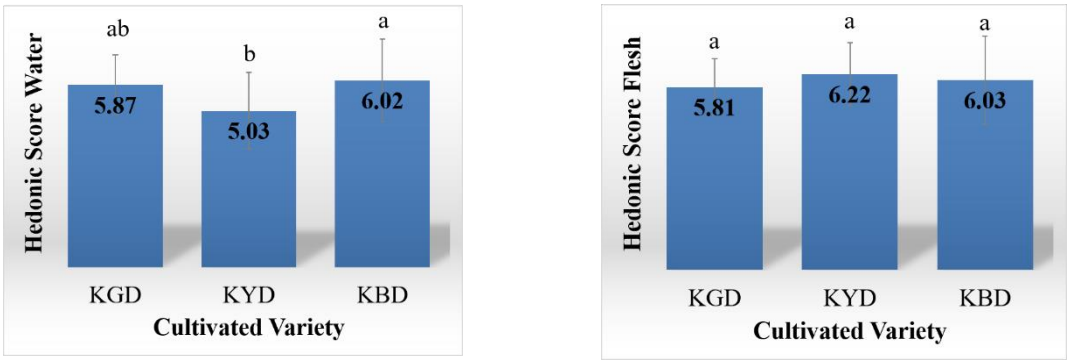

Figure 4.5. Hedonic scores of Kopyor coconut water (A) and flesh (B) for three cultivated varieties based on ANOVA and Tukey Post Hoc Test at 5% significance level

Subsequently, a correlation analysis was performed between the hedonic scores and the metabolomic data to identify the compounds contributing to the hedonic ratings of both Kopyor coconut water and flesh. This analysis was conducted using Pearson correlation at a 95% confidence level, allowing for the identification of specific metabolites that are significantly associated with consumer preferences.

Table 4.4. Correlation Between Hedonic Scores and Metabolite Concentrations in Kopyor Water Based on Pearson Correlation

No	Correlation Hedonic vs.	*p*-value			Pearson *r*		
		p (two-tailed)	*p*-value summary	Significant ? (α = 0.05)	*r*	95% confidence interval ((*CI*)*r*)	*R* squared
1	Citric acid	<0.0001	****	Yes	-0.99	-1.0 to -0.97	0.99
2	Phosphate	<0.0001	****	Yes	-0.99	-1.0 to -0.97	0.99
3	Pyroglutamic acid	<0.0001	****	Yes	-0.95	-0.99 to -0.77	0.9
4	Tryptophan	<0.0001	****	Yes	-0.98	-1.0 to -0.89	0.96
5	Valine	0.000	***	Yes	-0.94	-0.99 to -0.74	0.89
6	Proline	0.000	***	Yes	-0.93	-0.98 to -0.68	0.86
7	Quinic acid	0.001	***	Yes	-0.91	-0.98 to -0.64	0.84
8	Inositol	0.001	***	Yes	-0.9	-0.98 to -0.59	0.81
9	Sucrose	0.001	***	Yes	-0.9	-0.98 to -0.59	0.81
10	Xylitol	0.002	**	Yes	-0.88	-0.98 to -0.53	0.78
11	Isoleucine	0.002	**	Yes	-0.88	-0.98 to -0.53	0.78
12	Serine	0.002	**	Yes	-0.88	-0.97 to -0.52	0.77

No	Correlation Hedonic vs.	*p*-value			Pearson *r*		
		p (two-tailed)	*p*-value summary	Significant ? (α = 0.05)	*r*	95% confidence interval ((*CI*)*r*)	*R* squared
13	Fructose	0.002	**	Yes	0.87*	0.49 to 0.97	0.76
14	Tagatose	0.002	**	Yes	0.87*	0.49 to 0.97	0.76
15	Glucose	0.003	**	Yes	0.87*	0.48 to 0.97	0.75
16	Lysine	0.003	**	Yes	-0.87	-0.97 to -0.47	0.75
17	Methionine	0.003	**	Yes	-0.86	-0.97 to -0.45	0.74
18	Aspartic acid	0.004	**	Yes	-0.85	-0.97 to -0.42	0.72
19	Meso erythritol	0.004	**	Yes	-0.84	-0.97 to -0.40	0.71
20	β-Alanine	0.006	**	Yes	-0.82	-0.96 to -0.35	0.68
21	Galactose	0.008	**	Yes	0.81*	0.31 to 0.96	0.65
22	Turanose	0.013	*	Yes	-0.78	-0.95 to -0.24	0.61
23	2-Aminoethanol	0.016	*	Yes	-0.76	-0.95 to -0.20	0.58
24	Maltitol	0.019	*	Yes	-0.75	-0.94 to -0.18	0.57
25	Succinic acid	0.024	*	Yes	0.74*	0.14 to 0.94	0.54
26	Xylonic acid	0.042	*	Yes	-0.68	-0.93 to -0.037	0.47
27	Gentiobiose	0.046	*	Yes	0.68*	0.022 to 0.92	0.46

Note: The asterisk (*) indicates metabolites that show a **significant correlation** with the hedonic scores.

Table 4.5. Correlation between hedonic scores and metabolite concentrations in Kopyor flesh based on Pearson correlation

No	Correlation Hedonic vs.	*p*-value			Pearson *r*		
		p (two-tailed)	*p*-value summary	Significant (α = 0.05)	*r*	95% confidence interval (*CI* (*r*))	*R* squared
1	Galactitol	0.001	**	Yes	-0.888	-0.976 to -0.544	0.788
2	Sorbitol	0.002	**	Yes	-0.870	-0.972 to -0.486	0.756
3	Fumaric acid	0.006	**	Yes	-0.827	-0.962 to -0.361	0.684
4	Succinic acid	0.011	*	Yes	-0.790	-0.954 to -0.266	0.625
5	Fructose	0.013	*	Yes	-0.779	-0.951 to -0.237	0.606
6	Malic acid	0.017	*	Yes	-0.763	-0.947 to -0.201	0.583
7	Galactinol	0.035	*	Yes	-0.703	-0.932 to -0.0724	0.494

The results of the hedonic correlation test using Pearson correlation reveal significant relationships between the hedonic ratings of Kopyor water and its metabolomic profile (**Table 4.4.**). A total of 27 metabolites exhibits significant correlations with the hedonic ratings, as indicated by *p*-values below 0.05. While the majority of these metabolites display a negative correlation, meaning that higher concentrations tend to reduce the hedonic scores and potentially diminish the sensory appeal of Kopyor water, six metabolites consisting of fructose, tagatose, glucose, galactose, succinic acid, and gentibiose exhibit a positive correlation with the hedonic scores. The following compounds are suggested to indicate a potential association with the factors contributing to KBD being more preferable.

Among the Kopyor varieties, KBD water shows the strongest correlation with hedonic ratings, outperforming KGD and KYD. It is suggested that these six positively correlated compounds could influence consumer perceptions of Kopyor water. Their possible role in the flavor and sensory profile may contribute to KBD water being viewed as a preferred variety.

The results of the Pearson correlation analysis on Kopyor coconut flesh (**Table 4.5.)** reveal that 7 metabolites exhibit significant correlations with the hedonic ratings at the 0.05 significance level. Notably, all of these metabolites show a negative correlation, indicating that as the concentration of these compounds increases, the hedonic scores decrease. Although the

hedonic test for flesh did not reveal statistically significant differences between varieties, the variety KGD consistently exhibited the lowest hedonic score. This finding is particularly important as the 7 negatively correlated metabolites are predominantly accumulated in KGD, suggesting that these compounds play a crucial role in lowering the hedonic score of Kopyor coconut flesh.

Further investigation is needed to determine whether these metabolites act independently to reduce hedonic scores or if they collaborate with other compounds, possibly acting as triggers or synergistic agents in a more complex network of interactions (Grabež et al., 2019). Understanding whether these metabolites function alone or in concert with others will be crucial in deciphering the mechanisms behind the reduction of sensory appeal in Kopyor flesh. The endosperm plays a key role in seed-specific developmental processes (Lopes & Larkins, 1993). Metabolite accumulation can vary between each variety, ultimately influencing the sensory profile in a specific way in edible fruit.

4.4 Conclusion

The conclusion of this chapter highlights that specific metabolite accumulation differs between varieties, with contrasting patterns in water and flesh. It indicates a potential association between the preference for Kopyor Brown Dwarf (KBD) coconut water and its sensory attributes and key metabolites. In contrast, the flesh is equally well-liked across all varieties.

Chapter 5

Conclusion and Future Perspective

This study comprehensively characterizes the sensory attributes, metabolite profiles, physicochemical properties, and proximate composition of Kopyor coconut to address the general challenge of its potential being limited by incomplete information, particularly regarding its sensory characteristics and metabolite profiles. Chapter 2 demonstrates that Kopyor coconut possesses a rich metabolite profile and introduces the sensory wheel as a comprehensive tool for characterizing its attributes. In Chapter 3, results show that a higher endosperm quantity enhances metabolite accumulation and improves nutrient bioavailability, with valine identified as a potential biomarker. Chapter 4 indicates a potential association between the preference for Kopyor Brown Dwarf (KBD) coconut water and its sensory attributes and key metabolites. Collectively, this study establishes a foundational framework for broader applications of Kopyor coconut. The findings serve as a valuable reference not only for the study of Kopyor but also for other unique coconut varieties worldwide.

For future perspectives, there are two main categories: research development potential and product development potential. This study represents an extension of ongoing research into the unique characteristics of Kopyor. However, much remains unexplored regarding Kopyor's potential applications, particularly in the fields of food science, health, and agriculture, offering substantial opportunities for future development. Current metabolomic studies focusing on widely targeted hydrophilic compounds could be expanded to include hydrophobic compounds and proteomics, providing a more comprehensive profile of Kopyor's bioactive components. This expansion would allow for deeper insights into the complex biochemical pathways involved, supporting further pathway analysis to elucidate the metabolic and proteomic processes that contribute to Kopyor’s unique characteristics.

Pathway analysis plays a crucial role in advancing biotechnology, especially for optimizing Kopyor coconuts. By identifying critical metabolic pathways, researchers can leverage biotechnology tools such as gene editing (e.g., CRISPR-Cas9), transgenic technology, or metabolic engineering to modify or enhance these pathways. This approach aims to achieve better control over specific Kopyor traits that currently exhibit suboptimal characteristics. Through the targeted modification of key genetic and metabolic factors, pathway analysis can support efforts to increase the proportion of Kopyor coconuts within each harvest. Furthermore, this method has the potential to enhance Kopyor quality by improving endosperm quality (EQ) levels, thus yielding fruits with more consistent and superior attributes. These targeted interventions offer a promising means to stabilize and elevate Kopyor production, aligning it more closely with both market demand and quality standards.

The next research focus is on the analysis of Kopyor aroma. Although Kopyor-scented products are already sold by small-scale industries in Indonesia, a detailed study on the compounds responsible for Kopyor's unique aroma has not yet been conducted. This research has confirmed that Kopyor has a distinct aroma compared to regular mature and young coconuts. Sensory testing reveals that Kopyor has a milky, creamy, and nutty aroma, but the specific compounds contributing to this profile remain unidentified. Therefore, a study using GC-MS olfactometry for volatile compound analysis, employing the HS-SPME method, is essential to identify these unique aroma compounds accurately. In the future, the findings from this research could serve as a foundation for product development to meet the market demand for natural food aromas, offering consumers an authentic and natural Kopyor aroma for various culinary applications.

The next research potential lies in exploring the unique varieties of coconuts worldwide, including studies on the preservation of Kopyor and other rare coconut types. Kopyor is one such rare coconut, with numerous others yet to be thoroughly investigated. However, sampling

these coconuts presents challenges due to their bulkiness, high cost, susceptibility to spoilage, and complex international permitting issues related to biodiversity protection and the risk of spreading plant pests and diseases. A promising solution lies in silica monolithic sampling technology, followed by metabolomics analysis with GC-MS. This method allows samples to dry easily, which suppresses enzyme activity and reduces fluctuations in metabolites. By stabilizing samples in this way, researchers can capture and analyze the metabolic profile of coconuts accurately without facing the logistical and regulatory obstacles associated with transporting fresh samples.

Moreover, research into the digestibility and antioxidant properties of Kopyor could establish a scientific foundation for its promotion as a functional food. Understanding the bioactive compounds responsible for these benefits would enhance its appeal in health-conscious markets and open up a range of applications.

Kopyor coconut holds significant potential for innovative product development, particularly in the culinary and health-focused markets. Promising applications include Kopyor-based flavor enhancers such as a “Kopyor sprinkle” seasoning, which brings the authentic coconut-Kopyor aroma and flavor to various dishes, appealing to consumers seeking unique, tropical flavors. Instant Kopyor beverages or functional Kopyor drinks could introduce Kopyor’s distinct taste to a broader audience, showcasing its high amino acid content, low fat, tropical aroma, and excellent digestibility. Another exciting avenue is the development of aroma-intensified Kopyor products as additives for the food industry, enhancing sensory experiences. Additionally, in the health sector, virgin coconut oil derived from Kopyor is already available, yet it has potential for further development and would benefit from comprehensive research to optimize its unique properties and applications.

References

Abraham, A., & Mathew, P. M. (1963). Cytology of coconut endosperm. Annals of Botany, 27(3), 505–512. https://doi.org/10.1093/oxfordjournals.aob.a083866

Adubofuor, J., Amoah, I., and Osei-Bonsu, I. (2016). Sensory and physicochemical properties of pasteurized coconut water from two varieties of coconut, Food Sci. Qual. Manag., 54, 26e32

Antu, M. Y., Maskromo, I., & Rindengan, B. (2021). Potensi daging kelapa kopyor sebagai bahan pangan sehat / Potency of Kopyor coconut meat as an ingredient of healthy food. Perspektif, 19(2), 95. https://doi.org/10.21082/psp.v19n2.2020.95-104

Azra, J. M., Setiawan, B., Nasution, Z., & Sulaeman, A. (2021). Effects of variety and maturity stage of coconut on physicochemical and sensory characteristics of powdered coconut drink. Foods and Raw Materials, 9(1), 43–51. https://doi.org/10.21603/2308-4057-2021-1-43-51

Bach, A., & Babayan, V. (1982). Medium-chain triglycerides: an update. The American Journal of Clinical Nutrition, 36(5), 950–962. https://doi.org/10.1093/ajcn/36.5.950

Bachmanov, A. A., Bosak, N. P., Glendinning, J. I., Inoue, M., Li, X., Manita, S., McCaughey, S. A., Murata, Y., Reed, D. R., Tordoff, M. G., & Beauchamp, G. K. (2016). Genetics of amino acid taste and appetite. In Advances in nutrition (Bethesda, Md.) 7 (4), pp. 806S-822S). https://doi.org/10.3945/an.115.011270

Baker, M. T., Lu, P., Parrella, J. A., & Leggette, H. R. (2022). Consumer acceptance toward functional foods: a scoping review. In International Journal of Environmental Research and Public Health 19 (3). https://doi.org/10.3390/ijerph19031217

Balasubramaniam, K. (1976). Polysaccharides of the kernel of maturing and matured coconuts. Journal of Food Science, 41(6), 1370–1373. https://doi.org/10.1111/j.1365-2621.1976.tb01174.x

Toan, N.B., & Thanh, V.C. (2011). Potential Development of Makapuno coconut in the Mekong Delta of Vietnam. International Journal of Renewable Energy, 6, 21-28.

Billet, K., Houillé, B., Dugé de Bernonville, T., Besseau, S., Oudin, A., Courdavault, V., Delanoue, G., Guérin, L., Clastre, M., Giglioli-Guivarc'h, N., & Lanoue, A. (2018). Field-based metabolomics of *Vitis vinifera* L. stems provides new insights for genotype discrimination and polyphenol metabolism structuring. Frontiers in Plant Science, 9. https://doi.org/10.3389/fpls.2018.00798

Che, L., Xu, M., Gao, K., Zhu, C., Wang, L., Yang, X., Wen, X., Xiao, H., Jiang, Z., & Wu, D. (2019). Valine increases milk fat synthesis in mammary gland of gilts through stimulating AKT/MTOR/SREBP1 pathway†. Biology of Reproduction, 101(1), 126–137. https://doi.org/10.1093/biolre/ioz065

Chen, Y., Chen, Y., Fang, Y., Pei, Z., & Zhang, W. (2024). Coconut milk treated by atmospheric cold plasma: Effect on quality and stability. Food Chemistry, 430, 137045. https://doi.org/10.1016/j.foodchem.2023.137045

Chowdhury, M. M., Aziz, M. G., and Uddin, M. B. (2005). Development of shelf-stable ready-to-serve green coconut water, Biotechnology, 4, 121e125

de O. Petkowicz, C. L., Reicher, F., Chanzy, H., Taravel, F. R., & Vuong, R. (2001). Linear mannan in the endosperm of Schizolobium amazonicum. Carbohydrate Polymers, 44(2), 107–112. https://doi.org/10.1016/S0144-8617(00)00212-5

Deliza, R., Macfie, H., & Hedderley, D. (2005). The consumer sensory perception of passion-fruit juice using free-choice profiling. Journal of Sensory Studies, 20(1), 17–27. https://doi.org/10.1111/j.1745-459X.2005.050604.x

Dixon, R. A., Gang, D. R., Charlton, A. J., Fiehn, O., Kuiper, H. A., Reynolds, T. L., Tjeerdema, R. S., Jeffery, E. H., German, J. B., Ridley, W. P., & Seiber, J. N. (2006). Applications of metabolomics in agriculture. In Journal of Agricultural and Food Chemistry (Vol. 54, Issue 24, pp. 8984–8994). https://doi.org/10.1021/jf061218t

Dyrløv Bendtsen, J., Nielsen, H., von Heijne, G., & Brunak, S. (2004). Improved prediction of signal peptides: SignalP 3.0. Journal of Molecular Biology, 340(4), 783–795. https://doi.org/10.1016/j.jmb.2004.05.028

Faramitha, Y., Dimawarnita, F., Sinta, M. M., Saptari, R. T., Riyadi, I., & Sumaryono. (2024). Observations on Kopyor coconut (*Cocos nucifera* var. Kopyor) characteristics during distribution. BIO Web of Conferences, 99, 02018. https://doi.org/10.1051/bioconf/20249902018

Gomide, A. I., Silva, R. de C. dos S. N., Nascimento, M., Minim, L. A., & Minim, V. P. R. (2021). Study of the influence of line scale length (9 and 15 cm) on the sensory evaluations of two descriptive methods. Journal of Food Science and Technology, 58(7), 2815–2824. https://doi.org/10.1007/s13197-020-04890-9

Grabež, V., Bjelanović, M., Rohloff, J., Martinović, A., Berg, P., Tomović, V., Rogić, B., & Egelandsdal, B. (2019). The relationship between volatile compounds, metabolites and sensory attributes: A case study using lamb and sheep meat. Small Ruminant Research, 181, 12–20. https://doi.org/10.1016/j.smallrumres.2019.09.022

Guo, K., Xia, K., & Yang, Z.-M. (2008). Regulation of tomato lateral root development by carbon monoxide and involvement in auxin and nitric oxide. Journal of Experimental Botany, 59(12), 3443–3452. https://doi.org/10.1093/jxb/ern194

Hanifah, A., Firmanto, H., Putri, S. P., & Fukusaki, E. (2022). Unique metabolite profiles of Indonesian cocoa beans from different origins and their correlation with temperature. Journal of Bioscience and Bioengineering, 134(2), 125–132. https://doi.org/10.1016/j.jbiosc.2022.05.001

Heo, J., Kim, S. S., Kim, M.-R., & Kwak, H. S. (2023). comparison of sensory profiling by descriptive analysis, free-choice profiling, and polarized sensory positioning on bottled water. Foods, 12(8), 1579. https://doi.org/10.3390/foods12081579

Ikram, M. M. M., Mizuno, R., Putri, S. P., & Fukusaki, E. (2021). Comparative metabolomics and sensory evaluation of pineapple (*Ananas comosus*) reveal the importance of ripening stage compared to cultivar. Journal of Bioscience and Bioengineering, 132(6), 592–598. https://doi.org/10.1016/j.jbiosc.2021.08.008

Ikram, M. M. M., Ridwani, S., Putri, S. P., & Fukusaki, E. (2020). GC-MS based metabolite profiling to monitor ripening-specific metabolites in pineapple (*Ananas comosus*). Metabolites, 10(4), 134. https://doi.org/10.3390/metabo10040134

Ismail, M., Halimah, L. S., Hengky, N., & Sudarsono, S. (2016). Xenia negatively affecting Kopyor nut yield in Kalianda Tall Kopyor and Pati Dwarf Kopyor coconuts. Emirates Journal of Food and Agriculture, 28(9), 644–652. https://doi.org/10.9755/ejfa.2015-07-552

Maskromo, I. & Sudarsono. (2013). Productivity of three dwarf Kopyor coconut varieties from Pati, Central Java, Indonesia. CORD, 29(2), 10. https://doi.org/10.37833/cord.v29i2.86

Kim, J., Lee, J. E., Lee, J. S., Park, J. S., Moon, J. O., & Lee, H. G. (2020). Phenylalanine and valine differentially stimulate milk protein synthetic and energy-mediated pathway in immortalized bovine mammary epithelial cells. Journal of Animal Science and Technology, 62(2), 263–275. https://doi.org/10.5187/jast.2020.62.2.263

Kotecka-Majchrzak, K., Sumara, A., Fornal, E., & Montowska, M. (2020). Oilseed proteins – properties and application as a food ingredient. Trends in Food Science & Technology, 106, 160–170. https://doi.org/10.1016/j.tifs.2020.10.004

Kumar, M., Saini, S. S., Agrawal, P. K., Roy, P., & Sircar, D. (2021). Nutritional and metabolomics characterization of the coconut water at different nut developmental stages. Journal of Food Composition and Analysis, 96, 103738. https://doi.org/10.1016/j.jfca.2020.103738

Kwon, K., Park, K. H., & Rhee, K. C. (1996). Fractionation and characterization of proteins from coconut (*Cocos nucifera* L.). Journal of Agricultural and Food Chemistry, 44(7), 1741–1745. https://doi.org/10.1021/jf9504273

Lawless, H. T., & Heymann, H. (2010). Sensory evaluation of food. Springer New York. https://doi.org/10.1007/978-1-4419-6488-5

Lim, J. (2011). Hedonic scaling: a review of methods and theory. Food Quality and Preference. https://doi.org/10.1016/j.foodqual.2011.05.008

Liñán, J., Arroyo, P., & Carrete, L. (2019). Conceptualizing healthy food: how consumer's values influence the perceived healthiness of a food product. Journal of Food and Nutrition Research, 7(9), 679–687. https://doi.org/10.12691/jfnr-7-9-10

Lopes, M. A., & Larkins, B. A. (1993). Endosperm origin, development, and function. The Plant Cell, 5(10), 1383–1399. https://doi.org/10.1105/tpc.5.10.1383

Ma, Y., Li, B., Zhang, X., Wang, C., & Chen, W. (2022). Production of gluconic acid and its derivatives by microbial fermentation: process improvement based on integrated routes. Frontiers in Bioengineering and Biotechnology, 10. https://doi.org/10.3389/fbioe.2022.864787

Mahbub, K., Octaviani, I. D., Astuti, I. Y., Sisunandar, S., & Dhiani, B. A. (2022). Oil from Kopyor coconut (*Cocos nucifera* var. Kopyor) for cosmetic application. Industrial Crops and Products, 186, 115221. https://doi.org/10.1016/j.indcrop.2022.115221

Maskromo, I., Novarianto, H., Sukendah, S., Sukma, D., & Sudarsono, S. (2014). Keragaman komponen buah dan kuantitas endosperma kelapa dalam Kopyor Kalianda dan kelapa genjah Kopyor Pati, endosperm quantity and fruit character variabilities of Kalianda Tall Kopyor and Pati Dwarf Kopyor coconut. Buletin Palma, 15, 102-109.

Chomchalow, N. (2013). Curd coconut: its mystery and potentialities (review article). CORD, 29(2), 6. https://doi.org/10.37833/cord.v29i2.89

Nayar, N. M. (2017). The coconut in the world. In the coconut (pp. 1–8). Elsevier. https://doi.org/10.1016/B978-0-12-809778-6.00001-2

Nguyen, Q. T., Bandupriya, H. D. D., Foale, M., & Adkins, S. W. (2016). Biology, propagation and utilization of elite coconut varieties (Makapuno and Aromatics). Plant Physiology and Biochemistry, 109, 579–589. https://doi.org/10.1016/j.plaphy.2016.11.003

Novarianto, H., Maskromo, I., Dinarti, D., & Sudarsono, S. (2014). Production technology for Kopyor coconut seednuts and seedlings in Indonesia. International Journal of Coconut Research and Development (CORD), 30(2), 31-40. https://doi.org/10.37833/cord.v30i2.77

Ohler, J. G. (1999). Modern coconut management: palm cultivation and products. Intermediate Technology Publications.

Patil, U., & Benjakul, S. (2018). Coconut milk and coconut oil: their manufacture associated with protein functionality. Journal of Food Science, 83(8), 2019–2027. https://doi.org/10.1111/1750-3841.14223

Pavagadhi, S., & Swarup, S. (2020). Metabolomics for evaluating flavor-associated metabolites in plant-based products. Metabolites, 10(5), 197. https://doi.org/10.3390/metabo10050197

Pereira, T. N. S., Neto, M. F., de Souza, M. M., da Costa Geronimo, I. G., de Melo, C. A. F., & Pereira, M. G. (2017). Cytological characterization of Brazilian Green Dwarf Coconut (*Cocos nucifera* L.); meiosis and conventional and differential karyotyping. Cytologia, 82(2), 167–174. https://doi.org/10.1508/cytologia.82.167

Pesik, A., Efendi, D., Novarianto, H., Dinarti, D., & Sudarsono, S. (2017). Development of SNAP markers based on nucleotide variability of WRKY genes in coconut and their validation using multiplex PCR. Biodiversitas Journal of Biological Diversity, 18(2), 465–475. https://doi.org/10.13057/biodiv/d180204

Prades, A., Dornier, M., Diop, N., & Pain, J.-P. (2012). Coconut water uses, composition and properties: a review. Fruits, 67(2), 87–107. https://doi.org/10.1051/fruits/2012002

Putri, S. P., & Fukusaki, E. (Eds.). (2016). Mass spectrometry-based metabolomics. CRC Press. https://doi.org/10.1201/b17793

Rachel, R. (2013). Sensory evaluation and sugars contents of coconut (*Cocos nucifera* L.) water during nuts ripening, Afr. J. Food Sci., 7, 186e192

Rahayu, M. S., Setiawan, A., Maskromo, I., Purwito, A., & Sudarsono, S. (2021). Genetic diversity analysis of Puan Kalianda kKopyor coconuts (*Cocos nucifera*) from South Lampung, Indonesia based on SSR markers. Biodiversitas Journal of Biological Diversity, 23(1). https://doi.org/10.13057/biodiv/d230126

Rahmawati, A., Volkaert, H. A., Dinarti, D., Maskromo, I., Hatta, A. N. N. L., & Sudarsono, S. (2021). Complete chloroplast genome sequences of coconut cv. Kopyor Green Dwarf and comparative genome analysis to oil palm, date palm, sago palm, and miniature sugar palm. In Oil Crop Genomics (pp. 189–216). Springer International Publishing. https://doi.org/10.1007/978-3-030-70420-9_10

Reeds, P. J., & Garlick, P. J. (2003). Protein and amino acid requirements and the composition of complementary foods. The Journal of Nutrition, 133(9), 2953S-2961S. https://doi.org/10.1093/jn/133.9.2953S

Rocchetti, G., & O'Callaghan, T. F. (2021). Application of metabolomics to assess milk quality and traceability. Current Opinion in Food Science, 40, 168–178. https://doi.org/10.1016/j.cofs.2021.04.005

Rozaki, Z., Mahardina, A., Kamarudin, M. F., Aziz Proklamalatu, M., & Utami, S. S. (2021). Farmers' motivation to produce kopyor coconut: a case in Ngagel Village, Pati Regency. E3S Web of Conferences, 316, 02039. https://doi.org/10.1051/e3sconf/202131602039

Saittagaroon, S., Kawakishi, S., & Namiki, M. (1983). Characterisation of polysaccharides of copra meal. Journal of the Science of Food and Agriculture, 34(8), 855–860. https://doi.org/10.1002/jsfa.2740340813

Samarajeewa, U. (2024). Coconut: nutritional and industrial significance. In nut consumption and usefulness in the modern world [Working Title]. IntechOpen. https://doi.org/10.5772/intechopen.1004173

Santoso, U., Kubo, K., Ota, T., Tadokorob, T., & Maekawab, A. (1996). Nutrient composition of Kopyor coconuts (*Cocos nucifera* L.). In Food Chemistry (Vol. 51, Issue 2).

Setiawan, A., Rahayu, M. S., Maskromo, I., Purwito, A., & Sudarsono. (2020). Inheritance pattern of endosperm quantity and Kopyor coconut (*Cocos nucifera* L.) fruit variations. IOP Conference Series: Earth and Environmental Science, 418(1), 012039. https://doi.org/10.1088/1755-1315/418/1/012039

Sisunandar, Alkhikmah, Husin, A., Julianto, T., Yuniaty, A., Rival, A., & Adkins, S. W. (2018). Ex vitro rooting using a mini growth chamber increases root induction and accelerates acclimatization of Kopyor coconut (*Cocos nucifera* L.) embryo culture-derived seedlings. In Vitro Cellular & Developmental Biology - Plant, 54(5), 508–517. https://doi.org/10.1007/s11627-018-9897-y

Stone, H., & Sidel, J. L. (1993). Sensory Evaluation Practices.

Sudarsono, S., Maskromo, I., & Dinarti, D. (2019). The genetics of unique coconut (*Cocos nucifera*) Kopyor endosperm mutants from Indonesia. Malaysia International Genetic Congress.

Sudha, R., Niral, V., Hebbar, K. B., & Samsudeen, K. (2019). Coconut inflorescence sap. Current Science, 116(11), 1809–1817. https://www.jstor.org/stable/27138131

Tanase, R., Senda, R., Matsunaga, Y., & Narukawa, M. (2022). Taste characteristics of various amino acid derivatives. In J Nutr Sci Vitaminol (Vol. 68).

Villarino, B. J., Dy, L. M., and Lizada, M. C. C. (2007). Descriptive sensory evaluation of virgin coconut oil and refined, bleached, and deodorized coconut oil, LWT-Food Sci. Technol., 40, 193e199

Wattanapahu, S., Suwonsichon, T., Jirapakkul, W., and Kasermsumran, S. (2012). Categorization of coconut milk products by their sensory characteristics, Kasetsart J. (Nat. Sci.), 46, 944e954

Wicaksono, A., Raihandhany, R., & Teixeira da Silva, J. A. (2021). Kopyor versus macapuno coconuts: are these two edible mutants of Southeast Asia the same? Planta, 254(5), 86. https://doi.org/10.1007/s00425-021-03740-y

Wichchukit, S., & O'Mahony, M. (2015). The 9-point hedonic scale and hedonic ranking in food science: some reappraisals and alternatives. Journal of the Science of Food and Agriculture, 95(11), 2167–2178. https://doi.org/10.1002/jsfa.6993

Xiao, Z., Ge, C., Zhou, G., Zhang, W., & Liao, G. (2019). 1H NMR-based metabolic characterization of Chinese Wuding chicken meat. Food Chemistry, 274, 574–582. https://doi.org/https://doi.org/10.1016/j.foodchem.2018.09.008

Yunindanova, M. B., Putri, S. P., Novarianto, H., & Fukusaki, E. (2024). Characteristics of kopyor coconut (*Cocos nucifera* L.) using sensory analysis and metabolomics-based approach. Journal of Bioscience and Bioengineering, 138(1), 44–53. https://doi.org/10.1016/j.jbiosc.2024.02.008

List of Publication

Original Paper:

Yunindanova, M. B., Putri, S. P., Novarianto, H., & Fukusaki, E. (2024). Characteristics of Kopyor coconut (*Cocos nucifera* L.) using sensory analysis and metabolomics-based approach. *Journal of Bioscience and Bioengineering*, *138*(1), 44–53. https://doi.org/10.1016/j.jbiosc.2024.02.008

Presentations:

1. **Yunindanova, M. B.**, Putri, S. P., Novarianto, H., & Fukusaki, E. (2023). Sensory evaluation and metabolomics approach to reveal the characteristics of Kopyor, Indonesian unique coconut. (*Oral presentation*) *The 75th Annual Meeting of the Society for Biotechnology, Japan (SBJ) – Nagoya University, Nagoya*

2. **Yunindanova, M. B.,** Fukusaki, E., Putri, S. P. (2023). Variety-related metabolites and sensory profiles of Kopyor (*Cocos nucifera* L.). *(Poster presentation) 3rd International BMS Symposium 2023 - Shimadzu Corporation, Kyoto*

3. **Yunindanova, M. B.,** Fukusaki, E., Putri, S. P. (2023). Investigation of Kopyor endosperm phenotype using proximate analysis and metabolomic approach. *(Poster presentation) 第 17 回メタボローム シンポジウム (17th Metabolome Symposium)- Shimadzu Tokyo Innovation Plaza in Tonomachi, Kanagawa*

Appendix

Supplementary Figure

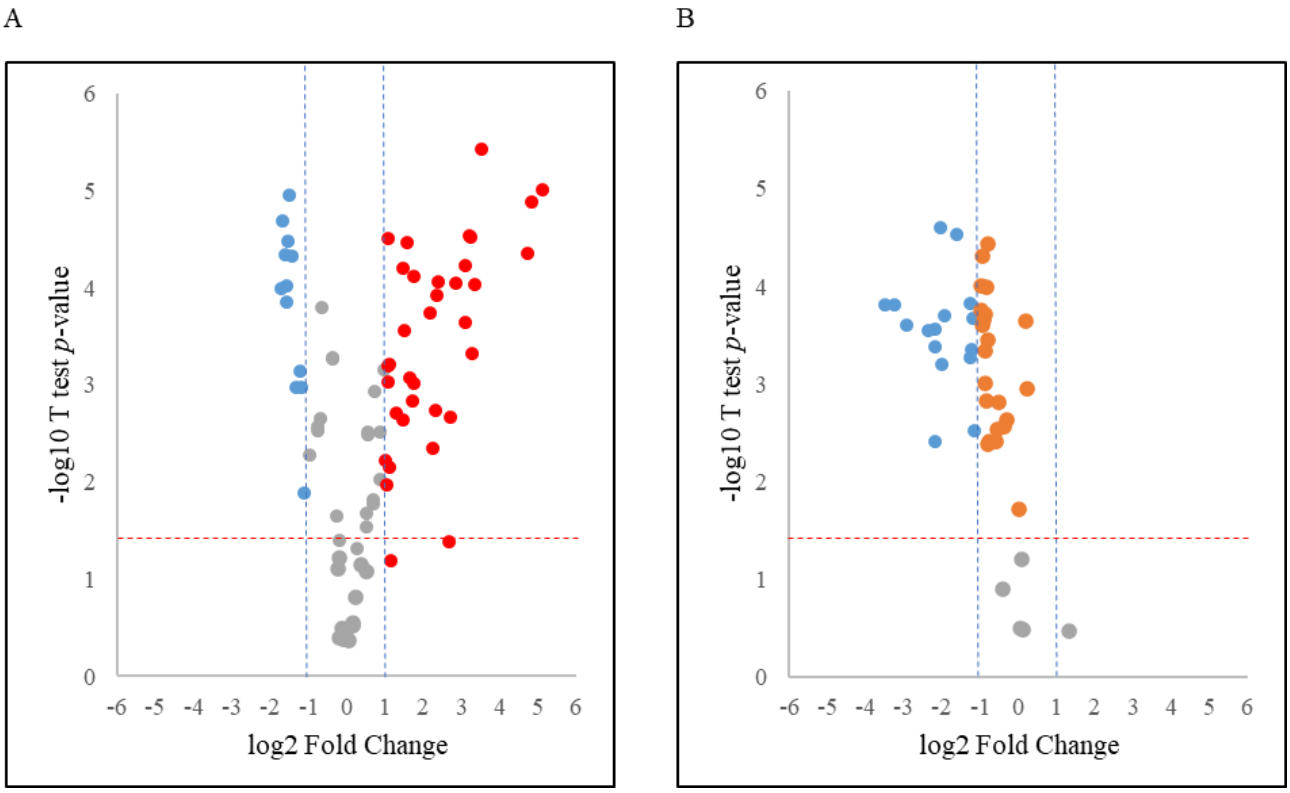

Figure S1. Differential analysis for detected metabolites in water (A) and flesh (B) of mature compared to young coconut. Volcano plot with the x-axis as the binary logarithm of fold changes and the y-axis as the negative common logarithm of the *p*-value from pairwise Student t-test of (A) water between mature and young; (B) flesh between mature and young. Comparing water of mature and young, 66 metabolites showed p-values lower than 0.05. Comparing flesh of mature and young, 48 metabolites showed *p*-values lower than 0.05.

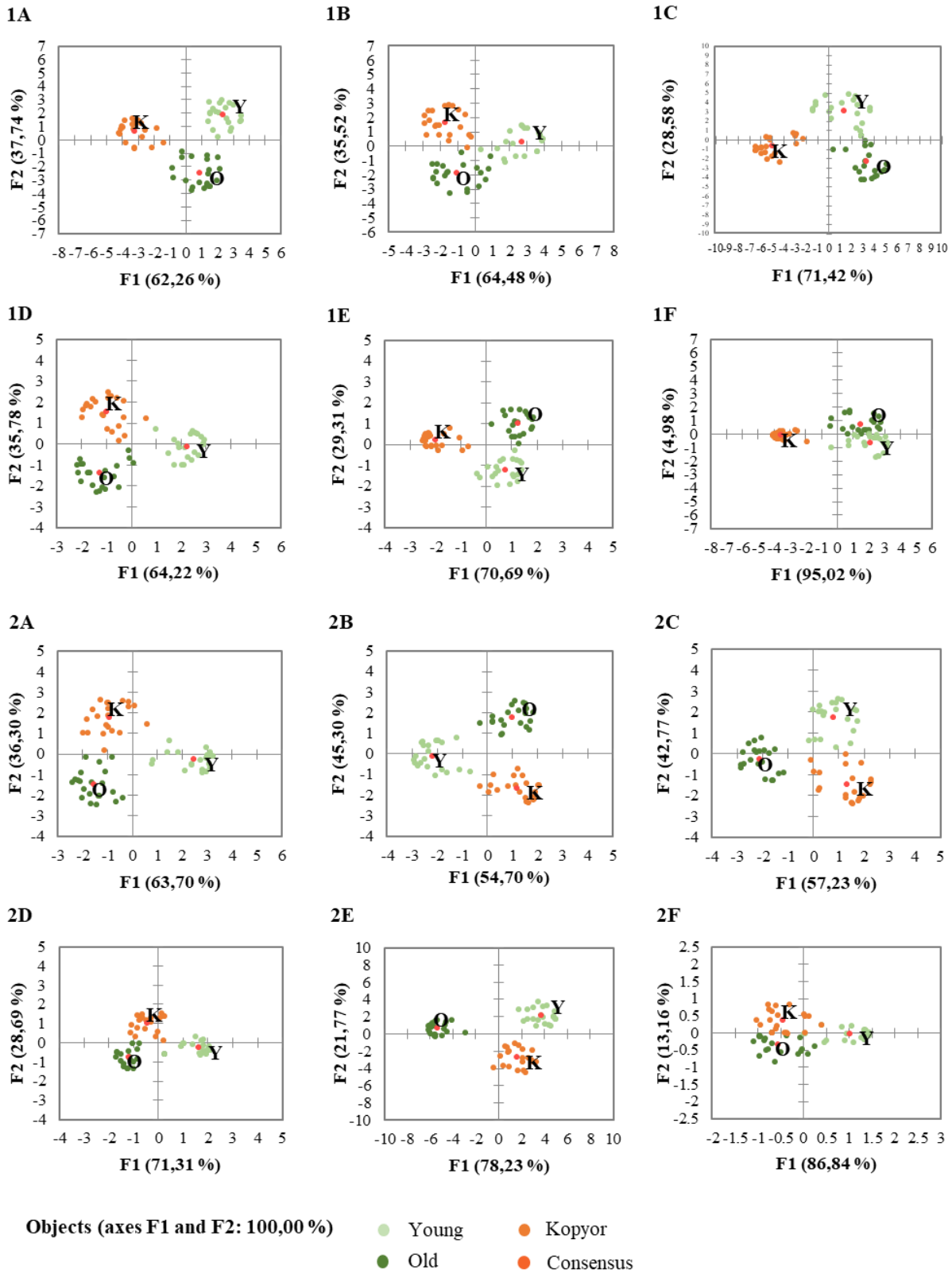

Figure S2. Biplot of Consensus from Generalized Procrustes Analysis (GPA) of water (1A-1F) and flesh (2A-2F) from kopyor, normal old, and normal young. (A) Taste of water, (B) flavor of water, (C) aroma of water, (D) aftertaste of water, (E) mouthfeel of water, (F) color of water, (G) taste of flesh, (H) flavor of flesh, (I) aroma of flesh, (J) aftertaste of flesh, (K) mouthfeel of flesh, (L) color of flesh.

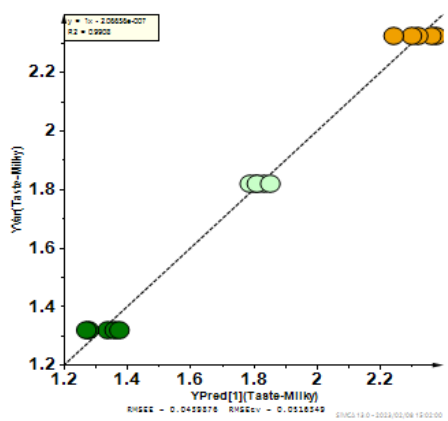

Taste Milky

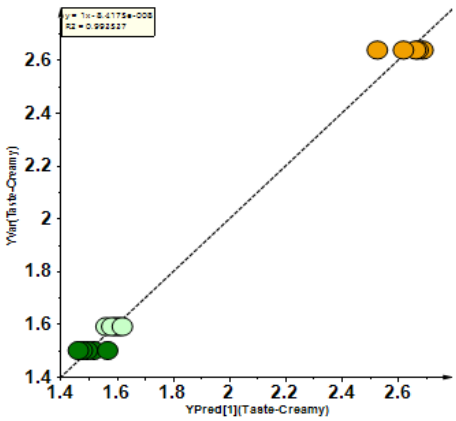

Taste Creamy

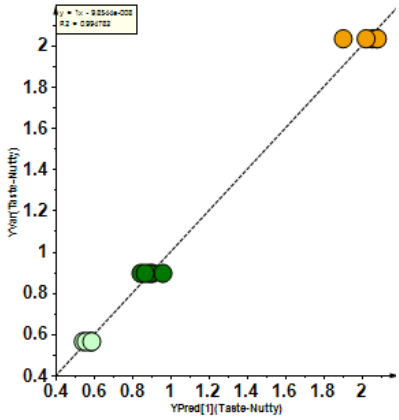

Taste Nutty

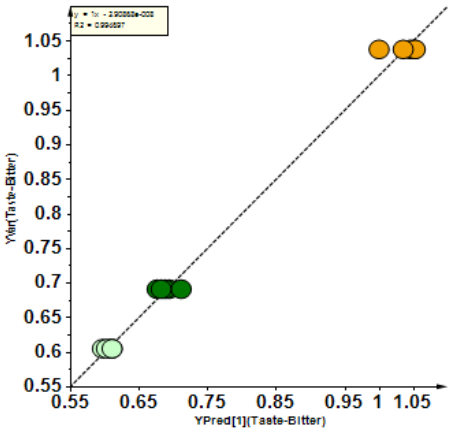

Taste Bitter

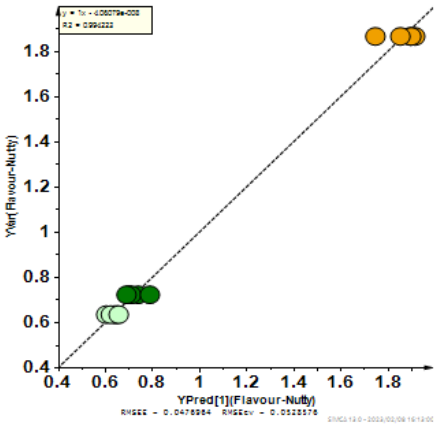

Flavor Nutty

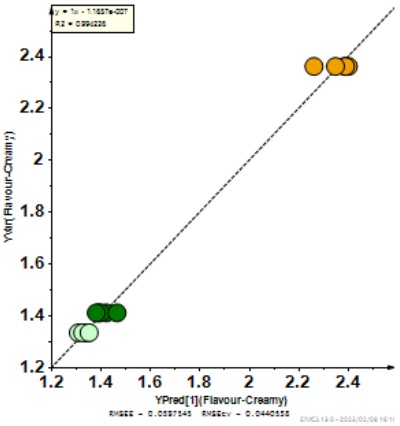

Flavor Creamy

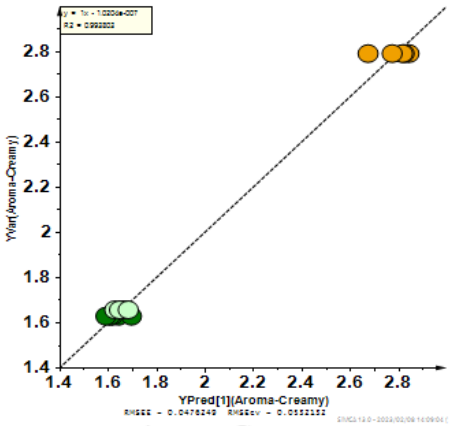

Aroma Creamy

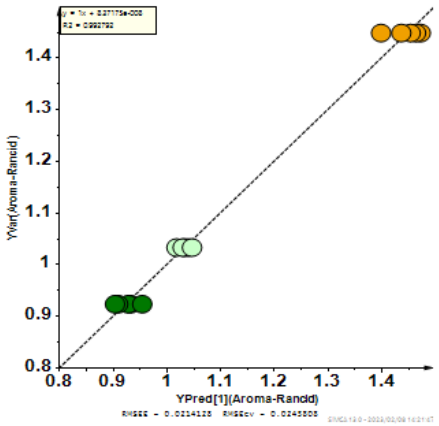

Aroma Rancid

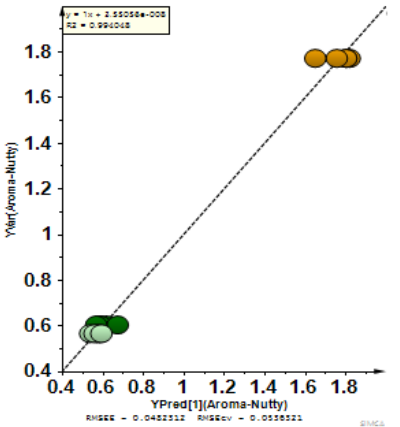

Aroma Nutty

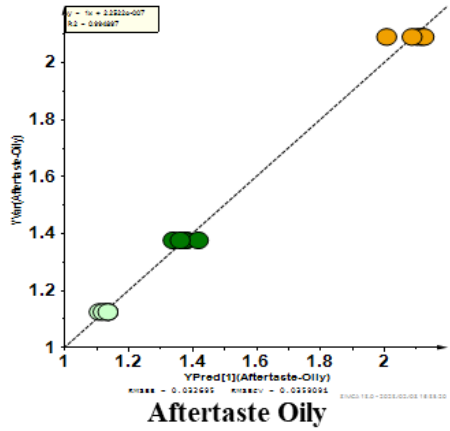

Aftertaste Oily

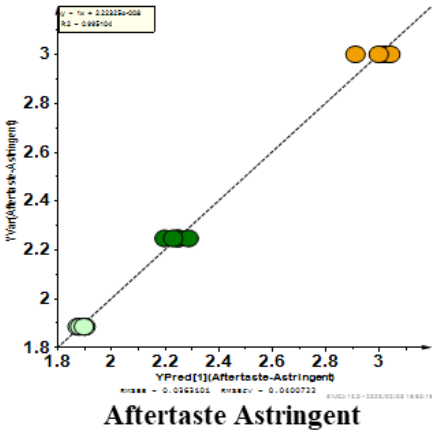

Aftertaste Astringent

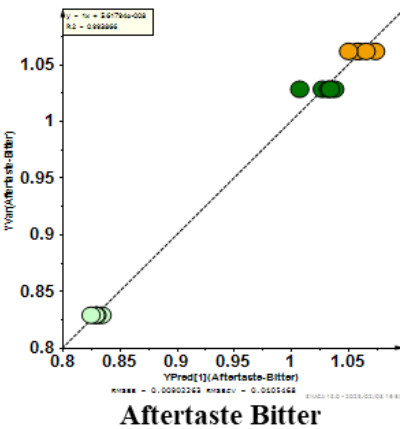

Aftertaste Bitter

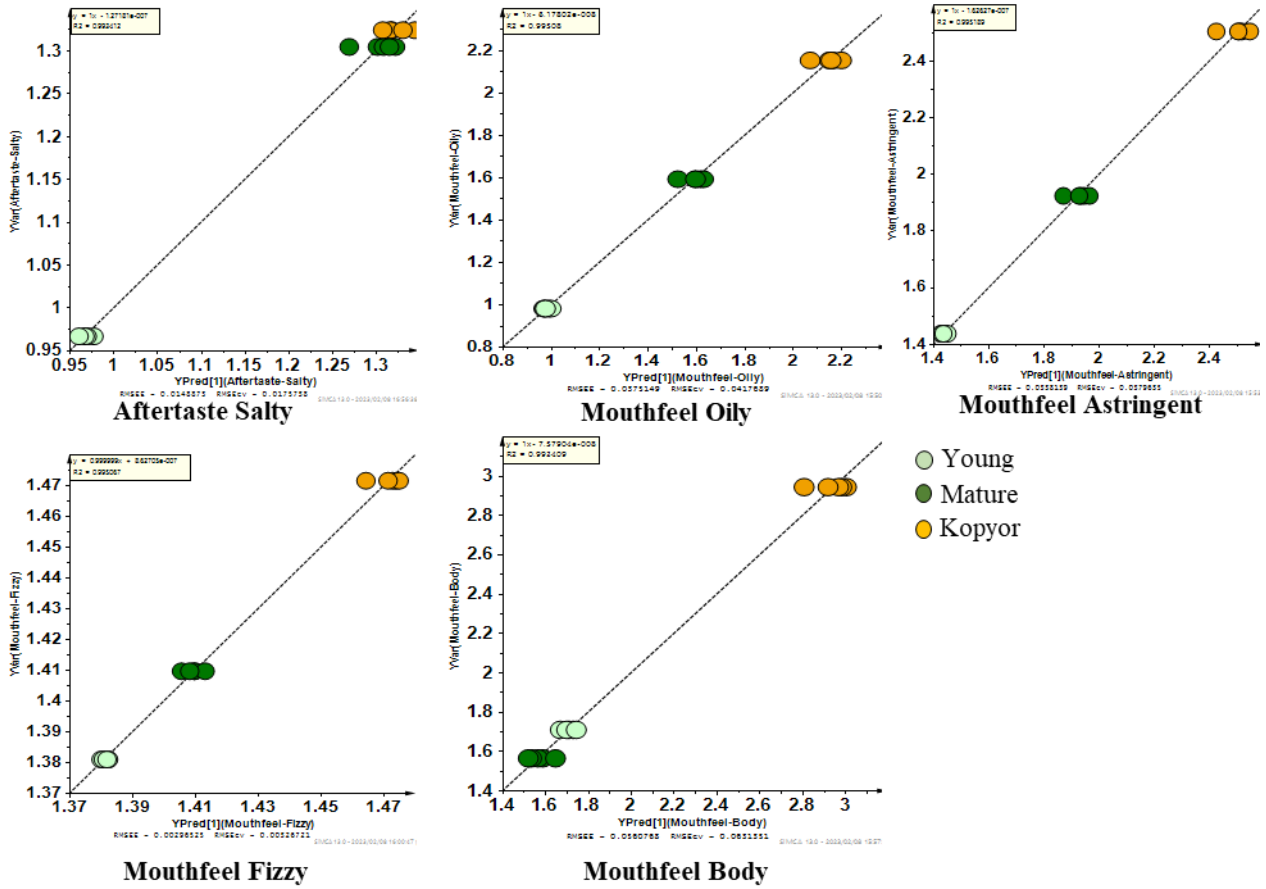

Figure S3. A summary of orthogonal partial least-square regression (OPLSR) models for attributes of Kopyor water.

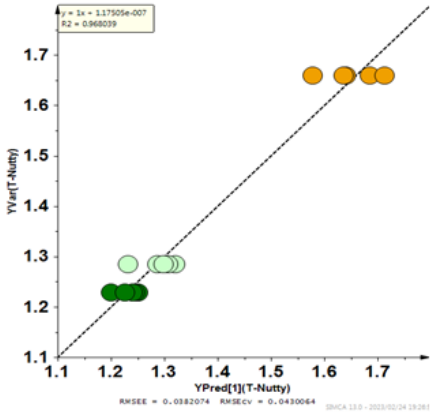

Taste Nutty

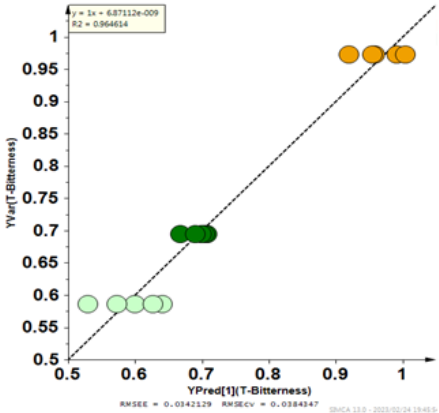

Taste Bitter

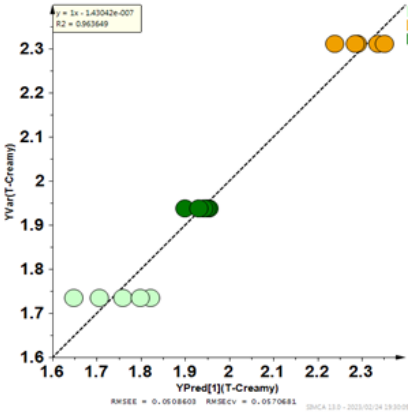

Taste Creamy

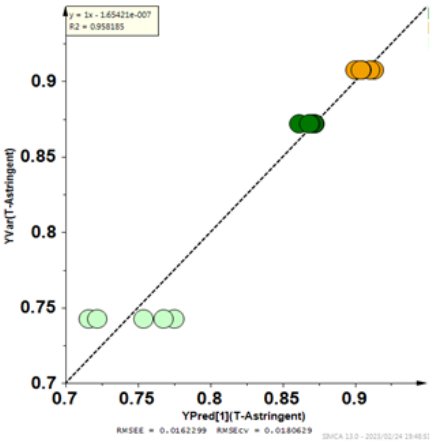

Taste Astringent

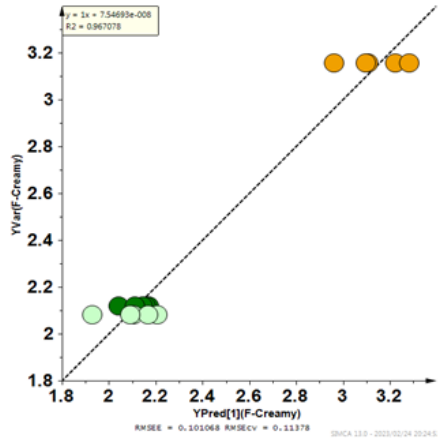

Flavor Creamy

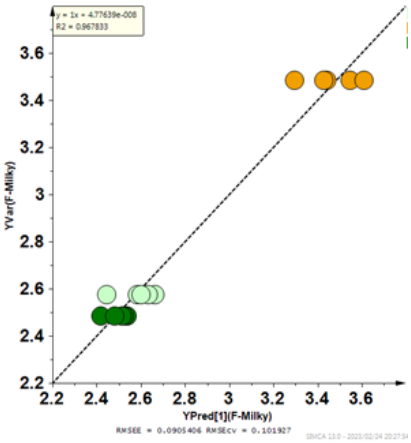

Flavor Milky

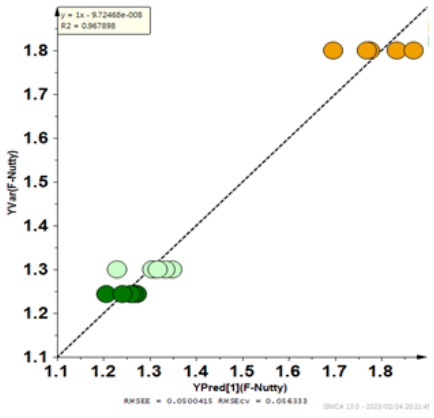

Flavor Nutty

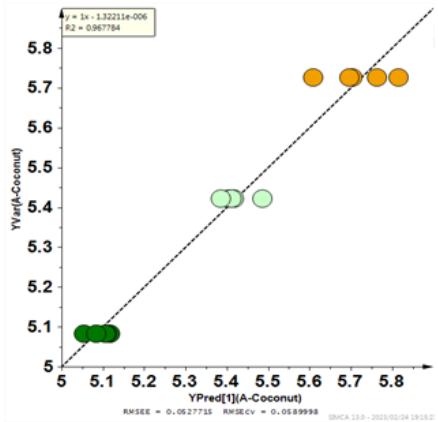

Aroma Coconut

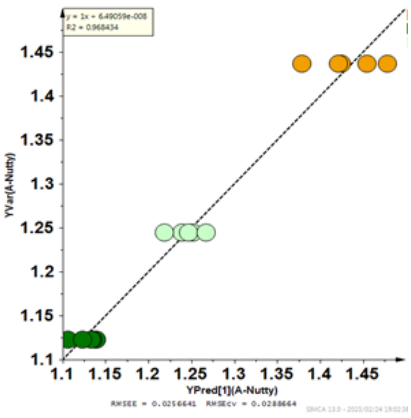

Aroma Nutty

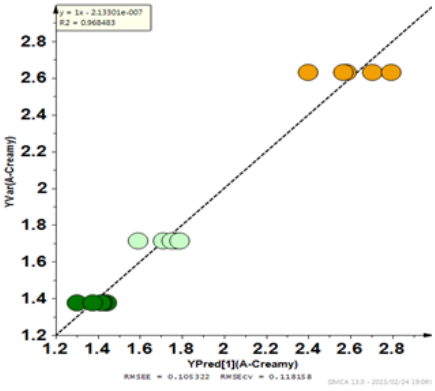

Aroma Creamy

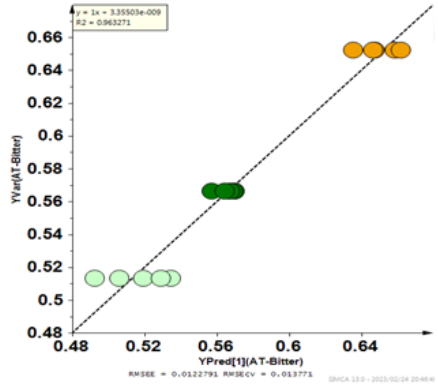

Aftertaste Bitter

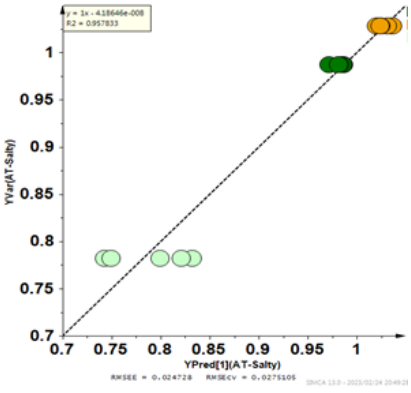

Aftertaste Salty

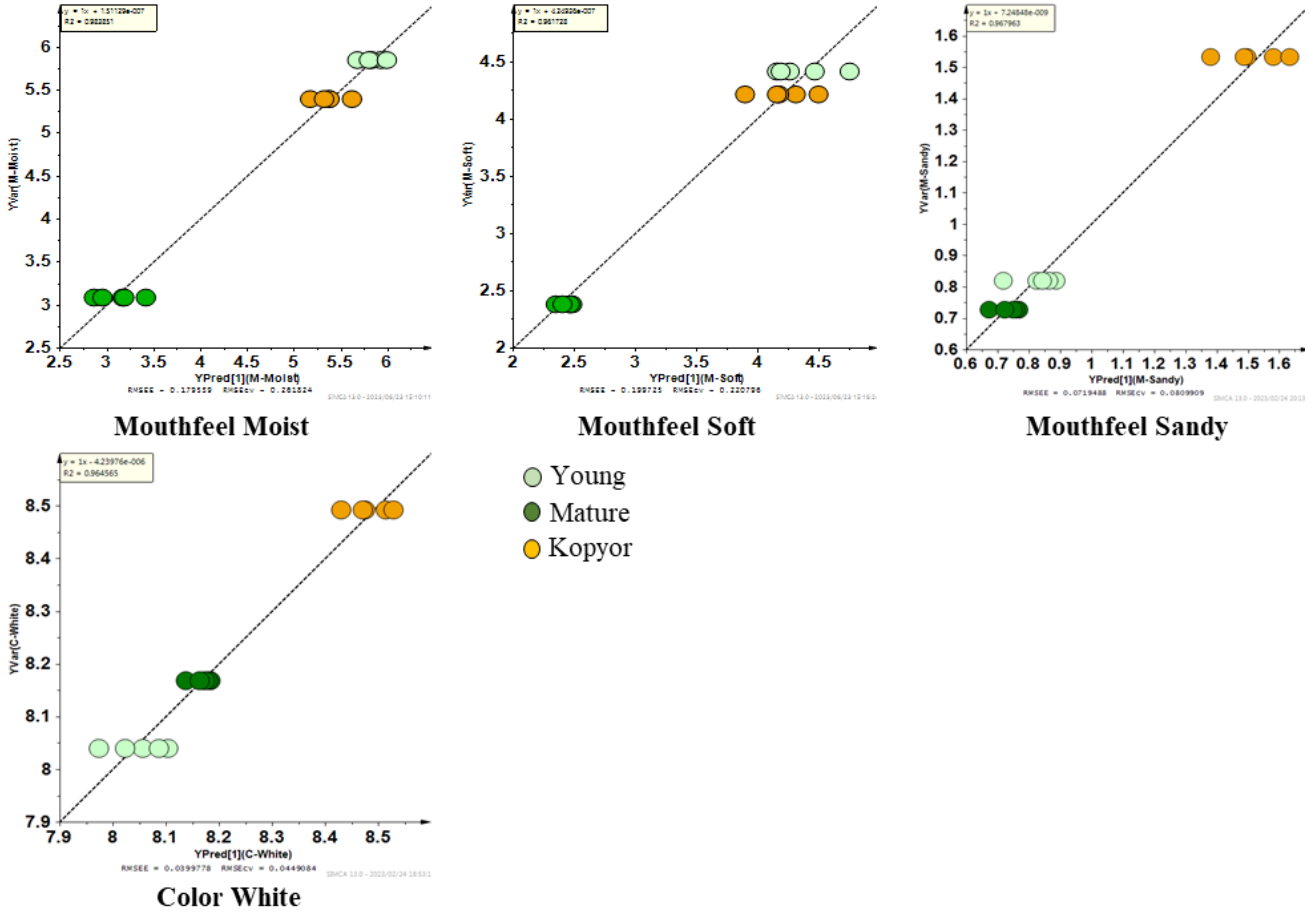

Figure S4. A summary of orthogonal partial least-square regression (OPLSR) models for attributes of Kopyor flesh.

Appendix

Supplementary Table

Table S1. Loading Score of PCA water based on PC1 and PC2

Number	Metabolite and Loading Score			
	Metabolite	PC1	Metabolite	PC2
1	Glutamic acid	0.13695	Galactose	0.22567
2	Alanine	0.13567	Mannitol	0.22528
3	Serine	0.13564	Sugar compound 2	0.22363
4	Maltitol	0.13534	Galactitol	0.22115
5	β-Alanine	0.13527	Dulcitol	0.22097
6	Sucrose	0.13467	Sorbitol	0.21942
7	Ornithine	0.13464	Myo-inositol	0.20286
8	Palatinose	0.13420	Mannose	0.16372
9	Lactulose	0.13360	Tetradecylglycerol	0.16017
10	Aspartic acid	0.13352	Sugar compound 3	0.15263
11	Pyroglutamic acid	0.13347	Trehalose	0.14673
12	Inositol	0.13326	Gentiobiose	0.12651
13	Butane	0.13320	Melibiose	0.11197
14	Proline	0.13296	Sugar alcohol compound	0.10845
15	Xylitol	0.13228	Arabitol	0.10431
16	Glycine	0.13218	Cellobiose	0.10071
17	α-D-xylopyranose	0.13214	Lyxose	0.06453
18	Turanose	0.13116	Meso erythritol	0.05901
19	Glycerol	0.13115	Quinic acid	0.05892
20	Citric acid	0.13113	β-Lactose	0.05884
21	Threonine	0.13098	Ribose	0.05605
22	Phosphate	0.13060	Sugar compound 1	0.04294
23	Cysteine	0.13032	Glycerol	0.04268
24	Lyxose	0.13002	Threitol	0.04000
25	Ribose	0.12980	Lactulose	0.03623
26	Phenylalanine	0.12975	Turanose	0.03375
27	Glutamine	0.12961	α-D-xylopyranose	0.02197
28	2-α-mannobiose	0.12957	Glycoside	0.00620
29	Succinic acid	0.12810	Maltitol	-0.00595
30	Leucine	0.12788	Glutamic acid	-0.00894
31	2-aminoethanol	0.12776	2-α-mannobiose	-0.02314

Number	Metabolite and Loading Score			
	Metabolite	PC1	Metabolite	PC2
32	Allothreonine	0.12736	Xylitol	-0.02765
33	Isoleucine	0.12717	Serine	-0.02882
34	Fumaric acid	0.12716	Alanine	-0.03457
35	Sugar compound 1	0.12628	Ornithine	-0.03462
36	Pentitol	0.12559	β-Alanine	-0.03659
37	Quinic acid	0.12534	Cysteine	-0.04117
38	Butanoic acid	0.12416	Sucrose	-0.04647
39	4-Aminobutyric acid	0.12392	Glucaric acid	-0.04659
40	Methionine	0.12321	Aspartic acid	-0.04660
41	Putrescine	0.12279	Pyroglutamic acid	-0.04957
42	Meso erythritol	0.12065	Palatinose	-0.04971
43	Phosphoric acid	0.11938	Inositol	-0.05469
44	Valine	0.11932	Butane	-0.05545
45	Glycoside	0.11677	Proline	-0.05567
46	Melibiose	0.11542	Glycine	-0.06177
47	Tetradecylglycerol	0.09645	Threonine	-0.06681
48	Trehalose	0.09073	Citric acid	-0.06685
49	Gentiobiose	0.08865	Phosphate	-0.06764
50	β-Lactose	0.07307	Phenylalanine	-0.07128
51	Sugar compound 3	0.06656	Glutamine	-0.07235
52	Arabitol	0.05977	Succinic acid	-0.08068
53	Myo-inositol	0.05676	Allothreonine	-0.08235
54	Shikimic acid	0.05469	2-aminoethanol	-0.08319
55	Cellobiose	0.05426	Methionine	-0.08350
56	Sugar alcohol compound	0.05421	Fumaric acid	-0.08422
57	Arabinose	0.03953	Leucine	-0.08436
58	Threitol	0.03814	Isoleucine	-0.08645
59	Sorbitol	0.03657	Pentitol	-0.08759
60	Butanedioic acid	0.03625	Phosphoric acid	-0.09165
61	Dulcitol	0.03478	α-D-glucopyranoside	-0.09421
62	Galactitol	0.03456	Putrescine	-0.09515
63	Malic acid	0.02742	Butanoic acid	-0.09644

Number	Metabolite and Loading Score			
	Metabolite	PC1	Metabolite	PC2
64	Galactose	-0.01807	Glucopyranose	-0.09765
65	Mannitol	-0.01906	4-Aminobutyric acid	-0.09905
66	Mannose	-0.02068	Sorbose	-0.09950
67	Sugar compound 2	-0.02429	Glucose	-0.10152
68	Lysine	-0.07424	Tagatose	-0.10391
69	β-D-mannopyranose	-0.09778	Xylose	-0.10592
70	Glucopyranose	-0.10507	Fructose	-0.10644
71	Talose	-0.11285	β-D-mannopyranose	-0.10779
72	α-D-glucopyranoside	-0.11841	Glyceryl-glycoside	-0.10826
73	Glyceryl-glycoside	-0.11938	Valine	-0.11255
74	Xylose	-0.12021	Talose	-0.12327
75	Fructose	-0.12035	Lysine	-0.18647
76	Tagatose	-0.12047	Arabinose	-0.19021
77	Glucose	-0.12139	Shikimic acid	-0.20043
78	Sorbose	-0.12265	Butanedioic acid	-0.20249
79	Glucaric acid	-0.13023	Malic acid	-0.20798

Table S2. Loading Score of PCA flesh based on PC1 and PC2

Number	Metabolite and Loading Score			
	Metabolite	PC1	Metabolite	PC2
1	Malic acid	0.15507	Threonine	0.38130
2	Inositol	0.15476	Rhamnose	0.37693
3	2-Aminoethanol	0.15455	Citric acid	0.36070
4	Lactulose	0.15447	Phenylalanine	0.30289
5	Talose	0.15447	Leucine	0.26763
6	Serine	0.15438	Sorbitol	0.19574
7	Sorbose	0.15427	Isoleucine	0.18445
8	Alanine	0.15423	Glycine	0.18292
9	Fructose	0.15421	Benzoic acid	0.14236
10	Pyroglutamic acid	0.15418	Fumaric acid	0.12527
11	Glutamic acid	0.15415	Succinic acid	0.11953
12	Aspartic acid	0.15410	Proline	0.10445

Number	Metabolite and Loading Score			
	Metabolite	PC1	Metabolite	PC2
13	Glucose	0.15394	Allothreonine	0.08675
14	Galactose	0.15355	α-D-glucopyranoside	0.07131
15	Valine	0.15347	Sucrose	0.06549
16	Tagatose	0.15339	Valine	0.04667
17	Galactinol	0.15327	Glycerol	0.04000
18	Mannitol	0.15313	4-Aminobutyric acid	0.03393
19	Sucrose	0.15308	Cysteine	0.03122
20	Mannose	0.15289	Sugar alcohol 2	0.02566
21	α-D-glucopyranoside	0.15277	Methionine	0.01605
22	Quinic acid	0.15276	Pyroglutamic acid	0.01442
23	Sugar compound 1	0.15183	Serine	0.00929
24	Meso-erythritol	0.15157	Talose	0.00657
25	Cysteine	0.15154	Malic acid	-0.00176
26	D-talopyranose	0.15129	Inositol	-0.00291
27	Glutamine	0.15051	Glutamic acid	-0.00292
28	Sugar alcohol 2	0.15024	Unknown 1	-0.00827
29	Methionine	0.14973	Aspartic acid	-0.02454
30	Putrescine	0.14906	Alanine	-0.02844
31	Maltose	0.14853	Meso-Erythritol	-0.04266
32	Raffinose	0.14796	β-Alanine	-0.04380
33	Allothreonine	0.14771	Lactulose	-0.04554
34	Proline	0.14756	Putrescine	-0.04624
35	Unknown 1	0.14734	2-Aminoethanol	-0.04737
36	Succinic acid	0.14658	Galactose	-0.04766
37	Fumaric acid	0.13904	Quinic acid	-0.05089
38	Glycine	0.13564	Glutamine	-0.05204
39	Isoleucine	0.13299	Sorbose	-0.05377
40	4-Aminobutyric acid	0.11716	Maltose	-0.05408
41	Sugar alcohol 1	0.11637	Fructose	-0.05435
42	Leucine	0.10975	Glucose	-0.05630
43	Phenylalanine	0.07241	Sugar compound 1	-0.05893
44	Dulcitol	0.06230	Mannose	-0.06016

Number	Metabolite and Loading Score			
	Metabolite	PC1	Metabolite	PC2
45	Benzoic acid	0.01431	Galactinol	-0.06117
46	Threonine	-0.00470	Tagatose	-0.06171
47	β-Alanine	-0.01769	Raffinose	-0.06421
48	Rhamnose	-0.02385	Mannitol	-0.06477
49	Citric acid	-0.04943	D-talopyranose	-0.08438
50	Sorbitol	-0.06430	Sugar alcohol 1	-0.20067
51	Phosphate	-0.11397	Phosphate	-0.23111
52	Glycerol	-0.13936	Dulcitol	-0.26279

Table S3. List of metabolites in volcano plot to compare water of kopyor and normal mature, which were significantly different based on *t*-test (*p*-value less than 0.05)

Fold Change 2 and more							
Number	Metabolite	Relative Intensity		Fold Change (FC) (Kopyor/Old)	*p*-value	log2FC	Minus log10 *p*-value
		Kopyor	Old				
1	Fumaric acid	0.0318	0.0013	25.0692	0.000	4.6478	4.9351
2	2-Aminoethanol	0.0371	0.0029	12.6091	0.000	3.6564	4.7567
3	Glutamine	0.0253	0.0023	10.8997	0.000	3.4462	4.7899
4	Succinic acid	0.0686	0.0074	9.2394	0.000	3.2078	5.3106
5	Isoleucine	0.0712	0.0085	8.3270	0.000	3.0578	5.1808
6	Allothreonine	0.0291	0.0036	7.9974	0.000	2.9995	5.2717
7	Leucine	0.1061	0.0152	7.0029	0.000	2.8080	4.9066
8	Phenylalanine	0.0180	0.0026	6.8266	0.000	2.7712	4.4873
9	Citric acid	0.0547	0.0083	6.6048	0.000	2.7235	4.4328
10	Glycine	0.1386	0.0212	6.5402	0.000	2.7093	4.8012
11	Pentitol	0.0164	0.0026	6.4085	0.000	2.6800	4.9707
12	Valine	0.1457	0.0264	5.5184	0.000	2.4642	4.7155
13	Proline	0.2416	0.0470	5.1370	0.000	2.3609	4.8266
14	Aspartic acid	0.0459	0.0090	5.1271	0.000	2.3581	3.7258
15	Methionine	0.0125	0.0025	5.0754	0.000	2.3435	4.0022
16	Threonine	0.0918	0.0202	4.5526	0.000	2.1867	4.3276

17	4-Aminobutyric acid	0.3348	0.0752	4.4496	0.000	2.1537	4.9930
18	Butane	0.2526	0.0583	4.3324	0.000	2.1152	4.9717
19	Pyroglutamic acid	0.0697	0.0165	4.2146	0.000	2.0754	3.9546
20	Butanoic acid	0.0657	0.0166	3.9559	0.000	1.9840	5.4381
21	Sucrose	28.0060	7.9739	3.5122	0.000	1.8124	5.4557
22	Palatinose	13.2509	3.8339	3.4563	0.000	1.7892	4.6828
23	Serine	0.1303	0.0391	3.3349	0.000	1.7376	4.4836
24	β-Alanine	0.0253	0.0076	3.3102	0.000	1.7269	6.5054
25	Ornithine	0.0085	0.0026	3.3073	0.000	1.7256	4.6464
26	Alanine	0.7816	0.2414	3.2374	0.000	1.6948	4.4816
27	Shikimic acid	0.0058	0.0019	3.0911	0.000	1.6281	3.4366
28	Putrescine	0.0054	0.0018	3.0194	0.000	1.5943	3.9999
29	Phosphate	0.1753	0.0602	2.9104	0.000	1.5412	5.1607
30	Inositol	0.0784	0.0276	2.8449	0.000	1.5084	5.8126
31	Glutamic acid	0.0519	0.0185	2.8134	0.000	1.4923	4.0110
32	Phosphoric acid	0.0133	0.0049	2.7392	0.001	1.4538	3.1993
33	Xylitol	0.0040	0.0015	2.6497	0.000	1.4058	3.9338
34	Maltitol	0.0074	0.0032	2.3378	0.000	1.2252	3.8480
35	Cysteine	0.0043	0.0019	2.2770	0.001	1.1871	2.9658
36	Arabinose	0.0082	0.0037	2.2233	0.002	1.1527	2.6405

Fold Change 0.5-2

Number	Metabolite	Relative Intensity			*p*-value	log2FC	Minus log10 *p*-value

		Kopyor	Old	Fold Change (FC) (Kopyor/Old)			
1	Lactulose	0.0159	0.0084	1.8907	0.000	0.9189	3.3251
2	α-D-xylopyranose	0.0116	0.0062	1.8644	0.001	0.8987	2.8639
3	2-α-mannobiose	0.0100	0.0057	1.7577	0.001	0.8137	3.2838
4	Glycoside	0.0128	0.0074	1.7263	0.019	0.7877	1.7258
5	Malic acid	1.2737	0.7398	1.7217	0.001	0.7839	3.0728
6	Butanedioic acid	0.2224	0.1296	1.7159	0.001	0.7790	3.1043
7	Ribose	0.0148	0.0095	1.5609	0.003	0.6424	2.5045
8	Lysine	0.0782	0.0515	1.5187	0.000	0.6029	3.8881
9	Quinic acid	0.0181	0.0120	1.5117	0.012	0.5962	1.9283
10	Lyxose	0.0320	0.0214	1.4967	0.002	0.5818	2.7932
11	Sugar compound 1	0.0136	0.0092	1.4794	0.020	0.5650	1.7007
12	Turanose	0.0252	0.0177	1.4208	0.004	0.5067	2.4551
13	Glycerol	0.1313	0.0950	1.3818	0.006	0.4666	2.2469
14	Meso erythritol	0.0076	0.0055	1.3759	0.046	0.4604	1.3355
15	Tetradecylglycerol	0.0639	0.0719	0.8889	0.044	-0.1700	1.3535
16	Glucaric acid	0.0377	0.0493	0.7646	0.002	-0.3872	2.7273
17	Glucopyranose	0.0144	0.0197	0.7325	0.023	-0.4492	1.6356
18	Talose	0.0639	0.0890	0.7178	0.003	-0.4783	2.4863
19	Myo-inositol	0.0231	0.0377	0.6133	0.003	-0.7054	2.5682
20	α-D-glucopyranoside	0.0055	0.0095	0.5767	0.000	-0.7940	3.3203
21	Glyceryl-glycoside	0.1060	0.2069	0.5123	0.000	-0.9650	3.4404

Fold Change less than 0.5							
Number	Metabolite	Relative Intensity		Fold Change (FC) (Kopyor/Old)	*p*-value	log2FC	Minus log10 *p*-value
		Kopyor	Old				
1	Xylose	1.1888	2.5338	0.4692	0.000	-1.092	3.556
2	Tagatose	0.2548	0.5519	0.4616	0.000	-1.115	3.570
3	Glucose	3.5704	7.9752	0.4477	0.000	-1.159	3.341
4	Fructose	2.5893	5.9317	0.4365	0.000	-1.196	3.928
5	Sorbose	4.5584	10.5001	0.4341	0.000	-1.204	3.599
6	Sorbitol	4.9485	11.4729	0.4313	0.000	-1.213	3.477
7	Galactitol	4.3089	10.3383	0.4168	0.000	-1.263	3.881
8	Dulcitol	3.9139	9.4389	0.4147	0.000	-1.270	4.041
9	Sugar compound2	0.0049	0.0291	0.1690	0.000	-2.564	4.633
10	Mannitol	0.0128	0.1047	0.1227	0.000	-3.027	4.309
11	Galactose	0.1208	0.9892	0.1221	0.000	-3.033	4.420
12	Mannose	0.0111	0.1364	0.0810	0.032	-3.625	1.491

Table S4. List of metabolites in volcano plot to compare water of kopyor and normal young, which were significantly different based on *t*-test (*p*-value less than 0.05)

Fold Change 2 and more							
Number	Metabolite	Relative Intensity		Fold Change (FC) (Old/Young)	*p*-value	log2FC	Minus log10 *p*-value
		Old	Young				
1	Aspartic acid	0.0459	0.0009	49.3911	0.000	5.6262	4.5152
2	Glutamic acid	0.0519	0.0018	28.5006	0.000	4.8329	5.5480
3	Glutamine	0.0253	0.0011	22.7816	0.000	4.5098	4.8455
4	Glycine	0.1386	0.0063	21.9363	0.000	4.4553	4.9594
5	Fumaric acid	0.0318	0.0015	21.9243	0.000	4.4545	4.9918
6	Lactulose	0.0159	0.0009	17.5189	0.000	4.1308	4.0658
7	Serine	0.1303	0.0087	14.9894	0.000	3.9059	4.9247
8	Dulcitol	3.9139	0.2746	14.2551	0.000	3.8334	4.8858
9	Proline	0.2416	0.0170	14.2074	0.000	3.8286	4.8452
10	Citric acid	0.0547	0.0040	13.6434	0.000	3.7701	5.2011
11	2-aminoethanol	0.0371	0.0031	12.1572	0.000	3.6037	4.6969
12	Pyroglutamic acid	0.0697	0.0058	11.9531	0.000	3.5793	4.2861
13	Galactitol	4.3089	0.3648	11.8102	0.000	3.5620	5.4772
14	Sorbitol	4.9485	0.4358	11.3541	0.000	3.5051	5.2340
15	Phenylalanine	0.0180	0.0017	10.8737	0.000	3.4428	4.6416
16	Succinic acid	0.0686	0.0066	10.3713	0.000	3.3745	4.6042

17	Ornithine	0.0085	0.0008	10.3031	0.000	3.3650	4.8899
18	Tetradecylglycerol	0.0639	0.0063	10.1958	0.000	3.3499	4.3817
19	Melibiose	0.0070	0.0007	10.0776	0.000	3.3331	4.5530
20	Alanine	0.7816	0.0806	9.6943	0.000	3.2771	4.9852
21	β-Alanine	0.0253	0.0028	9.0768	0.000	3.1822	6.2680
22	Butane	0.2526	0.0280	9.0343	0.000	3.1754	4.9413
23	Allothreonine	0.0291	0.0035	8.2939	0.000	3.0521	5.1113
24	Lyxose	0.0320	0.0041	7.8792	0.000	2.9780	5.2928
25	Ribose	0.0148	0.0019	7.8487	0.000	2.9725	4.8256
26	Maltitol	0.0074	0.0009	7.8462	0.000	2.9720	4.3549
27	Sucrose	28.0060	3.6539	7.6646	0.000	2.9382	6.1015
28	Isoleucine	0.0712	0.0097	7.3054	0.000	2.8690	5.0926
29	Quinic acid	0.0181	0.0025	7.2370	0.000	2.8554	4.9495
30	Leucine	0.1061	0.0157	6.7765	0.000	2.7605	5.0069
31	Palatinose	13.2509	1.9763	6.7050	0.000	2.7452	5.0747
32	Threonine	0.0918	0.0138	6.6522	0.000	2.7338	4.2981
33	α-D-xylopyranose	0.0116	0.0019	6.0901	0.000	2.6065	3.7940
34	Trehalose	0.0068	0.0011	5.9195	0.000	2.5655	4.2991
35	Xylitol	0.0040	0.0007	5.6313	0.000	2.4935	4.2691
36	Pentitol	0.0164	0.0030	5.4817	0.000	2.4546	4.9800
37	Methionine	0.0125	0.0026	4.7515	0.001	2.2484	3.2269
38	Myo-inositol	0.0231	0.0053	4.3743	0.000	2.1291	4.0600
39	Inositol	0.0784	0.0189	4.1381	0.000	2.0490	4.8551

40	Glycoside	0.0128	0.0033	3.8143	0.000	1.9314	3.4880
41	Phosphate	0.1753	0.0508	3.4476	0.000	1.7856	4.4391
42	4-Aminobutyric acid	0.3348	0.0972	3.4463	0.000	1.7850	4.9145
43	Meso erythritol	0.0076	0.0023	3.3707	0.002	1.7530	2.6722
44	Butanoic acid	0.0657	0.0200	3.2770	0.000	1.7124	4.5300
45	Valine	0.1457	0.0445	3.2744	0.000	1.7112	3.8615
46	Cysteine	0.0043	0.0013	3.2362	0.000	1.6943	4.2222
47	Sugar compound1	0.0136	0.0042	3.2339	0.000	1.6933	5.3638
48	Putrescine	0.0054	0.0020	2.6494	0.000	1.4057	4.7778
49	Glycerol	0.1313	0.0517	2.5399	0.000	1.3448	4.2881
50	2-α-mannobiose	0.0100	0.0040	2.5279	0.001	1.3379	3.2873
51	Phosphoric acid	0.0133	0.0053	2.5000	0.001	1.3219	3.0238
52	Turanose	0.0252	0.0106	2.3718	0.000	1.2460	3.6154

Fold Change 0.5-2

Number	Metabolite	Relative Intensity		Fold Change (FC) (Kopyor/Old)	*p*-value	log2FC	Minus log10 *p*-value
		Kopyor	Old				
1	Gentiobiose	0.0124	0.0071	1.7553	0.015	0.8117	1.8180
2	Sugar compound 3	0.0189	0.0132	1.4339	0.022	0.5199	1.6637
3	Arabitol	0.0109	0.0080	1.3558	0.021	0.4392	1.6706
4	Shikimic acid	0.0058	0.0047	1.2258	0.013	0.2938	1.8708
5	Galactose	0.1208	0.1057	1.1435	0.031	0.1934	1.5087
6	Glucaric acid	0.0377	0.0639	0.5894	0.000	-0.7627	3.5871

7	Lysine	0.0782	0.1384	0.5649	0.000	-0.8239	3.6474

Fold Change less than 0.5

Number	Metabolite	Relative Intensity		Fold Change (FC) (Kopyor/Old)	*p*-value	log2FC	Minus log10 *p*-value
		Kopyor	Old				
1	β-D-mannopyranose	0.0061	0.0170	0.3564	0.004	-1.4885	2.4447
2	Glucopyranose	0.0144	0.0424	0.3404	0.004	-1.5547	2.3963
3	α-D-glucopyranoside	0.0055	0.0219	0.2506	0.000	-1.9965	3.4701
4	Talose	0.0639	0.2917	0.2191	0.000	-2.1904	4.1288
5	Glyceryl-glycoside	0.1060	0.6236	0.1700	0.000	-2.5566	4.6223
6	Tagatose	0.2548	1.6479	0.1546	0.000	-2.6935	4.5752
7	Glucose	3.5704	23.2309	0.1537	0.000	-2.7019	4.8811
8	Xylose	1.1888	7.7577	0.1532	0.000	-2.7061	4.7267
9	Sorbose	4.5584	29.8822	0.1525	0.000	-2.7127	5.5608
10	Fructose	2.5893	19.1898	0.1349	0.000	-2.8897	4.9464

Table S5. List of metabolites in volcano plot to compare flesh of kopyor and normal mature, which were significantly different based on *t*-test (*p*-value less than 0.05)

Fold Change 2 and more							
Number	Metabolite	Relative Intensity		Fold Change (FC)	*p*-value	log2FC	Minus log10 *p*-value
		Kopyor	Old	(Kopyor/Old)			
1	Rhamnose	0.0488	0.0053	9.1219	0.000	3.1893	3.8528
2	Fumaric acid	0.0104	0.0013	7.8781	0.001	2.9778	3.1096
3	Threonine	0.0182	0.0023	7.7647	0.000	2.9569	3.5976
4	Isoleucine	0.0238	0.0036	6.6524	0.000	2.7339	3.4580
5	Leucine	0.0334	0.0051	6.5134	0.000	2.7034	3.8557
6	Putrescine	0.0041	0.0007	5.5723	0.000	2.4783	3.7472
7	Phenylalanine	0.0055	0.0011	5.2054	0.003	2.3800	2.5257
8	Sucrose	6.4815	1.3354	4.8534	0.000	2.2790	3.5236
9	Valine	0.0514	0.0112	4.5916	0.001	2.1990	3.1173
10	Cysteine	0.0027	0.0006	4.5505	0.004	2.1860	2.4449
11	Glucose	0.2356	0.0526	4.4773	0.002	2.1626	2.7403
12	Glycine	0.0439	0.0102	4.3245	0.000	2.1125	3.4613
13	α-D-glucopyranoside	2.7748	0.6521	4.2555	0.000	2.0893	3.6828
14	Sugar compound 1	0.0031	0.0007	4.2476	0.010	2.0867	2.0173
15	Talose	0.0089	0.0021	4.2173	0.000	2.0763	3.8636
16	Aspartic acid	0.0146	0.0038	3.8796	0.000	1.9559	4.1484

17	Citric acid	0.0391	0.0101	3.8584	0.000	1.9480	3.3738
18	Succinic acid	0.0449	0.0125	3.5790	0.000	1.8396	3.8855
19	Mannitol	0.0956	0.0268	3.5631	0.038	1.8331	1.4160
20	Proline	0.0730	0.0209	3.4877	0.001	1.8023	2.9865
21	Lactulose	0.0013	0.0004	3.2931	0.004	1.7194	2.3574
22	Alanine	0.2002	0.0611	3.2780	0.000	1.7128	3.7854
23	Glutamine	0.0031	0.0010	3.2439	0.009	1.6977	2.0234
24	Serine	0.0397	0.0136	2.9171	0.000	1.5445	3.5348
25	Sugar alcohol2	0.0026	0.0009	2.8846	0.001	1.5284	2.8689
26	Galactinol	0.0081	0.0029	2.7948	0.009	1.4827	2.0579
27	Mannose	0.0156	0.0058	2.7136	0.002	1.4402	2.8055
28	Pyroglutamic acid	0.0171	0.0069	2.4897	0.000	1.3160	3.8043
29	Allothreonine	0.0109	0.0045	2.4049	0.004	1.2660	2.4311
30	Methionine	0.0047	0.0020	2.3230	0.007	1.2160	2.1714
31	Sorbose	0.4137	0.1783	2.3199	0.004	1.2141	2.3491
32	Glutamic acid	0.0130	0.0057	2.2709	0.001	1.1833	2.8498
33	Fructose	0.2492	0.1114	2.2378	0.005	1.1621	2.3196
34	Inositol	0.0324	0.0148	2.1902	0.001	1.1311	3.0416
35	Unknown 1	0.0016	0.0008	2.0873	0.035	1.0616	1.4594
36	Malic acid	0.3067	0.1486	2.0645	0.007	1.0458	2.1694

Fold Change 0.5-2

Number	Metabolite	Relative Intensity		Fold Change (FC) (Kopyor/Old)	*p*-value	log2FC	Minus log10 *p*-value

		Kopyor	Old				
1	Galactose	0.0248	0.0129	1.9250	0.012	0.9449	1.9391
2	2-aminoethanol	0.0175	0.0100	1.7567	0.001	0.8129	3.1320
3	4-Aminobutyric acid	0.1902	0.1160	1.6396	0.024	0.7133	1.6261
4	Tagatose	0.0036	0.0025	1.4523	0.003	0.5383	2.5761
5	Maltose	0.0024	0.0017	1.4166	0.046	0.5025	1.3399
6	Sugar alcohol 1	0.0130	0.0193	0.6738	0.027	-0.5696	1.5619
7	Dulcitol	0.0106	0.0183	0.5791	0.012	-0.7882	1.9174
8	Phosphate	0.0410	0.0781	0.5244	0.002	-0.9314	2.7971

Table S6. List of metabolites in volcano plot to compare flesh of kopyor and normal young, which were significantly different based on t-test (*p*-value less than 0.05)

Fold Change 2 and more							
Number	Metabolite	Relative Intensity		Fold Change (FC) (Kopyor/Old)	*p-value*	log2FC	Minus log10 p-value
		Kopyor	Young				
1	Citric acid	0.0391	0.0093	4.2134	0.000	2.0750	3.6655
2	Rhamnose	0.0488	0.0120	4.0621	0.000	2.0222	3.4401
3	Threonine	0.0182	0.0067	2.7253	0.000	1.4464	3.8409
4	Glycerol	0.0268	0.0118	2.2684	0.001	1.1817	3.0873
Fold Change 0.5-2							
Number	Metabolite	Relative Intensity			*p*-value	log2FC	Minus log10 *p*-value

		Kopyor	Young	Fold Change (FC) (Kopyor/Old)			
1	Sorbitol	1.2223	0.8775	1.3930	0.047	0.4782	1.3291
2	Phosphate	0.0410	0.0337	1.2170	0.010	0.2834	1.9841
3	Isoleucine	0.0238	0.0332	0.7164	0.043	-0.4811	1.3679
4	Glycine	0.0439	0.0629	0.6990	0.005	-0.5167	2.2739
5	Succinic acid	0.0449	0.0781	0.5752	0.005	-0.7980	2.2919
6	Allothreonine	0.0109	0.0194	0.5613	0.017	-0.8333	1.7577
7	Proline	0.0730	0.1308	0.5581	0.005	-0.8414	2.2719
8	Dulcitol	0.0106	0.0196	0.5405	0.001	-0.8878	2.8826
9	Fumaric acid	0.0104	0.0200	0.5181	0.001	-0.9488	2.9907

Fold Change Less Than 0.5

Number	Metabolite	Relative Intensity		Fold Change (FC) (Kopyor/Old)	*p*-value	log2FC	Minus log10 *p*-value
		Kopyor	Young				
1	4-Aminobutyric acid	0.1902	0.4073	0.4669	0.011	-1.0987	1.9511
2	Sugar alcohol 1	0.0130	0.0280	0.4645	0.001	-1.1061	3.0501
3	α-D-glucopyranoside	2.7748	6.2080	0.4470	0.001	-1.1617	3.1448
4	Sucrose	6.4815	15.1651	0.4274	0.001	-1.2264	3.0531
5	Sugar alcohol 2	0.0026	0.0067	0.3926	0.001	-1.3488	2.9424
6	Valine	0.0514	0.1314	0.3914	0.005	-1.3533	2.3405
7	Pyroglutamic acid	0.0171	0.0470	0.3636	0.001	-1.4595	2.8949
8	Methionine	0.0047	0.0128	0.3631	0.007	-1.4617	2.1432
9	Cysteine	0.0027	0.0083	0.3267	0.001	-1.6140	3.2776

10	Malic acid	0.3067	0.9507	0.3226	0.001	-1.6321	3.0428
11	Glutamic acid	0.0130	0.0409	0.3173	0.002	-1.6563	2.6183
12	Serine	0.0397	0.1259	0.3156	0.001	-1.6637	2.9086
13	Inositol	0.0324	0.1041	0.3110	0.000	-1.6851	3.4123
14	Talose	0.0089	0.0310	0.2867	0.001	-1.8024	2.8825
15	Unknown 1	0.0016	0.0059	0.2767	0.010	-1.8534	2.0104
16	Meso-Erythritol	0.0048	0.0193	0.2471	0.000	-2.0166	4.2223
17	Quinic acid	0.0051	0.0264	0.1915	0.000	-2.3848	3.6406
18	Maltose	0.0024	0.0131	0.1852	0.004	-2.4326	2.4230
19	2-aminoethanol	0.0175	0.0964	0.1816	0.001	-2.4614	3.1606
20	Alanine	0.2002	1.1097	0.1804	0.001	-2.4705	2.8998
21	Galactose	0.0248	0.1376	0.1803	0.000	-2.4716	3.4910
22	Aspartic acid	0.0146	0.0835	0.1752	0.000	-2.5127	3.3487
23	Raffinose	0.0019	0.0109	0.1717	0.004	-2.5417	2.3645
24	D-talopyranose	0.0090	0.0621	0.1450	0.000	-2.7855	3.9409
25	Tagatose	0.0036	0.0259	0.1384	0.000	-2.8526	3.5561
26	Putrescine	0.0041	0.0324	0.1261	0.004	-2.9876	2.4349
27	Lactulose	0.0013	0.0106	0.1240	0.001	-3.0121	3.1085
28	Fructose	0.2492	2.1585	0.1154	0.000	-3.1147	3.6723
29	Sorbose	0.4137	3.6482	0.1134	0.000	-3.1405	3.5417
30	Glutamine	0.0031	0.0313	0.1000	0.004	-3.3224	2.4370
31	Mannose	0.0156	0.1704	0.0918	0.000	-3.4451	3.4543
32	Sugar compound 1	0.0031	0.0381	0.0818	0.001	-3.6122	3.1384

33	Glucose	0.2356	2.8822	0.0817	0.000	-3.6129	3.7891
34	Galactinol	0.0081	0.1316	0.0618	0.000	-4.0164	3.5653
35	Mannitol	0.0956	1.7416	0.0549	0.000	-4.1877	3.5433

Table S7. List of metabolites in volcano plot to compare old and young water, which were significantly different based on *t*-test (*p*-value less than 0.05)

Fold Change 2 and more							
Number	Metabolite	Relative Intensity		Fold Change (FC) (Old/Young)	*p*-value	log2FC	Minus log10 *p*-value
		Old	Young				
1	Dulcitol	9.4389	0.2746	34.3780	0.000	5.1034	5.0124
2	Galactitol	10.3383	0.3648	28.3362	0.000	4.8246	4.8816
3	Sorbitol	11.4729	0.4358	26.3242	0.000	4.7183	4.3549
4	Tetradecylglycerol	0.0719	0.0063	11.4705	0.000	3.5199	5.4320
5	Glutamic acid	0.0185	0.0018	10.1304	0.000	3.3406	4.0319
6	Aspartic acid	0.0090	0.0009	9.6333	0.000	3.2680	3.3269
7	Galactose	0.9892	0.1057	9.3623	0.000	3.2269	4.5213
8	Lactulose	0.0084	0.0009	9.2658	0.000	3.2119	4.5403
9	Melibiose	0.0060	0.0007	8.6275	0.000	3.1089	3.6468
10	Mannitol	0.1047	0.0122	8.6055	0.000	3.1053	4.2252
11	Myo-inositol	0.0377	0.0053	7.1330	0.000	2.8345	4.0488
12	Trehalose	0.0074	0.0011	6.4501	0.002	2.6893	2.6718

13	Mannose	0.1364	0.0216	6.3118	0.041	2.6581	1.3922
14	Lyxose	0.0214	0.0041	5.2643	0.000	2.3962	4.0614
15	Sugar compound 2	0.0291	0.0057	5.1535	0.000	2.3655	3.9291
16	Ribose	0.0095	0.0019	5.0283	0.002	2.3301	2.7431
17	Quinic acid	0.0120	0.0025	4.7872	0.004	2.2592	2.3476
18	Serine	0.0391	0.0087	4.4947	0.000	2.1682	3.7420
19	Maltitol	0.0032	0.0009	3.3563	0.000	1.7469	4.1130
20	Glycine	0.0212	0.0063	3.3541	0.001	1.7459	3.0187
21	α-D-xylopyranose	0.0062	0.0019	3.2666	0.001	1.7078	2.8373
22	Ornithine	0.0026	0.0008	3.1153	0.001	1.6394	3.0739
23	Alanine	0.2414	0.0806	2.9945	0.000	1.5823	4.4638
24	Pyroglutamic acid	0.0165	0.0058	2.8361	0.000	1.5039	3.5650
25	Proline	0.0470	0.0170	2.7657	0.002	1.4676	2.6412
26	β-Alanine	0.0076	0.0028	2.7421	0.000	1.4553	4.2030
27	Meso erythritol	0.0055	0.0023	2.4498	0.002	1.2926	2.7040
28	Sugar compound 1	0.0092	0.0042	2.1860	0.007	1.1283	2.1567
29	Sucrose	7.9739	3.6539	2.1823	0.001	1.1258	3.2129
30	Xylitol	0.0015	0.0007	2.1252	0.001	1.0876	3.0268
31	Glutamine	0.0023	0.0011	2.0901	0.000	1.0636	4.5099
32	Butane	0.0583	0.0280	2.0853	0.001	1.0603	3.2025
33	Citric acid	0.0083	0.0040	2.0657	0.011	1.0466	1.9706
34	Cellobiose	0.0053	0.0026	2.0262	0.006	1.0188	2.2261

Fold Change 0.5-2

Number	Metabolite	Relative Intensity		Fold Change (FC) (Old/Young)	*p*-value	log2FC	Minus log10 *p*-value
		Old	Young				
1	Palatinose	3.8339	1.9763	1.9400	0.001	0.9560	3.1536
2	Glycerol	0.0950	0.0517	1.8381	0.003	0.8782	2.5145
3	Gentiobiose	0.0127	0.0071	1.8065	0.009	0.8532	2.0278
4	Turanose	0.0177	0.0106	1.6693	0.001	0.7393	2.9357
5	Sugar compound 3	0.0212	0.0132	1.6067	0.015	0.6841	1.8118
6	Phenylalanine	0.0026	0.0017	1.5928	0.017	0.6716	1.7695
7	Threonine	0.0202	0.0138	1.4612	0.003	0.5472	2.4812
8	Inositol	0.0276	0.0189	1.4546	0.003	0.5406	2.5190
9	2-α-mannobiose	0.0057	0.0040	1.4381	0.028	0.5242	1.5454
10	Cysteine	0.0019	0.0013	1.4213	0.021	0.5072	1.6785
11	β-Lactose	0.0070	0.0059	1.1912	0.048	0.2524	1.3194
12	Isoleucine	0.0085	0.0097	0.8773	0.039	-0.1888	1.4036
13	Butanoic acid	0.0166	0.0200	0.8284	0.023	-0.2716	1.6463
14	4-Aminobutyric acid	0.0752	0.0972	0.7745	0.001	-0.3686	3.2639
15	Glucaric acid	0.0493	0.0639	0.7709	0.001	-0.3754	3.2769
16	Butanedioic acid	0.1296	0.2098	0.6178	0.002	-0.6948	2.6501
17	Malic acid	0.7398	1.2451	0.5942	0.003	-0.7510	2.5256
18	Valine	0.0264	0.0445	0.5934	0.003	-0.7530	2.5722
19	Arabinose	0.0037	0.0073	0.5035	0.005	-0.9899	2.2749
20	Arabinose	0.0037	0.0073	0.5035	0.005	-0.9899	2.2749

Fold Change less than 0.5							
Number	Metabolite	Relative Intensity		Fold Change (FC) (Old/Young)	*p*-value	log2FC	Minus log10 *p*-value
		Old	Young				
1	Glucopyranose	0.0197	0.0424	0.4647	0.013	-1.1055	1.8859
2	α-D-glucopyranoside	0.0095	0.0219	0.4345	0.001	-1.2025	2.9759
3	β-D-mannopyranose	0.0073	0.0170	0.4292	0.001	-1.2204	3.1443
4	Shikimic acid	0.0019	0.0047	0.3966	0.001	-1.3344	2.9718
5	Lysine	0.0515	0.1384	0.3720	0.000	-1.4268	4.3299
6	Sorbose	10.5001	29.8822	0.3514	0.000	-1.5089	4.9581
7	Glucose	7.9752	23.2309	0.3433	0.000	-1.5425	4.4752
8	Tagatose	0.5519	1.6479	0.3349	0.000	-1.5781	4.0171
9	Glyceryl-glycoside	0.2069	0.6236	0.3318	0.000	-1.5916	3.8561
10	Xylose	2.5338	7.7577	0.3266	0.000	-1.6143	4.3412
11	Fructose	5.9317	19.1898	0.3091	0.000	-1.6938	4.6906
12	Talose	0.0890	0.2917	0.3052	0.000	-1.7120	3.9995

Table S8. List of metabolites in volcano plot to compare old and young flesh, which were significantly different based on *t*-test (*p*-value less than 0.05)

Fold Change 0.5-2							
Number	Metabolite	Relative Intensity		Fold Change (FC) (Old/Young)	*p*-value	log2FC	Minus log10 *p*-value
		Old	Young				

1	Phosphate	0.0781	0.0669	1.1679	0.001	0.2239	2.9509
2	Glycerol	0.0293	0.0255	1.1462	0.000	0.1969	3.6485
3	Sugar alcohol 1	0.0193	0.0189	1.0198	0.019	0.0283	1.7168
4	Phenylalanine	0.0011	0.0013	0.8130	0.002	-0.2987	2.6312
5	Rhamnose	0.0053	0.0069	0.7757	0.003	-0.3664	2.5633
6	Allothreonine	0.0045	0.0065	0.6959	0.002	-0.5230	2.8073
7	Threonine	0.0023	0.0034	0.6827	0.003	-0.5507	2.5367
8	4-Aminobutyric acid	0.1160	0.1764	0.6574	0.004	-0.6052	2.4125
9	Methionine	0.0020	0.0034	0.5898	0.004	-0.7616	2.4180
10	Unknown 1	0.0008	0.0013	0.5791	0.004	-0.7880	2.3830
11	Meso-Erythritol	0.0034	0.0060	0.5723	0.000	-0.8052	4.4294
12	Succinic acid	0.0125	0.0219	0.5719	0.000	-0.8061	3.4480
13	D-talopyranose	0.0105	0.0185	0.5642	0.000	-0.8256	3.9943
14	Glutamic acid	0.0057	0.0103	0.5566	0.001	-0.8453	2.8307
15	Proline	0.0209	0.0380	0.5512	0.000	-0.8592	3.7199
16	Leucine	0.0051	0.0093	0.5497	0.000	-0.8634	3.3467
17	Malic acid	0.1486	0.2794	0.5317	0.000	-0.9114	3.6607
18	Pyroglutamic acid	0.0069	0.0131	0.5254	0.000	-0.9284	3.5979
19	Glycine	0.0102	0.0196	0.5185	0.000	-0.9477	4.3056
20	Inositol	0.0148	0.0289	0.5123	0.000	-0.9648	4.0028
21	Quinic acid	0.0035	0.0068	0.5113	0.000	-0.9677	3.7562
22	Quinic acid	0.0035	0.0068	0.5113	0.000	-0.9677	3.7562
Fold Change Less Than 0.5							

Number	Metabolite	Relative Intensity		Fold Change (FC) (Old/Young)	*p*-value	log2FC	Minus log10 *p*-value
		Old	Young				
1	Sugar alcohol 2	0.0009	0.0020	0.4557	0.000	-1.1338	3.6120
2	Serine	0.0136	0.0303	0.4503	0.000	-1.1510	3.4409
3	Maltose	0.0017	0.0038	0.4495	0.003	-1.1536	2.5242
4	Raffinose	0.0015	0.0034	0.4438	0.002	-1.1719	2.6228
5	α-D-glucopyranoside	0.6521	1.5002	0.4347	0.000	-1.2021	3.6790
6	2-aminoethanol	0.0100	0.0231	0.4320	0.000	-1.2108	3.3606
7	Valine	0.0112	0.0260	0.4311	0.001	-1.2139	2.9882
8	Tagatose	0.0025	0.0060	0.4151	0.000	-1.2683	3.6408
9	Galactose	0.0129	0.0311	0.4139	0.001	-1.2727	3.2708
10	Isoleucine	0.0036	0.0087	0.4126	0.000	-1.2770	3.8291
11	Sucrose	1.3354	3.2727	0.4081	0.000	-1.2931	3.6161
12	Talose	0.0021	0.0059	0.3566	0.000	-1.4877	3.4256
13	Cysteine	0.0006	0.0018	0.3223	0.000	-1.6334	4.5282
14	Fructose	0.1114	0.4237	0.2628	0.000	-1.9277	3.6988
15	Sorbose	0.1783	0.7089	0.2515	0.000	-1.9911	3.6001
16	Alanine	0.0611	0.2448	0.2495	0.001	-2.0031	3.2001
17	Fumaric acid	0.0013	0.0054	0.2424	0.000	-2.0448	4.5969
18	Glutamine	0.0010	0.0044	0.2216	0.004	-2.1740	2.4171
19	Lactulose	0.0004	0.0018	0.2202	0.000	-2.1832	3.3808
20	Aspartic acid	0.0038	0.0172	0.2189	0.000	-2.1914	3.5683

21	Mannose	0.0058	0.0299	0.1927	0.000	-2.3758	3.5507
22	Putrescine	0.0007	0.0056	0.1298	0.003	-2.9456	2.5672
23	Galactinol	0.0029	0.0224	0.1297	0.000	-2.9466	3.5996
24	Sugar compound 1	0.0007	0.0058	0.1256	0.001	-2.9937	3.0993
25	Glucose	0.0526	0.4987	0.1055	0.000	-3.2445	3.8169
26	Mannitol	0.0268	0.3020	0.0888	0.000	-3.4931	3.8074

Table S9. List of Metabolites with high VIP score and positive coefficient value from the Taste Nutty of Water model from OPLS regression analysis.

Number	Metabolites	VIP	Coefficient
1	β-alanine	1.279	0.023
2	Sucrose	1.276	0.023
3	Alanine	1.274	0.023
4	Palatinose	1.272	0.023
5	Serine	1.271	0.022
6	Inositol	1.269	0.023
7	Butane	1.269	0.023
8	Proline	1.267	0.023
9	Glutamic acid	1.266	0.022
10	Glycine	1.265	0.023

Table S10. List of Metabolites with high VIP score and positive coefficient value from the Taste Creamy of Water model from OPLS regression analysis.

Number	Metabolites	VIP	Coefficient
1	4-aminobutyric acid	1.348	0.028
2	Isoleucine	1.347	0.027
3	Butanoic acid	1.347	0.028
4	Leucine	1.345	0.027
5	Allothreonine	1.342	0.027
6	2-aminoethanol	1.342	0.027
7	Fumaric acid	1.341	0.027
8	Valine	1.338	0.029
9	Glutamine	1.337	0.027
10	Succinic acid	1.336	0.027

Table S11. List of Metabolites with high VIP score and positive coefficient value from the Taste Bitter of Water model from OPLS regression analysis.

Number	Metabolites	VIP	Coefficient
1	β-alanine	1.282	0.023
2	Sucrose	1.281	0.023
3	Alanine	1.277	0.023
4	Palatinose	1.277	0.023
5	Butane	1.276	0.023
6	Inositol	1.275	0.023
7	Proline	1.274	0.023
8	Serine	1.274	0.023
9	Glycine	1.272	0.023
10	Aspartic acid	1.269	0.023

Table S12. List of Metabolites with high VIP score and positive coefficient value from the Taste Milky of Water model from OPLS regression analysis.

Number	Metabolites	VIP	Coefficient
1	Valine	1.480	0.033
2	4-Aminobutyric acid	1.446	0.031
3	butanoic acid	1.436	0.031
4	Isoleucine	1.404	0.029
5	Leucine	1.393	0.029
6	Fumaric acid	1.390	0.029
7	2-Aminoethanol	1.388	0.029
8	Allothreonine	1.383	0.028
9	Succinic acid	1.373	0.028
10	Phosphoric acid	1.358	0.029

Table S13. List of Metabolites with high VIP score and positive coefficient value from the Flavor Nutty of Water model from OPLS regression analysis.

Number	Metabolites	VIP	Coefficient
1	Glutamine	1.303	0.025
2	Isoleucine	1.302	0.026
3	Leucine	1.302	0.026
4	Butane	1.301	0.024
5	Glycine	1.301	0.024
6	Sucrose	1.300	0.024
7	Citric acid	1.300	0.025
8	Allothreonine	1.300	0.026
9	Inositol	1.300	0.024
10	Proline	1.299	0.024

Table S14. List of Metabolites with high VIP score and positive coefficient value from the Flavor Creamy of Water model from OPLS regression analysis.

Number	Metabolites	VIP	Coefficient
1	Glutamine	1.303	0.025
2	Isoleucine	1.302	0.026
3	Leucine	1.301	0.026
4	Butane	1.301	0.024
5	Glycine	1.301	0.024
6	Sucrose	1.300	0.024
7	Citric acid	1.300	0.025
8	Allothreonine	1.300	0.026
9	Inositol	1.300	0.024
10	Proline	1.299	0.024

Table S15. List of Metabolites with high VIP score and positive coefficient value from the Aroma Creamy of Water model from OPLS regression analysis.

Number	Metabolites	VIP	Coefficient
1	Isoleucine	1.332	0.027
2	Leucine	1.330	0.027
3	4-Aminobutyric acid	1.329	0.027
4	Butanoic acid	1.329	0.027
5	Allothreonine	1.327	0.027
6	2-aminoethanol	1.327	0.027
7	Fumaric acid	1.327	0.027
8	Glutamine	1.326	0.026
9	Succinic acid	1.323	0.026
10	Citric acid	1.319	0.025

Table S16. List of Metabolites with high VIP score and positive coefficient value from the Aroma Rancid of Water model from OPLS regression analysis.

Number	Metabolites	VIP	Coefficient
1	Valine	1.394	0.031
2	4-Aminobutyric acid	1.392	0.030
3	Butanoic acid	1.389	0.029
4	Isoleucine	1.381	0.029
5	Leucine	1.376	0.028
6	Fumaric acid	1.372	0.028
7	2-aminoethanol	1.372	0.028
8	Allothreonine	1.371	0.028
9	Succinic acid	1.364	0.028
10	Glutamine	1.359	0.027

Table S17. List of Metabolites with high VIP score and positive coefficient value from the Aroma Nutty of Water model from OPLS regression analysis.

Number	Metabolites	VIP	Coefficient
1	Isoleucine	1.315	0.026
2	Leucine	1.315	0.026
3	Glutamine	1.314	0.026
4	Allothreonine	1.312	0.026
5	2-Aminoethanol	1.311	0.026
6	Fumaric Acid	1.311	0.026
7	Butanoic Acid	1.309	0.027
8	Citric Acid	1.309	0.025
9	Glycine	1.309	0.025
10	4-Aminobutyric Acid	1.308	0.027

Table S18. List of Metabolites with high VIP score and positive coefficient value from the Aftertaste Oily of Water model from OPLS regression analysis.

Number	Metabolites	VIP	Coefficient
1	β-alanine	1.272	0.023
2	Alanine	1.269	0.022
3	Sucrose	1.268	0.023
4	Serine	1.266	0.022
5	Glutamic acid	1.266	0.022
6	Palatinose	1.263	0.022
7	Inositol	1.259	0.023
8	Butane	1.259	0.023
9	Proline	1.257	0.023
10	Aspartic acid	1.256	0.022

Table S19. List of Metabolites with high VIP score and positive coefficient value from the Aftertaste Astringent of Water model from OPLS regression analysis.

Number	Metabolites	VIP	Coefficient
1	Glutamic acid	1.264	0.022
2	β-Alanine	1.259	0.022
3	Alanine	1.257	0.022
4	Serine	1.257	0.022
5	Sucrose	1.251	0.022
6	Palatinose	1.245	0.022
7	Inositol	1.240	0.022
8	Aspartic acid	1.239	0.022
9	Butane	1.239	0.022
10	Proline	1.236	0.022

Table S20. List of Metabolites with high VIP score and positive coefficient value from the Aftertaste Bitter of Water model from OPLS regression analysis.

Number	Metabolites	VIP	Coefficient
1	Tetradecylglycerol	1.319	0.032
2	Lyxose	1.310	0.025
3	Ribose	1.270	0.023
4	Glycerol	1.248	0.022
5	Quinic acid	1.243	0.023
6	Lactulose	1.242	0.021
7	Trehalose	1.220	0.029
8	Meso erythritol	1.211	0.023
9	Sugar compound 1	1.185	0.020
10	α-D-Xylopyranose	1.180	0.019

Table S21. List of Metabolites with high VIP score and positive coefficient value from the Aftertaste Salty of Water model from OPLS regression analysis.

Number	Metabolites	VIP	Coefficient
1	Tetradecylglycerol	1.379	0.034
2	Lyxose	1.312	0.025
3	Trehalose	1.273	0.031
4	Ribose	1.268	0.023
5	Quinic acid	1.243	0.023
6	Glycerol	1.240	0.022
7	Unknown 3	1.236	0.034
8	Lactulose	1.227	0.021
9	Meso erythritol	1.212	0.023
10	Gentiobiose	1.198	0.028

Table S22. List of Metabolites with high VIP score and positive coefficient value from the Mouthfeel Oily of Water model from OPLS regression analysis.

Number	Metabolites	VIP	Coefficient
1	Lyxose	1.250	0.023
2	Lactulose	1.249	0.022
3	Glutamic acid	1.241	0.021
4	Glycerol	1.231	0.021
5	Ribose	1.229	0.021
6	α-D-Xylopyranose	1.217	0.021
7	Serine	1.209	0.020
8	Alanine	1.203	0.019
9	β-Alanine	1.201	0.020
10	Quinic acid	1.193	0.021

Table S23. List of Metabolites with high VIP score and positive coefficient value from the Mouthfeel Astringent of Water model from OPLS regression analysis.

Number	Metabolites	VIP	Coefficient
1	Glutamic acid	1.252	0.021
2	Lactulose	1.241	0.021
3	Lyxose	1.230	0.022
4	Serine	1.228	0.021
5	Alanine	1.224	0.020
6	β-Alanine	1.224	0.021
7	Glycerol	1.219	0.021
8	α-D-Xylopyranose	1.215	0.020
9	Ribose	1.212	0.021
10	Sucrose	1.209	0.020

Table S24. List of Metabolites with high VIP score and positive coefficient value from the Mouthfeel Fizzy of Water model from OPLS regression analysis.

Number	Metabolites	VIP	Coefficient
1	Glutamic acid	1.264	0.022
2	β-Alanine	1.261	0.022
3	Alanine	1.259	0.022
4	Serine	1.258	0.022
5	Sucrose	1.254	0.022
6	Palatinose	1.248	0.022
7	Inositol	1.243	0.022
8	Aspartic acid	1.242	0.022
9	Butane	1.242	0.022
10	Proline	1.239	0.022

Table S25. List of Metabolites with high VIP score and positive coefficient value from the Mouthfeel Body of Water model from OPLS regression analysis.

Number	Metabolites	VIP	Coefficient
1	4-Aminobutyric acid	1.357	0.028
2	butanoic acid	1.355	0.028
3	Isoleucine	1.354	0.028
4	Leucine	1.351	0.027
5	Valine	1.349	0.029
6	2-Aminoethanol	1.348	0.027
7	Fumaric acid	1.348	0.027
8	Allothreonine	1.348	0.027
9	Glutamine	1.342	0.027
10	Succinic acid	1.342	0.027

Table S26. List of Metabolites with high VIP score and positive coefficient value from the Taste Nutty of Flesh model from OPLS regression analysis.

Number	Metabolite	VIP	Coefficient
1	Rhamnose	2.563	0.144
2	Citric acid	2.530	0.137
3	Threonine	2.508	0.144
4	Phenylalanine	1.777	0.114
5	Leucine	1.417	0.099
6	Sorbitol	1.265	0.061

Table S27. List of Metabolites with high VIP score and positive coefficient value from the Taste Bitterness of Flesh model from OPLS regression analysis.

Number	Metabolite	VIP	Coefficient
1	Citric acid	1.687	0.122
2	Rhamnose	1.595	0.126

Number	Metabolite	VIP	Coefficient
3	Threonine	1.479	0.124
4	Sorbitol	1.022	0.057
5	Glycerol	1.015	0.024

Table S28. List of Metabolites with high VIP score and positive coefficient value from the Taste Creamy of Flesh model from OPLS regression analysis.

Number	Metabolite	VIP	Coefficient
1	Citric acid	1.536	0.135
2	Rhamnose	1.430	0.142
3	Threonine	1.308	0.132
4	Glutamine	1.087	0.013
5	Putrescine	1.063	0.011
6	Glycerol	1.040	0.028

Table S29. List of Metabolites with high VIP score and positive coefficient value from the Taste Astringent of Flesh model from OPLS regression analysis.

Number	Metabolite	VIP	Coefficient
1	Raffinose	2.220	0.135
2	Maltose	2.193	0.140
3	Glycerol	2.106	0.139
4	Glutamine	1.317	0.108
5	Putrescine	1.197	0.061
6	Glutamic acid	2.220	0.135
7	Unknown 1	2.193	0.140
8	Valine	2.106	0.139
9	Methionine	1.317	0.108

Table S30. List of Metabolites with high VIP score and positive coefficient value from the Flavor Creamy of Flesh model from OPLS regression analysis.

Number	Metabolite	VIP	Coefficient
1	Citric acid	2.220	0.135
2	Rhamnose	2.193	0.140
3	Threonine	2.106	0.139
4	Phenylalanine	1.317	0.108
5	Sorbitol	1.197	0.061

Table S31. List of Metabolites with high VIP score and positive coefficient value from the Flavor Milky of Flesh model from OPLS regression analysis.

Number	Metabolite	VIP	Coefficient
1	Rhamnose	2.473	0.144
2	Citric acid	2.458	0.138
3	Threonine	2.409	0.143
4	Phenylalanine	1.655	0.113
5	Leucine	1.291	0.098
6	Sorbitol	1.254	0.061

Table S32. List of Metabolites with high VIP score and positive coefficient value from the Flavor Nutty of Flesh model from OPLS regression analysis.

Number	Metabolite	VIP	Coefficient
1	Rhamnose	2.500	0.144
2	Citric acid	2.480	0.138
3	Threonine	2.439	0.144
4	Phenylalanine	1.691	0.114
5	Leucine	1.328	0.099
6	Sorbitol	1.258	0.061

Table S33. List of Metabolites with high VIP score and positive coefficient value from the Aroma Coconut of Flesh model from OPLS regression analysis.

Number	Metabolite	VIP	Coefficient
1	Threonine	2.361	0.141
2	Rhamnose	2.279	0.140
3	Phenylalanine	2.229	0.120
4	Leucine	2.094	0.104
5	Citric acid	2.075	0.133
6	Isoleucine	1.670	0.075
7	Glycine	1.629	0.072
8	Fumaric acid	1.275	0.050
9	Succinic acid	1.264	0.048
10	Proline	1.234	0.046

Table S34. List of Metabolites with high VIP score and positive coefficient value from the Aroma Nutty of Flesh model from OPLS regression analysis.

Number	Metabolite	VIP	Coefficient
1	Threonine	2.723	0.146
2	Rhamnose	2.687	0.145
3	Citric acid	2.527	0.138
4	Phenylalanine	2.326	0.121
5	Leucine	2.081	0.105
6	Isoleucine	1.522	0.074
7	Glycine	1.456	0.070
8	Sorbitol	1.062	0.059
9	Succinic acid	1.019	0.046
10	Fumaric acid	1.018	0.046

Table S35. List of Metabolites with high VIP score and positive coefficient value from the Aroma Creamy of Flesh model from OPLS regression analysis.

Number	Metabolite	VIP	Coefficient
1	Rhamnose	2.768	0.146
2	Threonine	2.759	0.146
3	Citric acid	2.666	0.139
4	Phenylalanine	2.167	0.119
5	Leucine	1.849	0.103
6	Isoleucine	1.229	0.071
7	Sorbitol	1.225	0.060
8	Glycine	1.146	0.067

Table S36. List of Metabolites with high VIP score and positive coefficient value from the Aftertaste Bitter of Flesh model from OPLS regression analysis.

Number	Metabolite	VIP	Coefficient
1	Citric acid	1.481	0.114
2	Rhamnose	1.371	0.117
3	Threonine	1.247	0.115
4	Glycerol	1.047	0.026

Table S37. List of Metabolites with high VIP score and positive coefficient value from the Aftertaste Salty of Flesh model from OPLS regression analysis.

Number	Metabolite	VIP	Coefficient
1	Glycerol	1.084	0.031

Table S38. List of Metabolites with high VIP score and positive coefficient value from the Mouthfeel Moist of Flesh model from OPLS regression analysis.

Number	Metabolite	VIP	Coefficient
1	Glycine	1.366	0.067
2	Leucine	1.360	0.067
3	Isoleucine	1.343	0.059
4	Fumaric acid	1.299	0.085
5	Proline	1.276	0.056
6	Succinic acid	1.270	0.033
7	Phenylalanine	1.238	0.115
8	α-D-Glucopyranoside	1.210	0.028
9	Sucrose	1.200	0.028
10	Allothreonine	1.187	0.014

Table S39. List of Metabolites with high VIP score and positive coefficient value from the Mouthfeel Soft of Flesh model from OPLS regression analysis.

Number	Metabolite	VIP	Coefficient
1	Leucine	1.429	0.081
2	Glycine	1.404	0.064
3	Isoleucine	1.385	0.064
4	Phenylalanine	1.323	0.093
5	Fumaric acid	1.317	0.054
6	Proline	1.293	0.046
7	Succinic acid	1.289	0.046
8	α-D-Glucopyranoside	1.215	0.035
9	Sucrose	1.203	0.033
10	Allothreonine	1.197	0.035

Table S40. List of Metabolites with high VIP score and positive coefficient value from the Mouthfeel Sandy of Flesh model from OPLS regression analysis.

Number	Metabolite	VIP	Coefficient
1	Rhamnose	2.529	0.144
2	Citric acid	2.503	0.138
3	Threonine	2.471	0.144
4	Phenylalanine	1.729	0.114
5	Leucine	1.368	0.099
6	Sorbitol	1.261	0.061

Table S41. List of Metabolites with high VIP score and positive coefficient value from the Color White of Flesh model from OPLS regression analysis.

Number	Metabolite	VIP	Coefficient
1	Citric acid	1.679	0.122
2	Rhamnose	1.587	0.125
3	Threonine	1.470	0.124
4	Sorbitol	1.019	0.057
4	Glycerol	1.016	0.024

Table S42. Loading Scores for PC1 and PC2 of Annotated Metabolites from PCA of GC-MS Water Analysis Based on Endosperm Quantity

No	Metabolite	Loading Score	
		PC1	PC2
1	2-Aminoethanol	0.198	0.068
2	4-Aminobutyric acid	0.150	0.169
3	Alanine	0.173	0.014
4	Aspartic acid	0.201	-0.100
5	β-Alanine	0.156	0.220
6	Citric acid	0.178	0.019

No	Metabolite	Loading Score	
		PC1	PC2
7	Fructose	-0.180	0.012
8	Fumaric acid	0.173	-0.011
9	Galactose	-0.165	-0.221
10	Gentiobiose	-0.091	0.306
11	Gluconic acid	-0.054	0.029
12	Glucose	-0.177	0.053
13	Glutamine	0.194	-0.116
14	Glycine	0.201	0.087
15	Inositol	0.152	0.187
16	Isoleucine	0.203	-0.030
17	Leucine	0.202	0.009
18	Lysine	0.083	-0.308
19	Lyxose	-0.022	0.381
20	Malic acid	0.072	0.133
21	Maltitol	0.054	0.288
22	Maltose	0.061	-0.124
23	Melibiose	0.002	0.322
24	Meso erythritol	0.114	0.073
25	Methionine	0.196	0.039
26	Ornithine	0.169	-0.114
27	Phosphate	0.159	0.036
28	Pyroglutamic acid	0.194	-0.116
29	Quinic acid	0.180	0.009
30	Ribose	0.008	0.251
31	Serine	0.174	-0.201
32	Shikimic acid	0.110	0.196
33	Sorbitol	-0.119	-0.159
34	Succinic acid	0.175	0.026
35	Sucrose	0.179	0.042

No	Metabolite	Loading Score	
		PC1	PC2
36	Tagatose	-0.173	0.018
37	Threonine	0.197	-0.081
38	Turanose	0.169	-0.080
39	Tyrosine	-0.156	0.019
40	Valine	0.205	0.006
41	Xylitol	0.142	-0.162

Table S43. Loading Scores for PC1 and PC2 of Annotated Metabolites from PCA of GC-MS Flesh Analysis Based on Endosperm Quantity

No	Metabolite	Loading Score	
		PC1	PC2
1	2-Aminoethanol	0.184	-0.042
2	4-Aminobutyric acid	0.166	-0.132
3	Alanine	0.210	0.121
4	α-L-sorbopyranose	0.147	-0.335
5	Aspartic acid	0.209	0.057
6	β-Alanine	0.197	-0.140
7	Citric acid	0.152	0.030
8	Ethylene glycol	0.176	0.031
9	Fructose	0.149	-0.335
10	Fumaric acid	0.184	0.098
11	Galactinol	0.177	-0.098
12	Galactose	0.092	-0.349
13	Glucose	0.122	-0.366
14	Glutamic acid	0.198	0.076
15	Glycerol	0.087	-0.091
16	Glycine	0.212	0.052
17	Inositol	0.156	-0.144

No	Metabolite	Loading Score	
		PC1	PC2
18	Isoleucine	0.198	0.180
19	Leucine	0.208	0.123
20	Lysine	0.206	0.084
21	Malic acid	0.208	-0.020
22	Mannitol	0.109	0.027
23	Meso erythritol	-0.063	-0.017
24	Myristic acid	0.003	0.032
25	Palmitic acid	-0.038	0.087
26	Phenylalanine	0.183	0.200
27	Phosphate	-0.098	0.132
28	Phthalic acid	-0.037	0.109
29	Proline	0.209	0.068
30	Pyroglutamic acid	0.154	0.292
31	Quinic acid	0.151	0.001
32	Serine	0.153	0.299
33	Sorbitol	0.143	-0.176
34	Stearic acid	-0.017	0.054
35	Succinic acid	0.181	0.091
36	Sucrose	0.211	-0.019
37	UDP-N-acetylglucosamine	-0.137	0.181
38	Valine	0.208	0.121
39	Xylonic acid	-0.072	-0.044

Table S44. Analysis of Variance (ANOVA) and Tukey's HSD Results for Metabolite Differences in Water Samples

No	Metabolite	*F*-value	*p*-value	Tukey's HSD
1	Melibiose	33.810	0.000	10-0; 20-0; 30-0; 40-0; 50-0; 40-10; 50-10; 40-20; 50-20; 50-30
2	Turanose	21.462	0.000	40-0; 50-0; 40-10; 50-10; 40-20; 50-20; 40-30; 50-30
3	Galactose	17.869	0.000	10-0; 20-0; 30-0; 40-0; 50-0
4	Glutamic acid	14.866	0.000	40-0; 50-0; 50-10; 50-20; 50-30; 50-40
5	Glutamine	12.397	0.000	50-0; 50-10; 50-20; 50-30; 50-40
6	Valine	11.160	0.000	40-0; 50-0; 50-10; 50-20; 50-30
7	Sucrose	9.411	0.001	40-0; 50-0; 40-10; 50-10; 40-30; 50-30
8	Gentiobiose	9.272	0.001	50-0; 50-10; 50-20; 50-30
9	Fructose	9.186	0.001	40-0; 50-0; 40-10; 50-10; 40-20
10	Glucose	8.645	0.001	40-0; 50-0; 40-10; 50-10; 40-20
11	Inositol	7.052	0.003	50-0; 50-10; 50-20
12	Alanine	6.702	0.003	40-0; 50-0; 50-10; 50-20; 50-30
13	Tyrosine	6.686	0.003	40-0; 50-0; 40-10; 50-10
14	Tagatose	6.597	0.004	40-0; 50-0; 40-10; 50-10
15	Maltitol	6.450	0.004	50-0; 50-10; 50-40
16	Gluconic acid	6.401	0.004	40-0; 50-0; 50-10; 50-20
17	Glycine	5.467	0.008	50-0; 50-10; 50-20
18	Citric acid	5.280	0.009	40-0; 50-0; 40-10

No	Metabolite	*F*-value	*p*-value	Tukey's HSD
19	Xylitol	5.276	0.009	50-0; 50-10
20	Pyroglutamic acid	4.587	0.014	50-20; 50-30
21	Threonine	4.551	0.015	20-10; 40-20

Table S45. List of 16 Significant Metabolites from Water with *p*-values Below 0.05 for Correlation Analysis with Endosperm Quantity (EQ)

No	Metabolites	*p*-value	Pearson *r*	Confidence Interval of the Correlation Coefficient (*CI*(*r*))
1	Alanine	0.006	0.934	0.51 to 0.99
2	Citric acid	0.013	-0.905	-0.99 to -0.35
3	Fructose	0.002	-0.967	-1.0 to -0.72
4	Gentiobiose	0.014	0.903	0.34 to 0.99
5	Gluconic acid	0.005	0.944	0.57 to 0.99
6	Glucose	0.004	-0.949	-0.99 to -0.60
7	Glutamic acid	0.012	0.910	0.37 to 0.99
8	Glycine	0.017	0.892	0.29 to 0.99
9	Inositol	0.005	0.940	0.54 to 0.99
10	Melibiose	0.000	0.984	0.85 to 1.0
11	Sucrose	0.013	0.905	0.35 to 0.99

No	Metabolites	*p*-value	Pearson *r*	Confidence Interval of the Correlation Coefficient (*CI*(*r*))
12	Tagatose	0.001	-0.974	-1.0 to -0.77
13	Turanose	0.036	0.841	0.094 to 0.98
14	Tyrosine	0.005	-0.941	-0.99 to -0.55
15	Valine	0.023	0.875	0.22 to 0.99
16	Xylitol	0.008	0.925	0.46 to 0.99

Table S46. Analysis of Variance (ANOVA) and Tukey's HSD Results for Metabolite Differences in Flesh Samples

No	Metabolite	*F*-value	*p*-value	Tukey's HSD
1	Valine	18.120	0.000	20-0; 40-0; 50-0; 20-10; 40-10; 50-10; 50-30; 50-40
2	Glucose	17.857	0.000	10-0; 20-0; 30-0; 40-20; 50-20; 40-30; 50-30
3	Leucine	13.920	0.000	20-0; 40-0; 50-0; 20-10; 50-10; 50-30; 50-40
4	Alanine	13.631	0.000	20-0; 40-0; 50-0; 20-10; 40-10; 50-10; 50-30
5	Phenylalanine	13.031	0.000	20-0; 40-0; 50-0; 40-10; 50-10; 50-20; 50-30
6	Isoleucine	12.859	0.000	20-0; 40-0; 50-0; 50-10; 50-20; 50-30; 50-40
7	Glycine	12.687	0.000	20-0; 30-0; 40-0; 50-0; 20-10; 50-10
8	Sucrose	12.428	0.000	20-0; 30-0; 40-0; 50-0; 50-10
9	Aspartic acid	11.322	0.000	20-0; 40-0; 50-0; 50-10; 50-30; 50-40

No	Metabolite	*F*-value	*p*-value	Tukey's HSD
10	Lysine	11.169	0.000	20-0; 50-0; 50-10; 50-30; 50-40
11	Galactose	10.935	0.000	10-0; 20-0; 30-0; 40-10; 40-20; 50-20
12	Fumaric acid	9.258	0.000	20-0; 40-0; 50-0; 50-10
13	α-L-sorbopyranose	8.537	0.000	20-0; 30-0; 40-20; 40-30
14	Fructose	7.986	0.000	20-0; 30-0; 40-20
15	Succinic acid	7.829	0.000	40-0; 50-0; 50-10
16	Ethylene glycol	7.257	0.001	20-0; 40-0; 50-0
17	Serine	7.175	0.001	50-0; 50-10; 50-20; 50-30
18	Proline	6.200	0.002	20-0; 50-0; 50-10
19	Glutamic acid	5.871	0.002	20-0; 50-0; 20-10; 50-10
20	Phosphate	5.364	0.003	20-0; 30-0; 40-0
21	β-Alanine	4.690	0.006	20-0
22	Pyroglutamic acid	4.570	0.007	50-0; 50-10
23	Malic acid	4.412	0.008	50-0; 50-10
24	Sorbitol	4.352	0.009	30-0
25	Citric acid	3.684	0.018	50-0

Table S47. List of 17 Significant Metabolites from Flesh with *p*-values Below 0.05 for Correlation Analysis with Endosperm Quantity (EQ)

No	Metabolites	*p*-value	Pearson *r*	Confidence Interval of the Correlation Coefficient (*CI*(*r*))
1	Alanine	0.012	0.911	0.380 to 0.990
2	Aspartic acid	0.043	0.825	0.0412 to 0.980
3	Citric acid	0.018	0.889	0.276 to 0.988
4	Ethylene glycol	0.026	0.865	0.178 to 0.985
5	Fumaric acid	0.003	0.957	0.651 to 0.995
6	Glutamic acid	0.049	0.813	0.00525 to 0.979
7	Glycine	0.017	0.892	0.289 to 0.988
8	Isoleucine	0.014	0.901	0.333 to 0.989
9	Leucine	0.025	0.867	0.187 to 0.985
10	Lysine	0.049	0.814	0.00741 to 0.979
11	Phenylalanine	0.009	0.923	0.447 to 0.992
12	Proline	0.033	0.848	0.116 to 0.983
13	Pyroglutamic acid	0.006	0.936	0.519 to 0.993
14	Serine	0.032	0.850	0.123 to 0.983
15	Succinic acid	0.002	0.959	0.666 to 0.996
16	Sucrose	0.036	0.841	0.0939 to 0.982
17	Valine	0.023	0.873	0.212 to 0.986

Table S48. List of 8 Metabolites from Flesh with Non-Significant Correlation *p*-values Above 0.05

No	Metabolites	*p*-value
1	Sorbitol	0.085
2	Galactose	0.636
3	Glucose	0.594
4	α-L-sorbopyran	0.349
5	Fructose	0.382
6	β-Alanine	0.228
7	Malic acid	0.096
8	Phosphate	0.177

Table S49. Water Metabolites Sorted by Highest VIP Scores with Corresponding Coefficients Based on OPLSR Analysis

No	Metabolite	VIP	Coefficient
1	Glycine	1.281	0.038
2	Valine	1.252	0.029
3	Leucine	1.249	0.031
4	Aspartic acid	1.246	0.035
5	Sucrose	1.043	0.011
6	Alanine	1.034	0.018

Table 50. Flesh Metabolites Sorted by Highest VIP Scores with Corresponding Coefficients Based on OPLSR Analysis

No	Metabolite	VIP	Coefficient
1	Alanine	1.369	0.095
2	Valine	1.328	0.070
3	Glycine	1.297	0.079
4	Glutamic acid	1.206	0.075
5	Sucrose	1.152	0.052

Table S51. Confidence Intervals of the Correlation Coefficient (*CI*(*r*)) for Endosperm Quantity (EQ) and Various Flesh Proximate Analysis and Water Physicochemical Properties

	EQ	F-Fat	F-Total Fiber	F-Carbohydrate	F-Protein	F-Ash Content	F-Water Content	W-Absorbance	W-pH	W-Brix	W-EC
EQ		-0.97 to 0.13	-0.97 to 0.19	-0.99 to -0.46	-0.98 to -0.14	-0.98 to -0.060	-0.045 to 0.98	0.14 to 0.98	-0.081 to 0.97	-0.94 to 0.49	-0.049 to 0.98
F-Fat	-0.97 to 0.13		0.97 to 1.0	-0.22 to 0.97	0.80 to 1.0	0.75 to 1.0	-1.0 to -0.94	-1.0 to -0.71	-0.99 to -0.53	-0.81 to 0.81	-0.99 to -0.46
F-Total Fiber	-0.97 to 0.19	0.97 to 1.0		-0.27 to 0.96	0.78 to 1.0	0.65 to 1.0	-1.0 to -0.95	-1.0 to -0.63	-0.99 to -0.59	-0.83 to 0.79	-0.99 to -0.37
F-Carbohydrate	-0.99 to -0.46	-0.22 to 0.97	-0.27 to 0.96		0.042 to 0.98	-0.17 to 0.97	-0.97 to 0.16	-0.98 to 0.057	-0.96 to 0.34	-0.40 to 0.95	-0.97 to 0.22
F-Protein	-0.98 to -0.14	0.80 to 1.0	0.78 to 1.0	0.042 to 0.98		0.64 to 1.0	-1.0 to -0.92	-1.0 to -0.73	-0.99 to -0.58	-0.77 to 0.85	-0.99 to -0.35
F-Ash Content	-0.98 to -0.060	0.75 to 1.0	0.65 to 1.0	-0.17 to 0.97	0.64 to 1.0		-1.0 to -0.68	-1.0 to -0.93	-0.99 to -0.45	-0.75 to 0.86	-1.0 to -0.84
F-Water Content	-0.045 to 0.98	-1.0 to -0.94	-1.0 to -0.95	-0.97 to 0.16	-1.0 to -0.92	-1.0 to -0.68		0.71 to 1.0	0.68 to 1.0	-0.82 to 0.81	0.37 to 0.99
W-Absorbance	0.14 to 0.98	-1.0 to -0.71	-1.0 to -0.63	-0.98 to 0.057	-1.0 to -0.73	-1.0 to -0.93	0.71 to 1.0		0.47 to 0.99	-0.86 to 0.74	0.83 to 1.0
W-pH	-0.081 to 0.97	-0.99 to -0.53	-0.99 to -0.59	-0.96 to 0.34	-0.99 to -0.58	-0.99 to -0.45	0.68 to 1.0	0.47 to 0.99		-0.78 to 0.84	0.19 to 0.99
W-Brix	-0.94 to 0.49	-0.81 to 0.81	-0.83 to 0.79	-0.40 to 0.95	-0.77 to 0.85	-0.75 to 0.86	-0.82 to 0.81	-0.86 to 0.74	-0.78 to 0.84		-0.87 to 0.74

	EQ	F- Fat	F- Total Fiber	F- Carbohydrate	F- Protein	F- Ash Content	F- Water Content	W- Absorbance	W- pH	W- Brix	W- EC
W-EC	-0.049 to 0.98	-0.99 to -0.46	-0.99 to -0.37	-0.97 to 0.22	-0.99 to -0.35	-1.0 to -0.84	0.37 to 0.99	0.83 to 1.0	0.19 to 0.99	-0.87 to 0.74	

Table S52. Sensory Attributes of Water and Metabolites with Significant Pearson Correlation at the 0.05 Level

No	Attribute	Metabolites and Their Correlations
1	Color-Brightness	There are 19 metabolites, including Aspartic acid, beta-Alanine, Citric acid, Glutamic acid, Glycine, Lysine, Maltitol, Meso erythritol, Methionine, Ornithine, Phosphate, Proline, Pyroglutamic acid, Quinic acid, Serine, Threonine, Tryptophan, Turanose, and Valine. All of these compounds exhibit a negative correlation.
2	Color-Clearness	There are 11 metabolites, including 4-Aminobutyric acid, Fructose, Galactose, Gentiobiose, Glucose, Melibiose, Ribose, Shikimic acid, Succinic acid, and Tagatose, all of which exhibit a positive correlation, while Fumaric acid shows a negative correlation.
3	Aroma-Nutty	There are a total of 29 metabolites, with 8 showing a positive correlation, including Fructose, Glucose, Tagatose, Galactose, Melibiose, Gentiobiose, Succinic acid, and 4-Aminobutyric acid. Meanwhile, 21 metabolites exhibit a negative correlation, including beta-Alanine, Meso erythritol, Fumaric acid, Xylonic acid, Aspartic acid, Methionine, Lysine, 2-Aminoethanol, Quinic acid, Pyroglutamic acid, Proline, Valine, Serine, Tryptophan, Isoleucine, Xylitol, Phosphate, Sucrose, Citric acid, Inositol, and Turanose.

No	Attribute	Metabolites and Their Correlations
4	Aroma-Creamy	There are a total of 28 metabolites identified. Of these, 7 show a positive correlation, including Fructose, Glucose, Tagatose, Galactose, Succinic acid, Meliniose, and Gentiobiose. Meanwhile, 21 metabolites exhibit a negative correlation, including Xylonic acid, Maltitol, 2-Aminoethanol, beta-Alanine, Meso erythritol, Aspartic acid, Methionine, Lysine, Isoleucine, Xylitol, Inositol, Quinic acid, Sucrose, Proline, Pyroglutamic acid, Valine, Serine, Turanose, Tryptophan, Citric acid, and Phosphate.
5	Aroma-Milky	There are 13 metabolites that exhibit negative correlations, including Aspartic acid, beta-Alanine, Glutamic acid, Glycine, Lysine, Maltitol, Meso erythritol, Methionine, Ornithine, Pyroglutamic acid, Quinic acid, Serine, and Tryptophan.
6	Aroma-Coconut	There are 22 metabolites, including Aspartic acid, beta-Alanine, Citric acid, Glycine, Inositol, Isoleucine, Lysine, Maltitol, Meso erythritol, Methionine, Ornithine, Phosphate, Proline, Pyroglutamic acid, Quinic acid, Serine, Sucrose, Threonine, Tryptophan, Turanose, Valine, and Xylitol, exhibit negative correlations.
7	Aroma-Rancid	There are 28 metabolites in total, with 8 exhibiting positive correlations, including Fructose, Glucose, Tagatose, Galactose, Gentiobiose, Meliniose, Succinic acid, and 4-Aminobutyric acid. In contrast, 20 metabolites, such as Meso erythritol, Aspartic acid, Fumaric acid, Xylonic acid, Methionine, Lysine, Quinic acid, and others, show negative correlations.

No	Attribute	Metabolites and Their Correlations
8	Aroma-Sweet	A total of 24 metabolites were identified, with 3 showing positive correlations, including Fructose, Tagatose, and Glucose. In contrast, 21 metabolites, such as Glycine, Isoleucine, Ornithine, Xylitol, Inositol, Sucrose, Maltitol, Aspartic acid, Methionine, Lysine, Meso erythritol, Turanose, beta-Alanine, Proline, Valine, Quinic acid, Citric acid, Phosphate, Pyroglutamic acid, Serin, and Tryptophan, exhibit negative correlations.
9	Taste-Nutty	A total of 7 metabolites were identified, with 1 showing a positive correlation (Fumaric acid) and 6 exhibiting negative correlations, including Glycine, Shikimic acid, Meliniose, Gentiobiose, Ribose, and 4-Aminobutyric acid.
10	Taste-Creamy	A total of 29 metabolites were identified. The 8 metabolites that show positive correlations are Fructose, Glucose, Tagatose, Galactose, Meliniose, Gentiobiose, Succinic acid, and 4-Aminobutyric acid. Meanwhile, the 21 metabolites with negative correlations are Fumaric acid, beta-Alanine, Xylonic acid, Meso erythritol, Aspartic acid, 2-Aminoethanol, Methionine, Lysine, Quinic acid, Proline, Pyroglutamic acid, Valine, Isoleucine, Serin, Xylitol, Tryptophan, Inositol, Sucrose, Phosphate, Turanose, and Citric acid.
11	Taste-Milky	All 17 metabolites exhibit negative correlations: Citric acid, Glutamic acid, Proline, Phosphate, Valine, Methionine, Lysine, Aspartic acid, Tryptophan, Quinic acid, Serin, Pyroglutamic acid, Meso erythritol, beta-Alanine, Ornithine, Glycine, and Maltitol.

No	Attribute	Metabolites and Their Correlations
12	Taste-Coconut	A total of 28 metabolites were identified. Seven metabolites exhibit positive correlations: Fructose, Tagatose, Glucose, Galactose, Succinic acid, Meliniose, and Gentiobiose. Meanwhile, 21 metabolites show negative correlations, including Xylonic acid, Maltitol, 2-Aminoethanol, beta-Alanine, Meso erythritol, Aspartic acid, Lysine, Methionine, Isoleucine, Xylitol, Inositol, Sucrose, Quinic acid, Proline, Valine, Pyroglutamic acid, Turanose, Serin, Tryptophan, Citric acid, and Phosphate.
13	Taste-Sweet	A total of 25 metabolites were identified. Five metabolites exhibit positive correlations: Fructose, Glucose, Tagatose, Galactose, and Succinic acid. In contrast, 20 metabolites show negative correlations, including 2-Aminoethanol, Maltitol, Isoleucine, Xylitol, beta-Alanine, Inositol, Aspartic acid, Meso erythritol, Methionine, Sucrose, Lysine, Proline, Quinic acid, Turanose, Valine, Pyroglutamic acid, Serin, Tryptophan, Citric acid, and Phosphate.
14	Taste-Fizzy	All 18 metabolites exhibit positive correlations: Aspartic acid, beta-Alanine, Citric acid, Glutamic acid, Glycine, Lysine, Maltitol, Meso erythritol, Methionine, Ornithine, Phosphate, Proline, Pyroglutamic acid, Quinic acid, Serin, Tryptophan, Turanose, and Valine.

No	Attribute	Metabolites and Their Correlations
15	Taste-Salty	A total of 29 metabolites were identified. Of these, 21 metabolites exhibit positive correlations, including Citric acid, Phosphate, Turanose, Inositol, Isoleucine, Sucrose, Tryptophan, Xylitol, Serin, Valine, Proline, Pyroglutamic acid, Quinic acid, 2-Aminoethanol, Lysine, Methionine, Aspartic acid, Meso erythritol, Xylonic acid, beta-Alanine, and Fumaric acid. In contrast, 8 metabolites show negative correlations, including 4-Aminobutyric acid, Gentiobiose, Succinic acid, Meliniose, Galactose, Fructose, Glucose, and Tagatose.
16	Taste-Astringent	A total of 22 metabolites were identified. Of these, 13 exhibit positive correlations, including Inositol, Isoleucine, Sucrose, Xylitol, Fumaric acid, Turanose, Citric acid, 2-Aminoethanol, Phosphate, Xylonic acid, Tryptophan, Proline, and Valine. In contrast, 9 metabolites show negative correlations, including Shikimic acid, Succinic acid, 4-Aminobutyric acid, Galactose, Fructose, Gentiobiose, Glucose, Meliniose, and Tagatose.
17	Taste-Bitter	All 6 metabolites exhibit negative correlations: 4-Aminobutyric acid, Gentiobiose, Glycine, Meliniose, Ribose, and Shikimic acid.
18	Mouthfeel-Oily	All six metabolites exhibit negative correlations: 4-Aminobutyric acid, Gentiobiose, Glycine, Meliniose, Ribose, and Shikimic acid.

No	Attribute	Metabolites and Their Correlations
19	Mouthfeel-Astringent	A total of 19 metabolites were identified. Of these, 10 exhibit positive correlations, including Inositol, Isoleucine, Sucrose, Xylitol, Fumaric acid, Turanose, 2-Aminoethanol, Citric acid, Xylonic acid, and Phosphate. In contrast, 9 metabolites show negative correlations, including Shikimic acid, Succinic acid, Galactose, Fructose, Glucose, Tagatose, 4-Aminobutyric acid, Gentiobiose, and Meliniose.
20	Mouthfeel-Body	All six metabolites exhibit negative correlations: beta-Alanine, Glycine, Maltitol, Meso erythritol, Ornithine, and Ribose.
21	Mouthfeel-Fizzy	A total of 28 metabolites were identified. Of these, 21 exhibit positive correlations, including Citric acid, Phosphate, Turanose, Isoleucine, Tryptophan, Serin, Inositol, Proline, Pyroglutamic acid, Valine, Sucrose, Xylitol, Quinic acid, Lysine, Methionine, Aspartic acid, Meso erythritol, 2-Aminoethanol, beta-Alanine, Xylonic acid, and Maltitol. In contrast, 7 metabolites show negative correlations, including Gentiobiose, Meliniose, Succinic acid, Galactose, Fructose, Glucose, and Tagatose.
22	Flavour-Nutty	A total of 27 metabolites were identified. Of these, 19 exhibit positive correlations, including Inositol, Sucrose, Citric acid, Turanose, Xylitol, Isoleucine, Phosphate, Tryptophan, Serin, Valine, Proline, 2-Aminoethanol, Pyroglutamic acid, Fumaric acid, Quinic acid, Xylonic acid, Lysine, Methionine, and Aspartic acid. In contrast, 8 metabolites

No	Attribute	Metabolites and Their Correlations
		show negative correlations, including 4-Aminobutyric acid, Succinic acid, Galactose, Gentiobiose, Meliniose, Fructose, Glucose, and Tagatose.
23	Flavour-Creamy	A total of 24 metabolites were identified. Two metabolites exhibit positive correlations, Fructose and Tagatose. In contrast, 22 metabolites show negative correlations, including Alanine, Glycine, Inositol, Sucrose, Xylitol, Isoleucine, Ornithine, Aspartic acid, Lysine, Methionine, Turanose, Maltitol, Meso erythritol, Proline, beta-Alanine, Valine, Citric acid, Quinic acid, Phosphate, Pyroglutamic acid, Tryptophan, and Serin.
24	Flavour-Milky	All 13 metabolites exhibit negative correlations: Ribose, Lysine, Tryptophan, Aspartic acid, Serin, Glutamic acid, Quinic acid, Pyroglutamic acid, Meso erythritol, beta-Alanine, Maltitol, Ornithine, and Glycine.
25	Flavour-Coconut	All 19 metabolites exhibit negative correlations: Threonine, Glutamic acid, Turanose, Glycine, Methionine, Proline, Lysine, Ornithine, Aspartic acid, Citric acid, Valine, Phosphate, Meso erythritol, Quinic acid, Tryptophan, beta-Alanine, Maltitol, Pyroglutamic acid, and Serin.

No	Attribute	Metabolites and Their Correlations
26	Flavor-Sweet	A total of 29 metabolites were identified. Of these, 8 exhibit positive correlations, including Fructose, Glucose, Tagatose, Galactose, Succinic acid, Meliniose, Gentiobiose, and 4-Aminobutyric acid. In contrast, 21 metabolites show negative correlations, including Maltitol, Xylonic acid, beta-Alanine, 2-Aminoethanol, Meso erythritol, Aspartic acid, Lysine, Methionine, Quinic acid, Proline, Xylitol, Isoleucine, Pyroglutamic acid, Valine, Inositol, Sucrose, Serin, Tryptophan, Turanose, Phosphate, and Citric acid.
27	After taste-Sweet	A total of 29 metabolites were identified. Of these, 8 exhibit positive correlations, including Fructose, Glucose, Tagatose, Galactose, Meliniose, Succinic acid, Gentiobiose, and 4-Aminobutyric acid. In contrast, 21 metabolites show negative correlations, including Fumaric acid, Xylonic acid, beta-Alanine, Meso erythritol, Aspartic acid, 2-Aminoethanol, Methionine, Lysine, Quinic acid, Proline, Pyroglutamic acid, Valine, Xylitol, Isoleucine, Serin, Sucrose, Inositol, Tryptophan, Phosphate, Turanose, and Citric acid.
28	After taste-Oily	There are 19 metabolites that exhibit negative correlations: Aspartic acid, beta-Alanine, Citric acid, Glutamic acid, Glycine, Lysine, Maltitol, Meso erythritol, Methionine, Ornithine, Phosphate, Proline, Pyroglutamic acid, Quinic acid, Serin, Threonine, Tryptophan, Turanose, and Valine.

No	Attribute	Metabolites and Their Correlations
29	After taste-Astringent	There are 22 metabolites that exhibit positive correlations: Aspartic acid, beta-Alanine, Citric acid, Glycine, Inositol, Isoleucine, Lysine, Maltitol, Meso erythritol, Methionine, Ornithine, Phosphate, Proline, Pyroglutamic acid, Quinic acid, Serin, Sucrose, Threonine, Tryptophan, Turanose, Valine, and Xylitol.
30	After taste-Bitter	There are 4 metabolites that exhibit positive correlations: Glycine, Maltitol, Ornithine, and Ribose.
31	After taste-Salty	There are 7 metabolites that exhibit positive correlations: beta-Alanine, Glutamic acid, Glycine, Maltitol, Meso erythritol, Ornithine, and Ribose.
32	After taste-Umami	A total of 28 metabolites were identified. Of these, 21 exhibit positive correlations, including Citric acid, Phosphate, Tryptophan, Turanose, Serin, Pyroglutamic acid, Valine, Inositol, Proline, Sucrose, Isoleucine, Quinic acid, Xylitol, Lysine, Methionine, Aspartic acid, Meso erythritol, beta-Alanine, 2-Aminoethanol, Maltitol, and Xylonic acid. In contrast, 7 metabolites show negative correlations, including Gentiobiose, Meliniose, Succinic acid, Galactose, Glucose, Fructose, and Tagatose.

Table S53. Sensory Attributes of Flesh and Metabolites with Significant Pearson Correlation at the 0.05 Level

No	Sensory attribute	Metabolites and Their Correlations
1	Appearance-White	There are 11 compounds, which consist of: Fructose, Fumaric acid, Glucose, Galactinol, Galactitol, Malic acid, Succinic acid, 2-Aminoethanol, Glycine, Galactose, and Sorbitol (all positively correlated above 70%).
2	Appearance-Chocolate	There are 7 compounds, which consist of: Galactitol, Sorbitol, Fumaric acid, Succinic acid, Fructose, Malic acid, and Galactinol (all negatively correlated).
3	Aroma-Nutty	There are 10 compounds, which consist of: 2-Aminoethanol, Proline, Glycine, Fumaric acid, 4-Aminobutyric acid, Glutamic acid, Fructose, Glucose, Galactose, and Galactinol (All of these compounds are positively correlated.)
4	Aroma-Creamy	There are 11 compounds, which consist of: Fructose, Glucose, Fumaric acid, Galactinol, 2-Aminoethanol, Glycine, Galactose, 4-Aminobutyric acid, Malic acid, Galactitol, and Succinic acid. All of these compounds are positively correlated.
5	Aroma-Milky	There are 2 compounds, which consist of Glutamic acid (negatively correlated) and Sucrose (positively correlated).

No	Sensory attribute	Metabolites and Their Correlations
6	Aroma-Coconut	There are 9 compounds, which consist of: 2-Aminoethanol, Proline, Glycine, 4-Aminobutyric acid, Glutamic acid, Fructose, Glucose, Galactose, and Galactinol. All of these compounds are positively correlated.
7	Aroma-Rancid	There are 5 compounds, which consist of: Proline, 4-Aminobutyric acid, Glutamic acid, and Galactose (all positively correlated), while Sucrose is negatively correlated.
8	Taste-Nutty	There are 9 compounds, which consist of: 2-Aminoethanol, Proline, Glycine, 4-Aminobutyric acid, Glutamic acid, Fructose, Glucose, Galactose, and Galactinol. All of these compounds are positively correlated.
9	Taste-Creamy	There are 11 compounds, which consist of: 2-Aminoethanol, Glycine, Succinic acid, Fumaric acid, Malic acid, 4-Aminobutyric acid, Fructose, Glucose, Galactose, Galactitol, and Galactinol. All of these compounds are positively correlated.
10	Taste-Milky	There are 7 compounds, which consist of: Succinic acid, Fumaric acid, Malic acid, Fructose, Galactitol, Sorbitol, and Galactinol. All of these compounds are positively correlated.
11	Taste-Coconut	There are 6 compounds, which consist of: 2-Aminoethanol, Proline, 4-Aminobutyric acid, Glutamic acid, Glucose, and Galactose. All of these compounds are positively correlated.

No	Sensory attribute	Metabolites and Their Correlations
12	Taste-Bitter	There are 6 compounds, which consist of: 2-Aminoethanol, Proline, 4-Aminobutyric acid, Glutamic acid, Glucose, and Galactose. All of these compounds are positively correlated.
13	Taste-Astringent	There are 2 compounds, which consist of: Galactitol and Sorbitol. Both of these compounds are positively correlated.
14	Mouthfeel-Oily	There are 9 compounds, which consist of: 2-Aminoethanol, Proline, Glycine, 4-Aminobutyric acid, Glutamic acid, Fructose, Glucose, Galactose, and Galactinol. All of these compounds are positively correlated.
15	Mouthfeel-Soft	There are 5 compounds, which consist of: Succinic acid, Fumaric acid, Malic acid, Galactitol, and Sorbitol. All of these compounds are negatively correlated.
16	Mouthfeel-Moist	There are 8 compounds, which consist of: Succinic acid, Fumaric acid, Malic acid, Fructose, Glucose, Galactitol, Sorbitol, and Galactinol. All of these compounds are positively correlated.
17	Mouthfeel-Slimy	There are 11 compounds, which consist of: 2-Aminoethanol, Glycine, Succinic acid, Fumaric acid, Malic acid, 4-Aminobutyric acid, Fructose, Glucose, Galactose, Galactitol, and Galactinol. All of these compounds are positively correlated.
18	Mouthfeel-Crispy	There are 3 compounds, which consist of: 4-Aminobutyric acid and Glutamic acid (both positively correlated), while Sucrose is negatively correlated.

No	Sensory attribute	Metabolites and Their Correlations
19	Mouthfeel-Sandy	There are 10 compounds, which consist of: 2-Aminoethanol, Glycine, Succinic acid, Fumaric acid, Malic acid, Fructose, Glucose, Galactitol, Sorbitol, and Galactinol. All of these compounds are negatively correlated.
20	Mouthfeel-Astringent	There are 6 compounds, which consist of: Succinic acid, Fumaric acid, Malic acid, Fructose, Galactitol, and Sorbitol. All of these compounds are negatively correlated.
21	Flavor-Nutty	There are 3 compounds, which consist of: 4-Aminobutyric acid and Glutamic acid (both positively correlated), while Sucrose is negatively correlated.
22	Flavor-Creamy	There are 12 compounds, which consist of: 2-Aminoethanol, Glycine, Succinic acid, Fumaric acid, Malic acid, 4-Aminobutyric acid, Glutamic acid, Fructose, Glucose, Galactose, Galactitol, and Galactinol. All of these compounds are positively correlated.
23	Flavor-Milky	There is 1 compound, which is Sucrose, and it is positively correlated.
24	Flavor-Coconut	There are 2 compounds, which consist of: Sorbitol and Sucrose. Both of these compounds are positively correlated.
25	Flavor-Umami	There are 7 compounds, which consist of: Succinic acid, Fumaric acid, Malic acid, Fructose, Galactitol, Sorbitol, and Galactinol. All of these compounds are negatively correlated.

No	Sensory attribute	Metabolites and Their Correlations
26	After taste-Oily	There are 6 compounds, which consist of: Succinic acid, Fumaric acid, Malic acid, Fructose, Galactitol, and Sorbitol. All of these compounds are positively correlated.
27	After taste-Bitter	There are 6 compounds, which consist of: 2-Aminoethanol, Proline, 4-Aminobutyric acid, Glutamic acid, Glucose, and Galactose. All of these compounds are positively correlated.
28	After taste-Salty	There are 10 compounds, which consist of: 2-Aminoethanol, Proline, Glycine, Fumaric acid, 4-Aminobutyric acid, Glutamic acid, Fructose, Glucose, Galactose, and Galactinol. All of these compounds are positively correlated.
29	After taste-Umami	There are 10 compounds, which consist of: 2-Aminoethanol, Proline, Glycine, Fumaric acid, 4-Aminobutyric acid, Glutamic acid, Fructose, Glucose, Galactose, and Galactinol. All of these compounds are positively correlated.
30	After taste-Astringent	There are 9 compounds, which consist of: 2-Aminoethanol, Glycine, Fumaric acid, 4-Aminobutyric acid, Glutamic acid, Fructose, Glucose, Galactose, and Galactinol. All of these compounds are positively correlated.

Note: Sensory data presented based on sensory attributes with compounds that show a significant correlation using Pearson's test at a 0.05 level